Studies into Hydrogen Atom Abstraction from Amino Acids and Peptides

A thesis submitted for the degree of Doctor of Philosophy of
The Australian National University

by

Zachary Ivan Watts

January 2006

THE AUSTRALIAN NATIONAL UNIVERSITY

Declaration

This is to declare that the work presented herein represents original work that I carried out during my Ph.D. candidature from April 2002 to January 2006, except that in "Chapter 5: Radical Stabilisation and its Affect on Reaction Rate", the bond dissociation energies and radical stabilisation energies were determined by Prof. L. Radom and Mr. G.P.F. Wood, University of Sydney.

To the best of my knowledge, this thesis does not contain material that has been previously published or accepted for the award of any other degree or diploma in any university or other tertiary institution. Published or written work by another person has been acknowledge by citation throughout the text.

I give consent for a copy of my thesis to be deposited in the University library and be available for loan and photocopying.

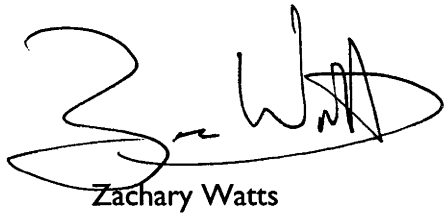

Zachary Watts

January 2006

Acknowledgements

Firstly, thanks go to Prof. Chris Easton, my supervisor. Arguably the best Ph.D. supervisor I have ever had. He has been supportive and enthusiastic about my project even when I wasn't. You've got to hand it to him; he knows what he's on about.

Secondly, thanks go to the numerous members of the Easton Group. Academically, Dr. Jamie Simpson was invaluable during the beginning phase of my studies as a sounding board for ideas. Dr. Adam Wright took over this role after Jamie departed. Tony Herlt is a technician of whose prowess can not be surpassed. Dr. Lorna Barr and Dr. Hideki Onagi helpt proof this theseis. The remainder of the group proved to be a remarkably nice bunch of people to work with, and so in order to not offend anyone by their absence I must thank: Amy, Ryan, Rodger, Georgie, Saara, Alex, Iris, Candace, Daarshana, Subashani, Marta, Ken and Dave.

For the best bit about working in Canberra: not working. Thanks to Heather, Rian and Lorraine.

To whomever I forgot to list above, I couldn't have done it without you.

And of course to the Research School of Chemistry for, despite its best efforts, not burning to the ground in August 2005.

Abstract

The reactions of protonated α-amino acids with chlorine radicals have been investigated. The identity of the products, the relative amount of each product and the rate at which the amino acids react has been used to calculate the reactivity of various types of hydrogen within amino acids. The results indicate that hydrogen atom abstraction preferentially occurs at positions more distant from the α-centre, and that abstraction at the α- and β-positions of protonated α-amino acids is highly disfavoured. These results reflect a large polar effect.

In an identical manner, the reactions of chlorine radicals with *N*-acetylated amino acids have been studied. The reactivity of these compounds follows a similar pattern; for α- and β-positions there is little reaction when compared to more distal positions. Again, this is indicative of a polar effect operating, albeit a slightly weaker one than for the protonated amino acids.

The reactivities per hydrogen obtained in the above mentioned studies were used to predict the selectivity of radical chlorination of four tripeptides. A high level of agreement was found between the prediction and experimental observation as regards both the identity and the amount the major product, or products, formed in each case.

Theoretical calculations at the RB3-LYP/6-311+G(3df,2p)//UB3-LYP/6-31G(d) level of theory of the stability of the radicals formed through hydrogen abstraction from protonated and *N*-acetylated amino acids were compared with the rates of formation of those radicals. There was little correlation. In particular, the α-carbon-centred radicals of *N*-acetylated amino acids showed very high radical stabilisation energies but their rates of formation were extremely slow. These results provide a measure of the polar effect seen in the chlorination experiments.

An alternative approach to the investigation of hydrogen atom abstraction from protonated and *N*-acetylated amino acids involved using oxygen-centred radicals. These experiments provided the relative rates of reaction, and the reactivity per hydrogen for various types of methyl hydrogens. Qualitatively, these results are similar

to those of the chlorinations, as α- and β-hydrogens displayed a significant decrease in reactivity compared to hydrogens at positions further along the amino acid side-chains.

These results provide insight to numerous biological processes involving amino acids and peptides and free radicals as intermediates.

Table of Contents

Chapter 1: Introduction

1.1 Biological Aspects of Amino Acid Radicals

Proteins are ubiquitous in nature as, among other things, enzymes[1] and hormones[1,2] and as structural components of cells.[3] The basic building blocks of these molecules are α-amino acids,[1] of which (including structurally related compounds) more than 700 are found in nature.[4] Despite this variety, only 20 are found commonly in proteins.[5-7] The wide variety arises through functionalisation of the more common amino acids during biosynthethic processes, such as secondary metabolism.[4]

Amino acid radicals have been shown to have pathological significance.[8-20] Prolonged attack by free radicals results in a build up of damaged, potentially toxic proteins.[8-11] Oxidative modification of proteins is a marker for protease degradation. Oxidative damage to proteins is associated with numerous disease states such as ageing (including premature ageing diseases such as progeria and Werner's syndrome), ischemia-reperfusion (oxidative damage after restricted blood flow is restored), muscular dystrophy, pulmonary diseases, rheumatoid arthritis, cataract formation, atherosclerosis and diabetes.[21] The toxicity of carbon tetrachloride[13] and cigarette smoke[18] has been attributed to radical processes. The presence of radical species has been detected in enzymatic reactions.[22-30]

Biological systems have an abundance of so-called reactive oxygen species (ROS) which include such radicals as superoxide anion ($O_2^{\bullet-}$), peroxyl and hydroperoxyl radicals ($ROO^{\bullet}$ and $HOO^{\bullet}$) and hydroxyl radical ($HO^{\bullet}$).[31] In biological systems there is a variety of reductive systems which catalyse the transformation of molecular oxygen into superoxide anion, such as NAD^+ (Figure 1.1) and cytochrome a (Figure 1.2).

$$NAD^+ \xrightarrow{+\,e^-} NAD^{\bullet} \xrightarrow{O_2} NAD^+ + O_2^{\bullet-}$$

Figure 1.1: Formation of superoxide anion by NAD^+

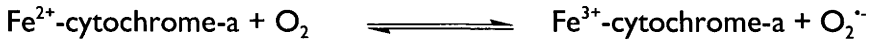

Figure 1.2: Formation of superoxide anion by cytochrome a

Superoxide anion is not in itself a reactive radical, because the unpaired spin is resonance delocalised and in general superoxide itself is not an important mediator of O_2 toxicity. However, subsequent transformations lead to much more reactive species.[31] Superoxide anion exists in an equilibrium with its conjugate acid, the hydroperoxyl radical, HOO$^{\bullet}$ (Figure 1.3). In general, at biological pH the amount of hydroperoxyl radical is small, but non-negligible (at pH 6 up to 4% is hydroperoxyl radical).[31]

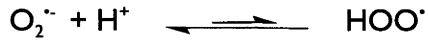

Figure 1.3: The equilibrium between superoxide anion and hydroperoxyl radical

The other main pathway for the formation of more reactive species is via disproportionation (Figure 1.4), such as through the action of superoxide dismutase.[32]

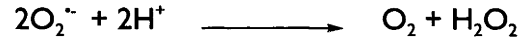

Figure 1.4: Disproportionation of superoxide anion catalysed by superoxide dismutase

Such peroxides can undergo Fenton-type chemistry to yield hydroxyl and hydroperoxyl radicals (Figure 1.5).[21]

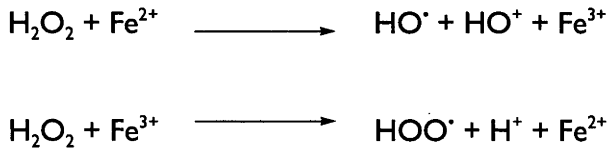

Figure 1.5: The Fenton reaction

The relative reactivity increases from superoxide anion to hydroperoxyl and peroxyl radicals to hydroxyl radical.[31] Because of the significantly higher reactivity of hydroxyl radicals as well as generally low concentrations of hydroperoxyl and peroxyl radicals, hydroxyl radicals are the primary hydrogen atom abstracting species *in vivo*.[31]

Regardless of the species, hydrogen abstraction can damage all the important biological molecules, such as DNA, lipids and proteins.

DNA damage can occur through two main processes: abstraction of hydrogen from the deoxyribose moiety, which results in ring opening and dephosphorylation which results in a break in the DNA chain, or by addition to the π systems of the bases, which disrupts the pairing due to hydrogen bonding (Figure 1.6). Radical damage occurs on 10^4-10^5 bases per cell per day.[33]

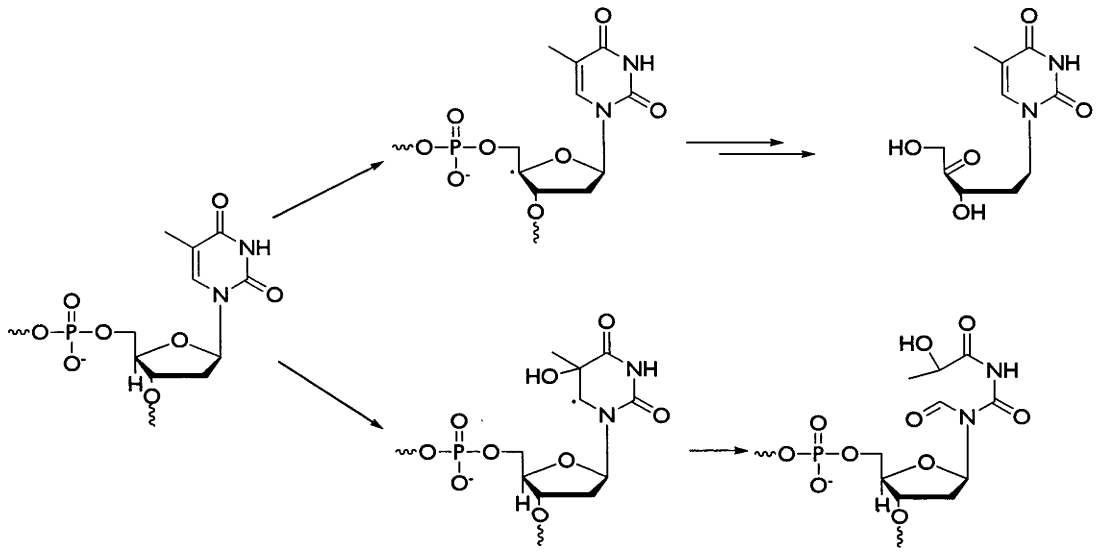

Figure 1.6: Radical reactions resulting in DNA damage

Unsaturated lipids can be damaged by abstraction of allylic hydrogens, and because of delocalisation of the formed radicals, multiple products can result (Figure 1.7). This mechanism is, however, not completely adverse as such processes are required for the synthesis of compounds such as prostaglandins and leukotrienes.[33]

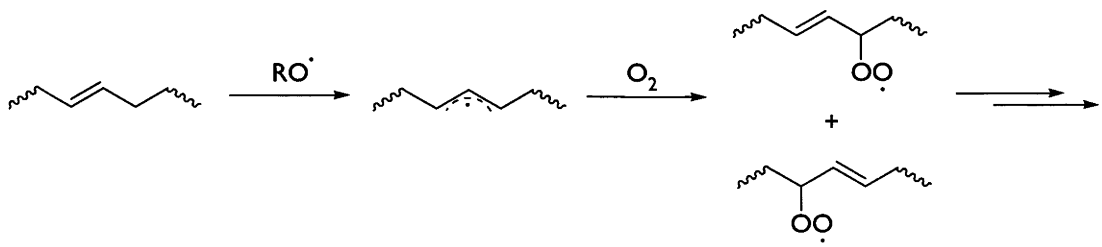

Figure 1.7: Radical reactions resulting in lipid damage

Biological oxidations of amino acids also involve ROS. Examples of hydroxylated amino acids in natural products, presumably produced through such processes, are listed in Figure 1.8.

Natural Product	Amino Acid
actinomycin X0β[34]	γ-HO-proline
aureobasidin[35]	β-HO-valine
berninamycin A[36]	β-HO-valine
bleomycin[37]	β-HO-histidine
bouvardin[38]	β-HO-tyrosine
BZR-cotoxin II[39]	δ-HO-leucine
calcium dependent antibiotic[40]	β-HO-asparagine
chloroeremycin[41]	β-HO-tyrosine
coumermycin A_1[42]	β-HO-tyrosine
cupolamide A[43]	γ-HO-proline
echinocandins C, D[44]	β-HO-proline
factor IX[45]	β-HO-aspartate
funebrine[46]	γ-HO-isoleucine
glidobactins A, B, C[47]	γ-HO-lysine
halipeptin A[48]	δ-HO-leucine
γ-hydroxyconophan[49]	γ-HO-valine
γ-hydroxy-*N*-methylproline[50]	N/A
γ-hydroxynorvaline lactone[51]	N/A
janthinocins A,B,C[52]	β-HO-leucine
katanosin B[53]	β-HO-phenylalanine
	β-HO-leucine
lysobactin[54]	β-HO-phenylalanine
	β-HO-leucine
	β-HO-asparagine
microcolin A[55]	γ-HO-proline
nikkomycin X[56]	β-HO-histidine

Figure 1.8: Natural products containing hydroxylated amino acids

Natural Product	Amino Acid
nostropeptin H[57]	β-HO-proline
novobiocin[42]	β-HO-tyrosine
P168[58]	β-HO-leucine
phallacidin[59]	γ-HO-proline
	γ,δ-di-HO-leucine
phallicin[59]	γ-HO-proline
phallisacin[59]	γ-HO-proline
	γ,δ-di-HO-leucine
phallisin[59]	γ-HO-proline
	γ,δ-di-HO-leucine
phalloidin[59]	γ-HO-proline
	γ,δ-di-HO-leucine
phalloine[59]	γ-HO-leucine
	γ-HO-proline
phomopsin A[60]	β-HO-isoleucine
	β-HO-phenylalanine
plusbacin A_3[61]	β-HO-aspartate
	β-HO-proline
polyoxypeptin A[62]	β-HO-β-Me-proline
ramoplanin[63]	β-HO-asparagine
streptothricin[64]	β-HO-arginine
vancomycin[65]	β-HO-tyrosine
virotoxins[66]	β,γ-di-HO-proline
yunnanin E[67]	δ-HO-leucine

Figure 1.8 *cont.*: Natural products containing hydroxylated amino acids

Oxygenase enzymes, such as those in the cytochrome family, function via the formation of reactive oxygen intermediates which can abstract hydrogen atoms. However, in general, the reactions occur at the metal centre of an enzyme in a manner similar to that shown below (Figure 1.9), and free reactive oxygen species such as superoxide anion are not released (the main exception being the case of cytochrome a, which was addressed above).[31]

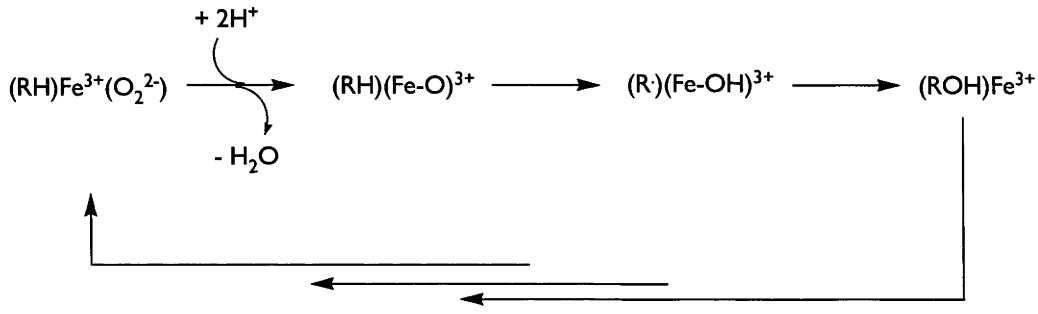

Figure 1.9: Radical oxidation facilitated by an oxygenase

In the absence of a substrate (or indeed in the presence of one) the cytochromes can catalyse the formation of peroxide, that is to say instead of converting R-H to R-OH, the enzymes produce H_2O_2 from H_2O.[31]

CmaB, one of five proteins involved in the synthesis of coronamic acid in certain phytopathogenic bacteria, is a non-haem Fe^{2+} halogenase. It has a high level of genetic homology with oxygenases, as well as with genes involved in the synthesis of halogenated natural products such as syringomycin E and barbamide.[68]

The step of particular interest is shown below, where *L-allo*-isoleucine (attached via a sulfur link to a carrier protein, CmaD) undergoes a radical chlorination to a γ-chloro-*L-allo*-isoleucine (Figure 1.10).

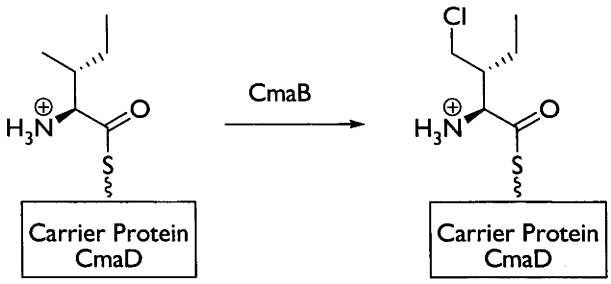

Figure 1.10: Formation of γ-chloroisoleucine-CmaD from isoleucine-CmaD

This process is thought to be radical in nature due to the dependence on iron and oxygen. The proposed mechanism of action of the CmaB protein is shown below (Figure 1.11).

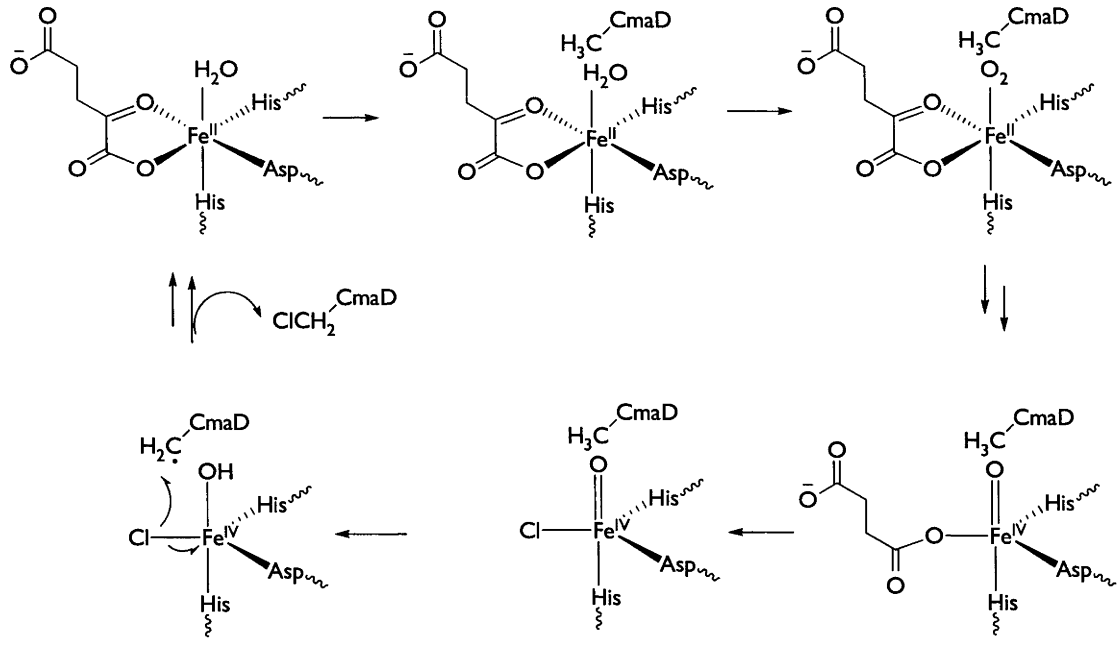

Figure 1.11: The proposed mechanism of the CmaB enzyme.

Depending on the experimental conditions, the Cma system can also act as an oxygenase.[68]

Many reactions of amino acids and their derivatives in biological systems involve hydrogen abstraction from the α-centres to give the corresponding radicals, however there are free radical mechanisms in addition to those discussed above which have been proposed whereby, rather than reactions at the α-centres, radical formation

occurs on the side-chains of the amino acids. In numerous studies of the biosynthesis of penicillin and related β-lactam antibiotics, radical based mechanisms have been proposed for the formation of the carbon-sulfur bond.[69-72] The proposed mechanisms proceed via hydrogen atom abstraction by the enzyme isopenicillin-*N*-synthetase (IPNS) from the *C*-terminal residue of the monocyclic intermediate (**1**) derived from the substrate δ-(*L*-α-aminoadipoyl)-*L*-cysteinyl-*D*-valine, to give the corresponding radical (**2**), which then cyclises onto the sulfur to give the product (**3**) (Figure 1.12).

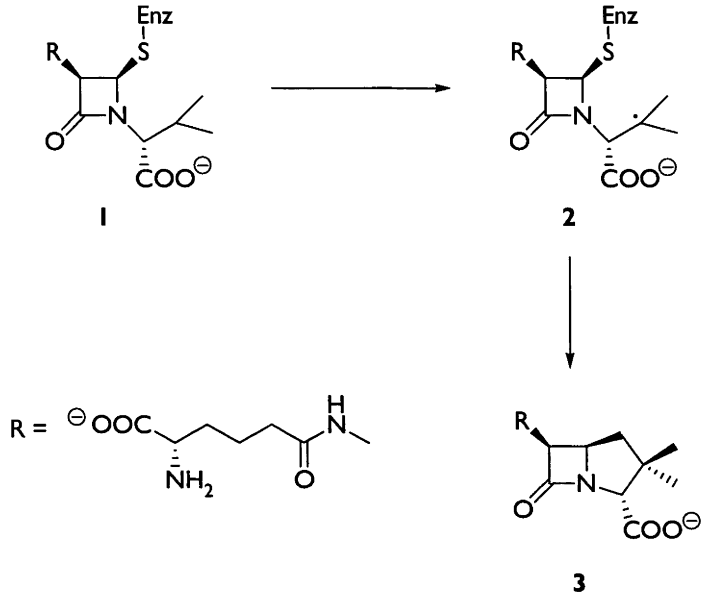

Figure 1.12: IPNS facilitated radical cyclisation to form the penicillin (**3**)

The above mentioned studies have demonstrated the dependence of IPNS on both Fe^{2+} and oxygen, which supports the hypothesis that penicillin biosynthesis follows a free radical mechanism. Further supporting evidence for this is that reaction of δ-(*L*-α-aminoadipoyl)-*L*-cysteinyl-*D*-allylglycine (**4**) with IPNS results in the products (**6**) and (**7**), which are indicative of those expected from formation of the allylic radical (**5**) (Figure 1.13). Additionally reaction of the substrate analogue (**8**) under free radical generating conditions gives the product (**9**) (Figure 1.14).[73]

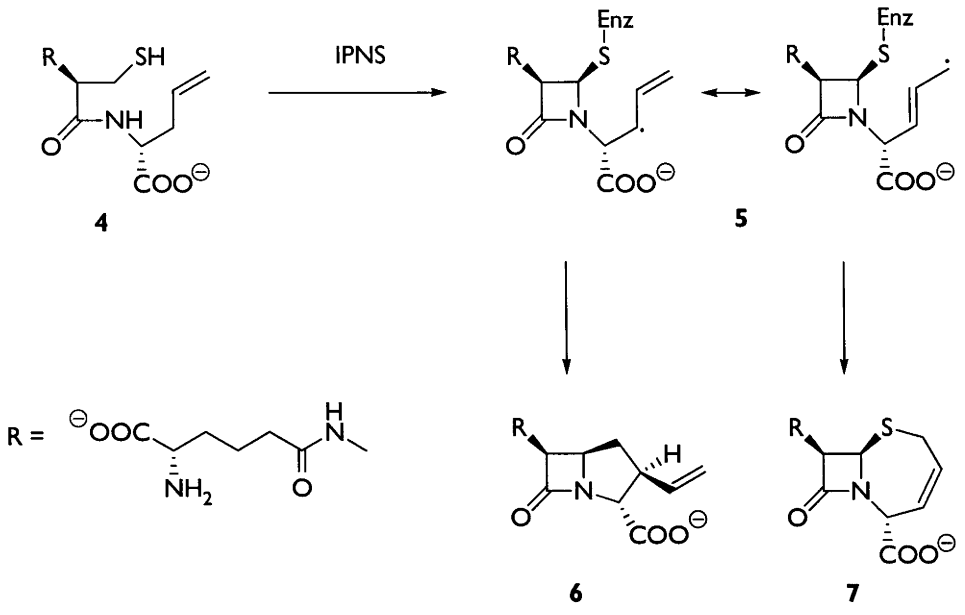

Figure 1.13: IPNS facilitated cyclisation of δ-(*L*-α-aminoadipoyl)-*L*-cysteinyl-*D*-allylglycine (**4**)

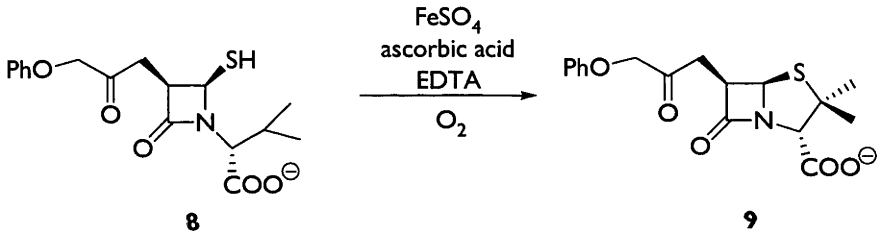

Figure 1.14: Cyclisation of the β-lactam (**8**) without IPNS

Other proposed free radical biosynthetic mechanisms include the production of clavulanic acid (**11**) which is suggested to occur in a manner analogous to that catalysed by IPNS. It has been demonstrated that the precursor of clavulanic acid (**11**) is the glutamic acid analogue (**10**). This would thus react via formation of a β-centred radical (Figure 1.15). Studies of this reaction have also shown its dependence on Fe^{2+} and oxygen.[74]

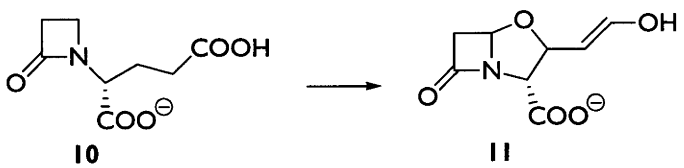

Figure 1.15: Formation of clavulinc acid (**11**) from the glutamic acid analogue (**10**)

The initial aims of the work described in this thesis were to examine fundamental free radical reactions of amino acids and their derivatives, in order to explore the reactivity and regioselectivity observed in biological systems such as those described above and to develop biomimetic synthetic methods.

1.2 Kinetics of Free Radical Reactions

The reactions examined in this thesis are chain processes and so they involve the steps outlined below (Figure 1.16), where X = Cl or HO.

X_2	$\longrightarrow$	$2\,X^{\bullet}$	(1)	*initiation*
$X^{\bullet} + RH$	$\longrightarrow$	$R^{\bullet} + XH$	(2)	*propagation*
$R^{\bullet} + O_2$	$\longrightarrow$	$ROO^{\bullet}$	(3)	
$R^{\bullet} + X_2$	$\longrightarrow$	$RX + X^{\bullet}$	(4)	
$ROO^{\bullet} + RH$	$\longrightarrow$	$ROOH + R^{\bullet}$	(5)	
$R^{\bullet} + X^{\bullet}$	$\longrightarrow$	RX	(6)	*termination*
$2R^{\bullet}$	$\longrightarrow$	RR	(7)	
$2X^{\bullet}$	$\longrightarrow$	X_2	(8)	
$ROO^{\bullet} + R^{\bullet}$	$\longrightarrow$	ROOR	(9)	

Figure 1.16: Reaction steps involved in chain processes[75-77]

The chain lengths of the reactions are large enough for the products of the termination reaction to be minor and therefore ignored in any analysis (chain lengths of typical radical chlorinations are generally greater than 1000).[76]

The rate constant for the hydrogen atom abstraction step (2) is defined as:

$$d[RH]/dt = k[X^{\bullet}][RH]$$

so to obtain k it is necessary to know both ($d[RH]/dt$) and the concentrations of $X^{\bullet}$ and RH. Because of the difficulty of this particularly with regard to determining [$X^{\bullet}$], it is more practical to determine relative rate constants, in which case the radical concentration can be ignored.

$$X^{\bullet} + R'H \xrightarrow{k'} R'^{\bullet} + XH \quad (10)$$

$$X^{\bullet} + R''H \xrightarrow{k''} R''^{\bullet} + XH \quad (11)$$

Figure 1.17: Hydrogen atom abstraction from two hydrocarbons, R'H and R"H

Now, the relative rates of consumption of the two hydrocarbons (Figure 1.17) defines k'/k'', or k_{rel} (Figure 1.18). The same holds for step (5). The value for $d[RH]/dt$ can be determined from the consumption of the starting material and/or from the formation of the products RX and ROOH.[75]

$$\frac{d[R'H]/dt}{d[R''H]/dt} = \frac{k'[X^{\bullet}][R'H]}{k''[X^{\bullet}][R''H]} = \frac{k'[R'H]}{k''[R''H]}$$

Figure 1.18: The equation which determines k_{rel} for reaction steps (10) and (11)

In order to reliably determine k_{rel} using this method the hydrogen abstraction reactions must not be reversible but this is a reasonable assumption given their exothermic nature and the relative ease of reaction steps (3) and (4).

If a reaction is endothermic, the transition state will resemble TS 1 (Figure 1.19), and the reactivity will be largely dependent on the stability of the generated radical $R^{\bullet}$. However, if a reaction is exothermic the transition state will more closely resemble TS 2 or TS 3 (Figure 1.19). There is less product radical character in these states, and so the reactivity will be less dependent on the stability of the product radical and more susceptible to the effects of charge development. If stabilisation of a partial charge is possible then the system will be more reactive (in other words there will be a reduction in the activation energy of the reaction).[78,79]

$R^{\delta\bullet}$----------H----$X^{\delta\bullet}$ (TS **1**)

$R^{\delta\bullet+}$---H----------$X^{\delta\bullet-}$ (TS **2**)

$R^{\delta\bullet-}$---H----------$X^{\delta\bullet+}$ (TS **3**)

Figure 1.19: Representations of transition states for the abstraction of hydrogen atoms

For reactive electrophilic radicals such as Cl$^{\bullet}$, HO$^{\bullet}$ and ROO$^{\bullet}$ the reactions are best represented by TS 2.[77,78] In the extreme this involves subsequent electron transfer and proton transfer steps (Figure 1.20).

$$R\text{-}H + X^{\bullet} \longrightarrow R\text{-}H^{\bullet+}\ X^{-} \longrightarrow R^{\bullet} + H\text{-}X$$

Figure 1.20: Hydrogen atom abstraction by subsequent electron transfer and proton transfer

The solvent in which a reaction is performed can affect the kinetics of a reaction in two ways. Firstly the rate of diffusion is dependent on the solvent viscosity (η):[79]

$$k_{diffusion} = (8RT/3)^{-3} \times \eta\ M^{-1}s^{-1}$$

The second possibility of a solvent effect is through the complexation of radicals by electron rich solvents.[77] Such complexes have altered reactivities. However, as the solvents which demonstrate such effects (such as aromatics and carbon disulfide) were not employed in the present experiments, this type of effect is not relevant in this study.

The general expectation for hydrogen atom abstraction reactions is for tertiary alkyl radicals to be formed in preference to secondary and primary alkyl radicals. The tertiary radicals are, in general, more thermodynamically stable,[77] which results in their preferred formation. Multiple factors contribute to the stability of radicals, such as

hyperconjugative stabilisation which involves interaction of the electron in the semi-occupied p-orbital of the radical centre with σ-bonds β to the radical centre. This kind of stabilisation is generally greater for tertiary radicals, due to the increased substitution compared to secondary and primary radicals. Another reason for the increased stability of tertiary radicals is relief of steric compression.[80,81] This occurs as the radical centre forms and becomes planar and the surrounding steric interactions are reduced. Again, this effect is greatest for centres with greater substitution.

An α-centred amino acid radical which is generally tertiary has enhanced stability over other tertiary radicals because of both the electron donating amino and electron withdrawing carboxyl substituents (Figure 1.21). Such an effect has been referred to variously as "push-pull stabilisation",[82-85] "merostabilisation"[86-88] and "captodative stabilisation".[89] The stability of α-centred radicals is not only greater than that of generic tertiary radicals but also greater than that expected based on the individual effects of amino and carboxyl substituents because of synergistic effects. Despite some historical contention about the magnitude of such effects[90-94] it is clear that radical reactions, such as brominations,[95-98] do preferentially occur at the α-position.

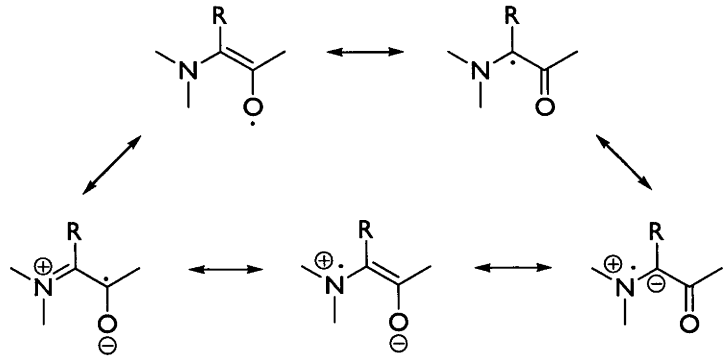

Figure 1.21: Resonance forms contributing to α-centred radicals

The same stabilising effects occur in peptides as in free amino acids, however the magnitude of the effects is reduced as the nitrogen electron pair is less able to contribute electron density because it is participating in the amide bond. This can be seen in the reduction of the stability of α-centred radicals between amino and amido acids,[94] and ESR measurements indicate that delocalisation of the α-centred radicals is reduced in acetylated amino acids compared to the non-acetylated analogues.[99]

The bond dissociation energies (BDEs) to give α-centred amino acid radicals are particularly low, between 316 and 369 kJ mol^{-1}, and most are below 350 kJ mol^{-1}.[100] In comparison, the BDE of the benzylic carbon-hydrogen bond of toluene is 371 kJ mol^{-1}, and that of methane is 435 kJ mol^{-1}.[101]

These BDEs can be used to compare the thermodynamic stabilities of radicals. A radical stabilisation energy (RSE) is defined as the difference in energy of a given radical compared to methyl radical. For example, the RSE of the benzylic radical is the difference in the BDEs of the corresponding carbon-hydrogen bonds of methane and toluene[102] (Figure 1.22).

$$\text{RSE } (PhC^{\cdot}H_2) = \text{BDE } (CH_4) - \text{BDE } (PhCH_3)$$

$$= 435 - 371 = 64 \text{ kJ mol}^{-1}$$

Figure 1.22: Calculation of the RSE of benzyl radical

$$\text{RSE } (NH_2C^{\cdot}HCOOH) = \text{BDE } (CH_4) - \text{BDE } (NH_2CH_2COOH)$$

$$= 435 - 350 = 85 \text{ kJ mol}^{-1}$$

Figure 1.23: Calculation of the RSE of the α-glycyl radical

In the same manner, the RSE of the α-glycyl radical is the difference in the BDEs of methane and glycine (Figure 1.23). The larger the RSE the more stable the radical. RSEs and BDEs can be determined experimentally or calculated theoretically. Recent theoretical studies have investigated the formation of numerous amino acid based radicals in the gas phase.[100,103-107]

1.3 Radical Reactions of Amino Acids

The radical chlorination of amino acids was first reported by Kollonitsch *et al.*,[108-110] in the 1960s. In strong acids such as hydrochloric acid, trifluoroacetic acid and chlorosulfuric acid, glycine did not react, however side chains on other amino acids underwent radical chlorination. The high reactivity of chlorine radicals resulted in cleavage of the relatively strong carbon-hydrogen bonds on the amino acid side-chains.

Kollonitsch *et al.*,[108-110] reported the isolation of a number of chlorinated amino acids (although in the current experiments it has not been possible to duplicate all of these), which are shown below (Figure 1.24).

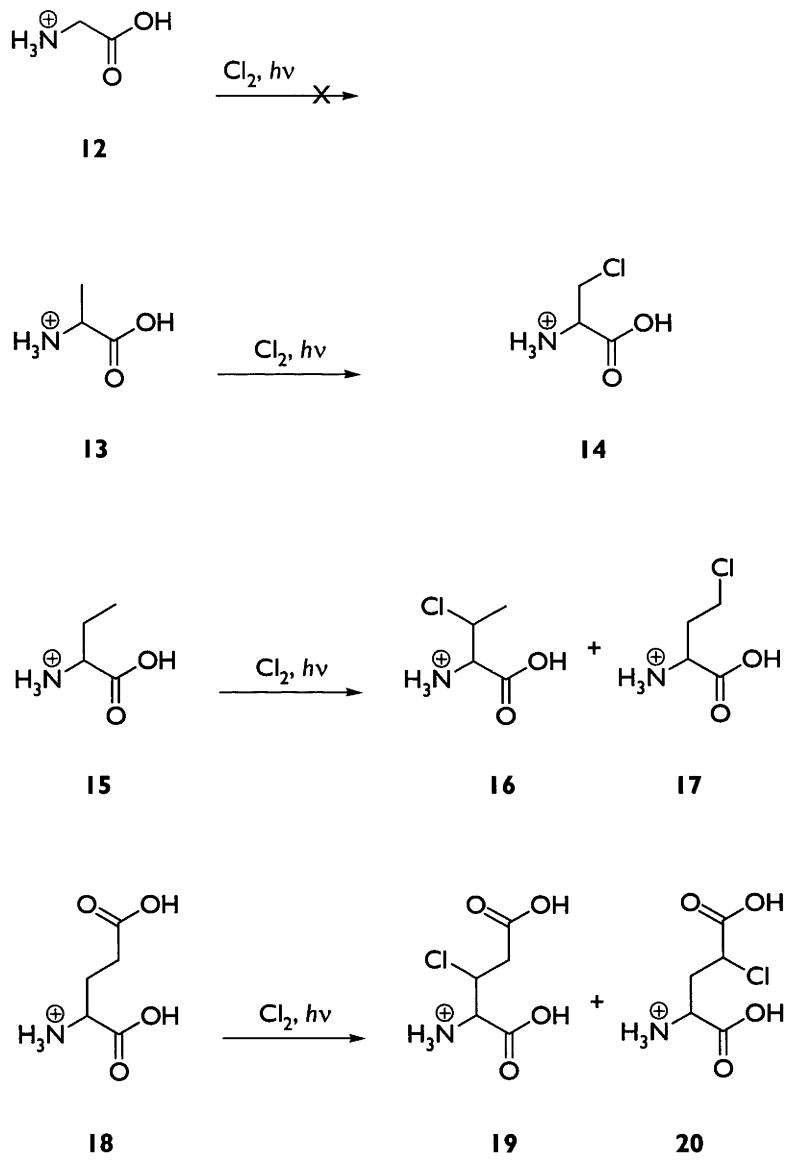

Figure 1.24: Reactions reported by Kollonitsch *et al.*[108-110]

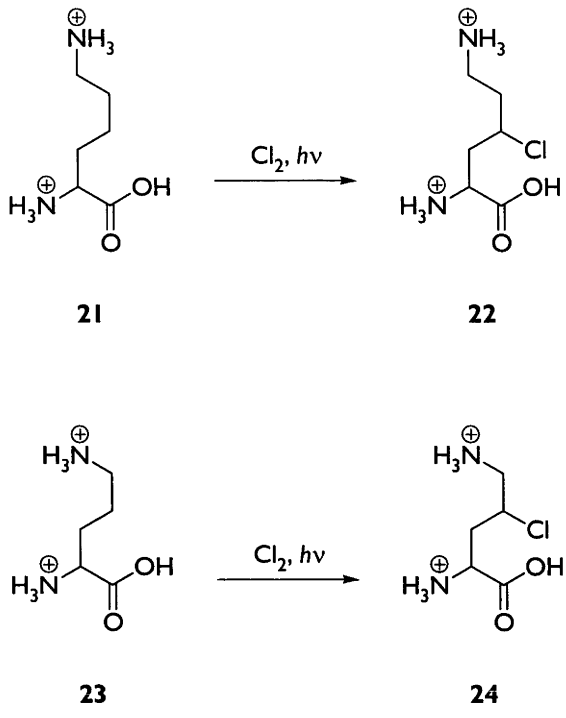

Figure 1.24 *cont.*: Reactions reported by Kollonitsch *et al.*[108-110]

Subsequent work by Dixon *et al.*,[111] resulted in the observation that the rate of chlorination varied in different acidic solvents, the fastest rate occurring in trifluoroacetic acid. Amino acids chlorinated by Dixon *et al.*,[111] and not by Kollonitsch *et al.*,[108-110] are shown below (Figure 1.25).

Historically, electron spin resonance (ESR) spectroscopy was the technique of choice for the detection of amino acid radicals. However, although a large variety of amino acid and peptide radicals (both α-centred radicals and side chain radicals) have been qualitatively examined,[112-125] only relatively recently have they been investigated quantitatively by these methods.[126,127] This has illustrated the variety of amino acid radicals that form besides α-centred radicals.

Product studies involved in the determination of hydrogen atom abstraction from amino acids and their derivatives by oxygen-centred radicals is more recent. Anderson *et al.*,[128,129] have developed a technique for determining the site of abstraction by quenching the radicals generated with a deuterated thiol (Figure 1.26), where the deuteration is then observed using ^{2}H NMR spectroscopy.

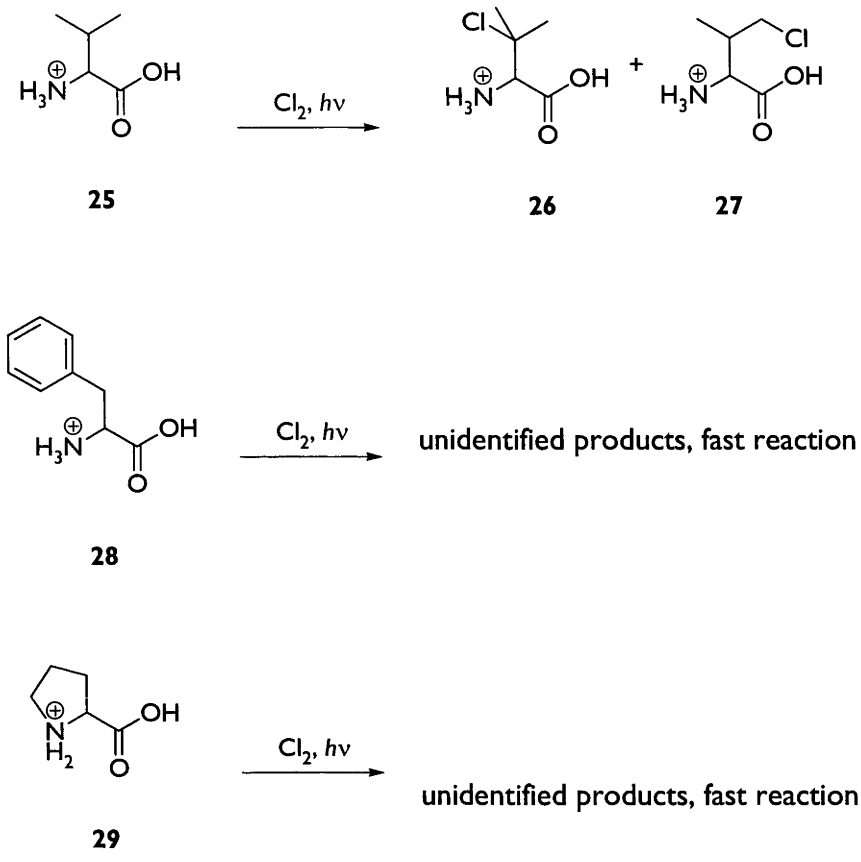

Figure 1.25: Reactions reported by Dixon *et al.*[111]

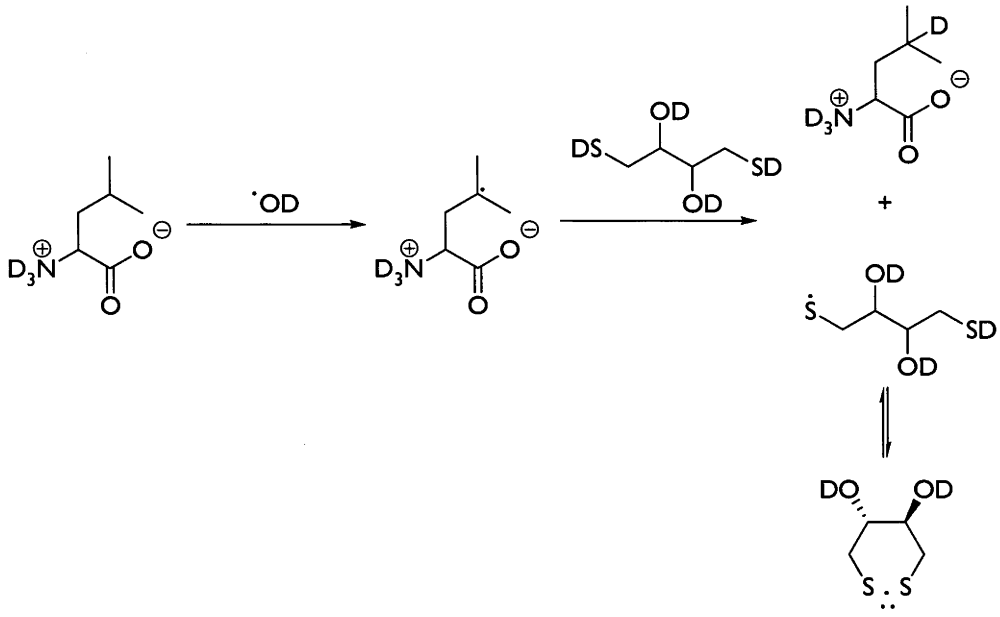

Figure 1.26: The technique used by Anderson *et al.*,[128,129] to identify the location of hydrogen atom abstraction

In these experiments they determined qualitatively the relative reactivity of a range of amino acids towards hydrogen abstraction (Figure 1.27) and observed, as with the chlorination experiments, that charged substituents deactivated the α-position towards reaction.

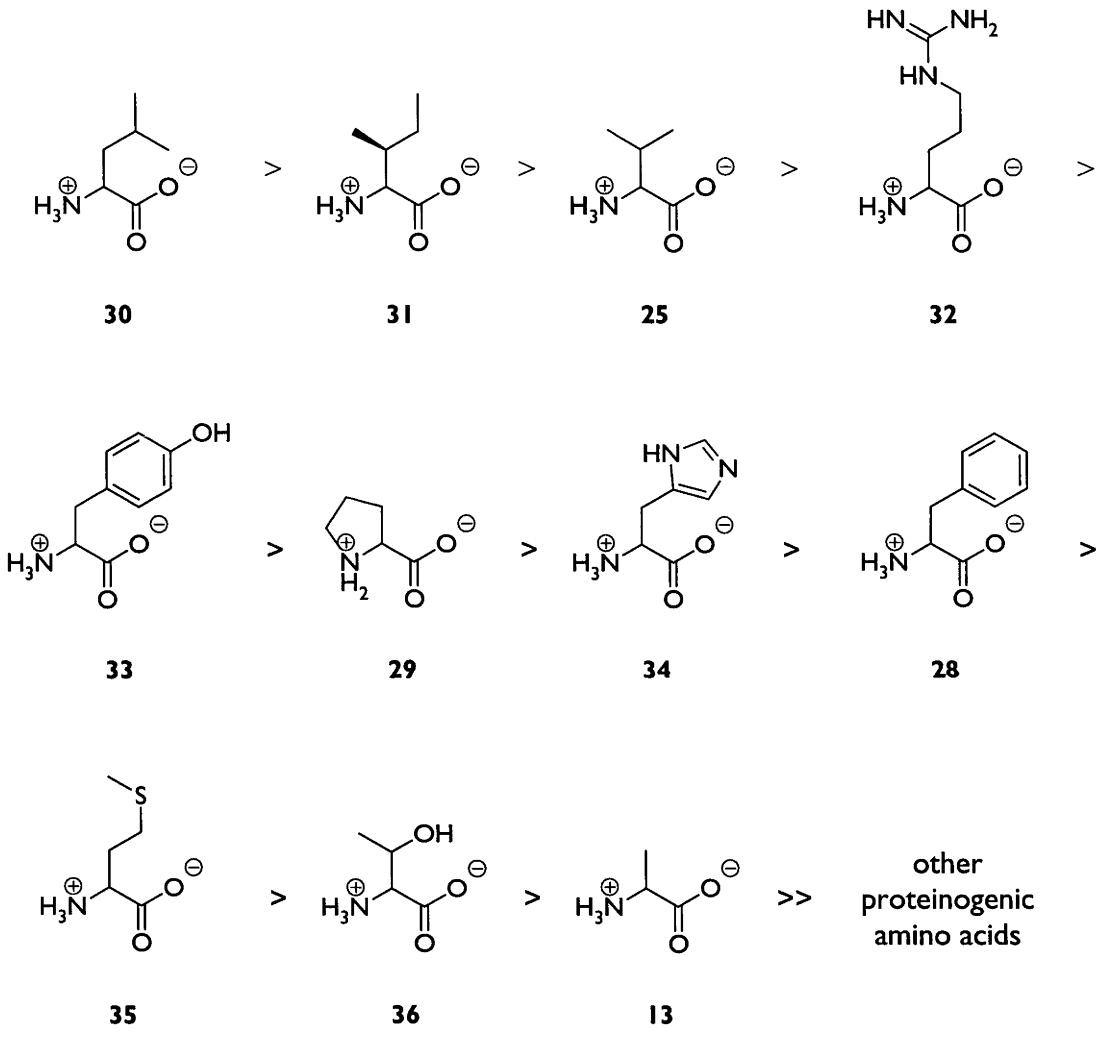

Figure 1.27: The order of reactivity of amino acids as determined by Anderson *et al.*[128,129]

Results such as these are challenging the view that the major pathway for oxidative peptide damage due to hydroxyl radicals is via α-hydrogen abstraction, although these studies are themselves compromised in that stable amino acid radicals would not be detected using this method. Their reactions with deuterated thiols would be endothermic to the extent that they would be unlikely to occur. The perception of reaction at the α-centres of amino acids dominating is probably due to a combination

of qualitative studies detailing protein fragmentation on exposure to hydroxyl radicals and molecular oxygen (Figure 1.28) and the predicted stability of the expected α-carbon centred radicals and their ease of formation through free radical bromination.[21]

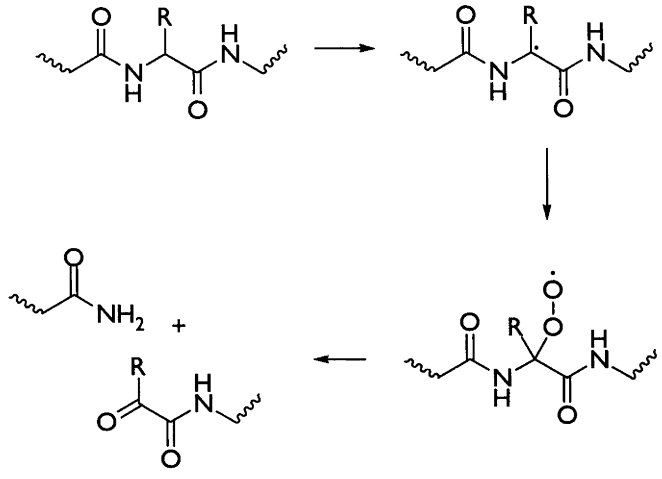

Figure 1.28: Peptide cleavage initiated by α-hydrogen atom abstraction

In order to better understand the way in which free radicals react with amino acids, peptides and proteins, and particularly the factors which control the rate at which hydrogen atom abstraction occurs and the location at which the abstraction occurs, several different reaction systems have been investigated in the work described in this thesis. This involved determination of rates of reaction and products formed for both chlorine radical hydrogen atom abstractions and oxygen-centred radical hydrogen atom abstractions, from both free and *N*-acetylated amino acids. The reliability of the data obtained in these experiments has been confirmed by using them to predict the selectivity of chlorination of several tripeptides. Theoretical calculations were also used to investigate the relationship between rates of hydrogen atom abstraction and the stabilities of the radicals formed.

Chapter 2: Results and Discussion

Hydrogen Atom Transfer from Amino Acids to Chlorine

Initially the reactions of free amino acids with chlorine were investigated. The free amino acids were of interest in their own right and as models of the *N*-terminal amino acid residues in peptides and proteins. Chlorination was studied as a way to assess the susceptibility of the amino acids to hydrogen atom transfer.

The choice of amino acids on which to study the effect of chlorine radical-facilitated hydrogen atom abstraction was determined by a number of factors. Firstly, for drawing conclusions relevant to biological systems it was desirable to examine the behaviour of naturally occurring, genetically encoded amino acids. Secondly, a number of isomers and homologues of naturally occurring amino acids were included, as they were expected to shed further light on the processes that occur. Homophenylalanine (**41**) is a homologue of phenylalanine (**28**), where the benzylic position is one carbon further away from the amino acid functionality. Ornithine (**23**), in a similar manner, is homologous with lysine (**21**), in that it has one methylene group less in its side chain. Valine (**25**), which has two γ-methyl groups on its side chain, forms a series of structurally similar compounds with α-aminobutyric acid (**15**) and *tert*-leucine (**40**), which have one and three γ-methyl groups, respectively. Likewise, α-aminobutyric acid (**15**), norvaline (**38**) and norleucine (**39**) form a series of amino acids with ethyl-, *n*-propyl- and *n*-butyl-side chains, respectively. Finally, a number of the proteinogenic amino acids are chemically incompatible with photochemical free radical chlorination and hydrogen atom transfer which precluded them from this particular study. A number of the aromatic amino acids (*i.e.*, tyrosine, tryptophan and histidine) are susceptible to electrophilic substitution, and rapidly react with molecular chlorine. Amino acids bearing hydroxyl functional groups are susceptible to ionic reactions, so serine and threonine were excluded from this investigation. The sulfur functionality of cysteine and methionine (**35**) is susceptible towards oxidation, and the thiol functionality of cysteine could interfere with the hydrogen atom transfer reactions, which would complicate any data obtained from such experiments. Asparagine, glutamine and arginine (**32**) are sufficiently structurally similar to glutamic acid (**18**),

aspartic acid (**37**) and ornithine (**23**) that it was thought that separate examination of their behaviour was not warranted.

This leaves a final set of sixteen compounds compromising glycine (**12**), alanine (**13**), valine (**25**), isoleucine (**31**), leucine (**30**), lysine (**21**), proline (**29**), phenylalanine (**28**), glutamic acid (**18**), aspartic acid (**37**), ornithine (**23**), α-aminobutyric acid (**15**), norvaline (**38**), norleucine (**39**), *tert*-leucine (**40**) and homophenylalanine (**41**). While glycine (**12**) is achiral, all other possible α-amino acids have at least one chiral centre. In general, the naturally occurring *S*-isomer was selected for experiments. This is primarily due to availability rather than for any other reason. Non-natural amino acids such as norleucine (**39**) were used as the cheaper racemates. Details are given in the Experimental. The chirality at the α-centre is not of great importance (and so in general, structures contained herein do not indicate stereochemistry), as the achiral nature of the chlorination reaction conditions means that enantiomers will have the same reactivity. Isoleucine (**31**) is the only naturally occurring diastereomeric amino acid and the only diastereomeric compund examined in these experiments, and it was used in its naturally occurring (2*S*,3*S*)-form.

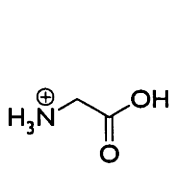

12

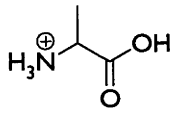

13

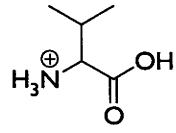

25

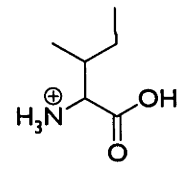

31

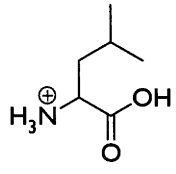

30

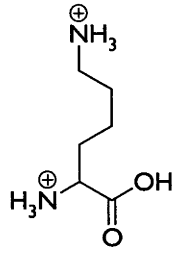

21

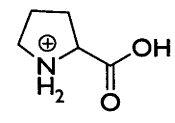

29

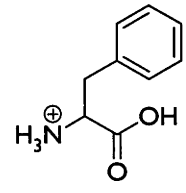

28

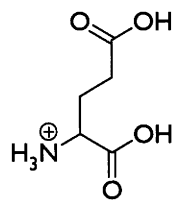

18

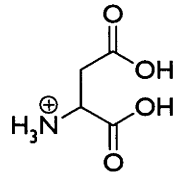

37

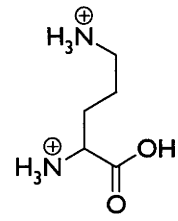

23

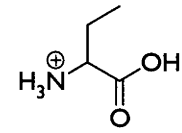

15

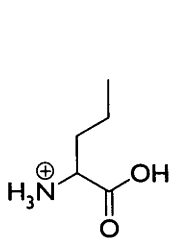

38

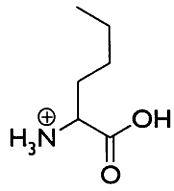

39

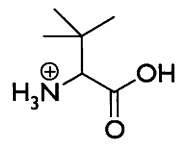

40

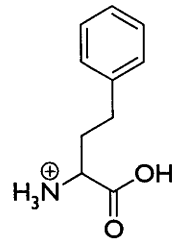

41

2.1 Reaction Products

The reactions of the amino acids (**12**), (**13**), (**15**), (**18**), (**21**), (**23**), (**25**), (**28-31**) and (**37-41**) were studied in trifluoroacetic acid saturated with molecular chlorine, with the mixtures being irradiated with a 300 W sunlamp for between 1-10 minutes depending on the reactivity of the substrate. Under these conditions the amino acids (**12**), (**13**), (**15**), (**18**), (**21**), (**23**), (**25**), (**28-31**) and (**37-41**) are expected to have been present in the form shown above (*i.e.*, fully protonated). The extent of substrate reaction was generally kept relatively low (less than 50%) to obtain good yields of mono-chlorinated products. The products were identified by direct analysis of crude reaction mixtures, after concentration under reduced pressure, using ^{1}H and 2D TOCSY (Total Correlation Spectroscopy) NMR experiments. HMQC (Heteronuclear Multiple Quantum Coherence) NMR experiments were also used to confirm ^{1}H resonance assignments by correlating them with ^{13}C resonances. Reactions were repeated in the presence of benzoic acid as an inert standard to determine the yields of the products and ascertain if they accounted for the starting amounts of the amino acids that had reacted.

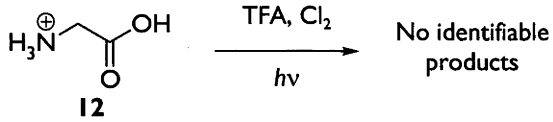

12

Figure 2.1: Reaction of glycine (**12**)

Glycine (**12**), when reacted using the conditions described above gave no observable products (Figure 2.1), however in the presence of benzoic acid as an internal standard it was shown to be slowly reacting. It is possible that α-chloroglycine is forming, which would eliminate HCl to form the corresponding imine, and decompose in the acid

medium. Other reactions could result in the degradation of glycine (**12**), possibly related to the observation that glycine (**12**) has been shown to decompose upon irradiation with UV light.[130]

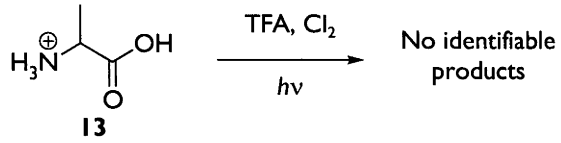

13

Figure 2.2: Reaction of alanine (**13**)

Alanine (**13**), like glycine (**12**), slowly reacts under the above conditions as demonstrated by the disappearance of starting material (Figure 2.2), but there is no evidence of reaction at the β-position to give β-chloroalanine (**14**). A singlet at δ2.3 ppm in the ^{1}H NMR spectrum of the product mixture is consistent with the formation of pyruvic acid,[131] that would result from chlorination at the α-position and subsequent reaction via the corresponding imine, as discussed above for glycine (**12**).

Glutamic acid (**18**) and aspartic acid (**37**), like glycine (**12**) and alanine (**13**), do not show any discrete products (Figure 2.3). Unlike glycine (**12**) and alanine (**13**), however, when the mass balance during reaction is monitored, it is seen that no discernible reaction is occurring in these cases.

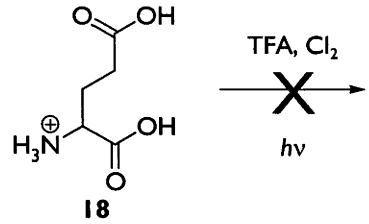

18

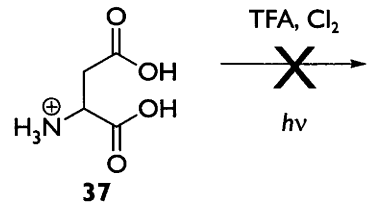

37

Figure 2.3: Reaction of glutamic acid (**18**) and aspartic acid (**37**)

When valine (**25**) is chlorinated three products are clearly identifiable by NMR spectroscopy (Figure 2.4), the yields of which account for at least 95% of the reacted starting material. One is β-chlorovaline (**26**), which is identifiable *via* its singlet α-

proton resonance, and the two singlet resonances of the methyl groups. The others are the diastereomers of γ-chlorovaline (**27**) which are produced in a 50:50 mixture.

The α-proton doublet resonances and the doublet resonances due to the non-chlorinated methyl group of each diastereomer can be used to identify these compounds. The methylenes bearing the chlorines give rise to complex splitting patterns. It is possible that some non-specific reactions analogous to those discussed for glycine (**12**) and alanine (**13**) are also occurring, but the magnitudes of such pathways are small compared to the chlorination reactions given the corrected yields of the products (**26**) and (**27**).

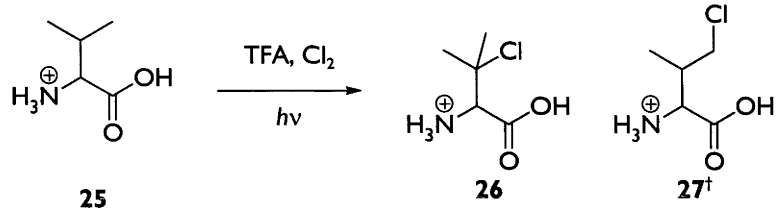

25 **26** **27**†

†Both diastereomers produced

Compound	¹H NMR Resonances (δ ppm)				
	αH	βH	γH	δH	εH
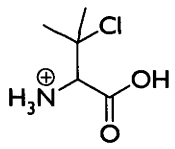 **26**	4.23 s	N/A	1.83 s 1.78 s		
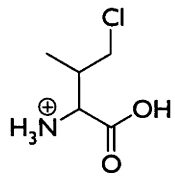 **27**	4.22 d 4 Hz† 4.21 d 4 Hz†	2.62 m† 2.40 m†	1.14 d 7 Hz† 1.13 d 7 Hz† 3.65 m		

Figure 2.4: Reaction of valine (**25**) and NMR data of the products (**26**) and (**27**)

The reaction of valine (**25**) is a good example to describe how the identification of products was verified using TOCSY NMR experiments. In Figure 2.5, a TOCSY spectrum of the products of the chlorination of valine (**25**), it can be seen how isolated spin systems (as indicated by the red and blue circles) can be correlated to resonances which can then be identified in the 1D ^{1}H NMR spectrum. This example (Figure 2.5) identifies the resonances due to the diastereomers of γ-chlorovaline (**27**). A TOCSY

experiment transfers spin from a given proton to a series of neighbouring bonded protons (up to 5 or 6 bonds away). This results in a series of crosspeaks (aligned vertically and horizontally) corresponding to the protons in each amino acid. To prove the validity of the method, a 2D HMQC spectrum was obtained which correlates the hydrogens identified above with their corresponding carbon resonances. The ^{1}H shifts identified for the products are completely consistent with the ^{13}C shifts (e.g., the methyl resonances of β-chlorovaline (**26**) have ^{1}H shifts of δ 1.83 ppm and δ 1.78 ppm which correlate to ^{13}C shifts of δ 30.5 ppm and δ 27.2 ppm, respectively).

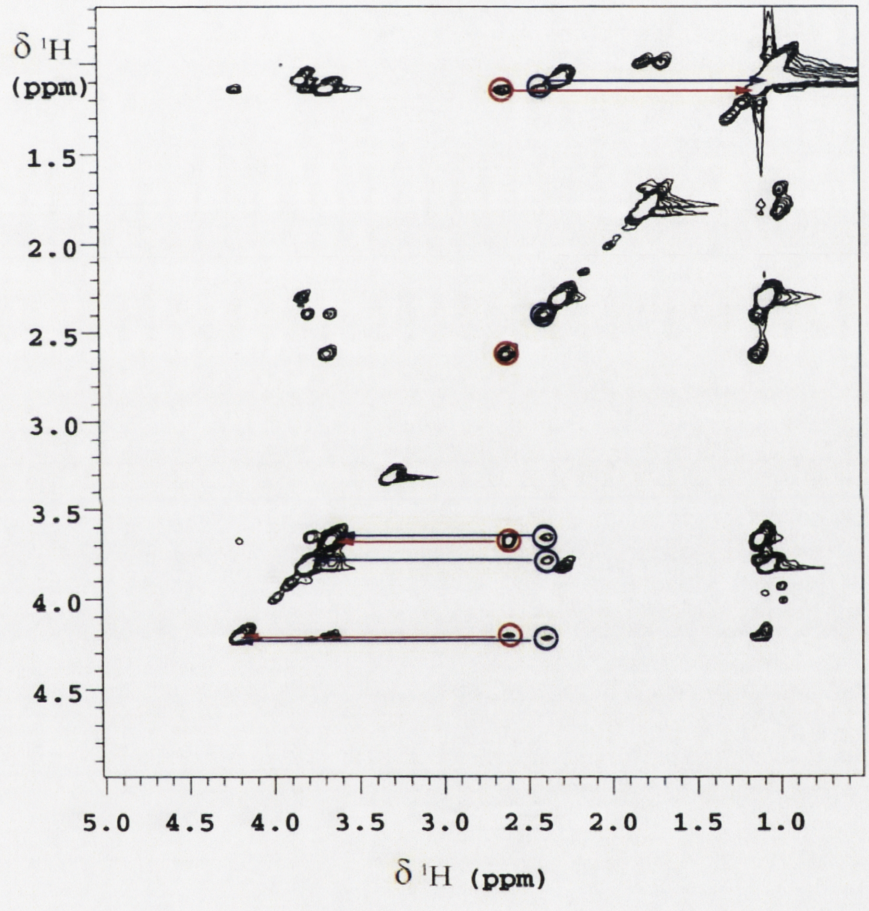

Figure 2.5: TOCSY NMR spectrum of the products from reaction of valine (**25**)

The identification of products from the chlorination of isoleucine (**31**) (Figure 2.7) is complicated not only because of the number of possible products, some of which are diastereomers, but also because the resonances of the methyl groups in many of the products are coincident in the ^{1}H NMR spectrum. However, using TOCSY experiments each group of resonances can be identified. Analysing the TOCSY spectrum (Figure 2.6) shows 6 separate products, including two sets of diastereomers,

two of which have only four cross peaks (compared to five for each of the others), which suggests they are the diastereomers of β-chloroisoleucine (**42**). The diastereomers of the γ-chloroisoleucine (**44**), the γ-chloroisoleucine (**43**) and δ-chloroisoleucine (**45**) can be identified by the α-proton resonances at ~δ4.0-4.5 ppm. The mixtures of diastereomers (**42**) and (**44**) occur in equal amounts, and the products (**42-45**) account for greater than 95% of the reacted starting material. Below is the TOCSY spectrum of the products of reaction of isoleucine (**31**) (Figure 2.6). As an example of the identification process, the resonances which have been assigned to δ-chloroisoleucine (**45**) are indicated in red.

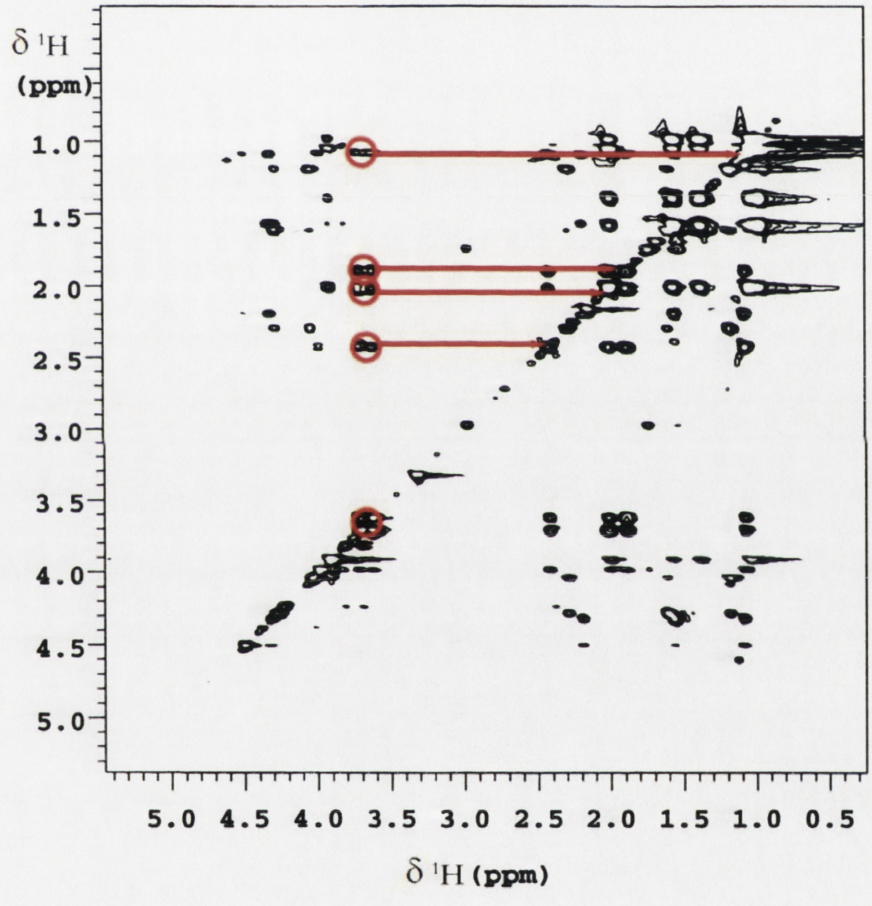

Figure 2.6: TOCSY NMR spectrum of the products from reaction of isoleucine (**31**)

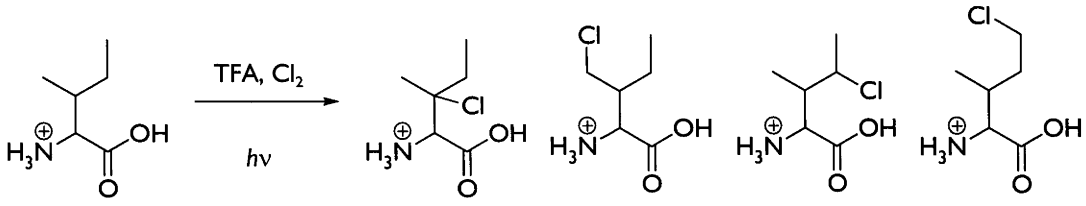

31 **42**† **43** **44**† **45**

†Both diastereomers produced

Compound	¹H NMR Resonances (δ ppm)				
	αH	βH	γH	δH	εH
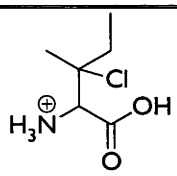 **42**	4.49 s† 4.50 s†	N/A	1.68 s† 1.74 s† 2.20 m	1.15*	
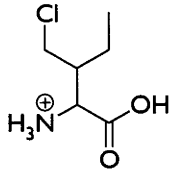 **43**	4.27 d 5.5 Hz	2.40 m	1.70 m* 3.80 m*	1.10*	
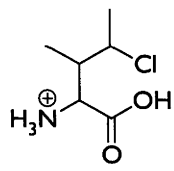 **44**	3.98 d 3 Hz† 4.03 d 6 Hz†	2.28 m	1.09 d 7 Hz† 1.18 d 7 Hz† 4.29 m*	1.56 d 6 Hz† 1.60 d 6 Hz†	
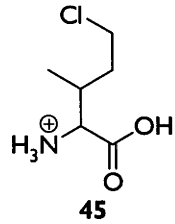 **45**	3.90*	2.41 m	1.07 d 7 Hz 1.88 m* 2.00 m*	3.68 m	

*Discrete resonance not detected in 1D ¹H NMR spectrum

Figure 2.7: Reaction of isoleucine (**31**) and NMR data of the products (**42-45**)

The chlorination of proline (**29**) results in a number of products (Figure 2.8), and the resulting ¹H NMR spectrum is complicated because the constrained ring causes discrete resonances for the diastereotopic protons, and both diastereomers are produced at each of the β- and γ-positions. Nonetheless, TOCSY experiments were used to deconvolute the ¹H NMR spectrum. The only resonances that occur in the

region between δ4-5 ppm are those due to α-protons and protons geminal to a chlorine. These can be used to identify the resonances belonging to each compound present. To determine the identity of each compound, the shift of each of these resonances can be compared to what is expected. In this manner, β-chloroproline (**46**) and γ-chloroproline (**47**) were identified. Below (Figure 2.9) is the TOCSY spectrum of the mixture of products from reaction of proline (**29**) with the spin systems assigned to one diastereomer of β-chloroproline (**46**) highlighted. The occurrence of resonances in pairs is indicative that mixtures of the diastereomers (**46**) and (**47**) were produced in equal amounts. The products (**46**) and (**47**) account for greater than 95% of the starting material consumed.

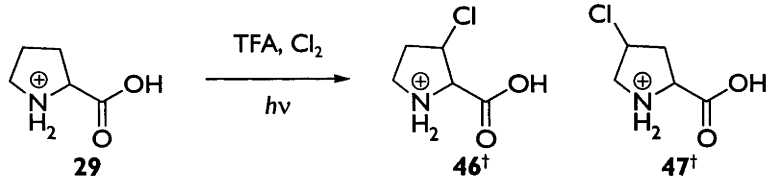

29 → **46**† + **47**†

†Both diastereomers produced

Compound	¹H NMR Resonances (δ ppm) αH	βH	γH	δH	εH
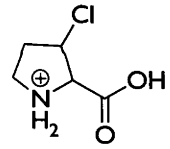 **46**	4.66 br†	4.98 m†	2.68 m†*	3.69 m†	
	4.80†*	5.02 m†	2.96 m†	3.78 m†	
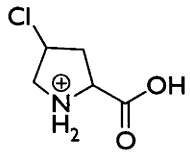 **47**	4.61 dd 4 Hz 10 Hz†	2.64 m†*	4.80 m†*	3.67 m†	
	4.74 dd 7 Hz 10 Hz†	2.75 m†*	4.89 m†	3.82 m†	

*Discrete resonance not detected in 1D ¹H NMR spectrum

Figure 2.8: Reaction of proline (**29**) and NMR data of the products (**46**) and (**47**)

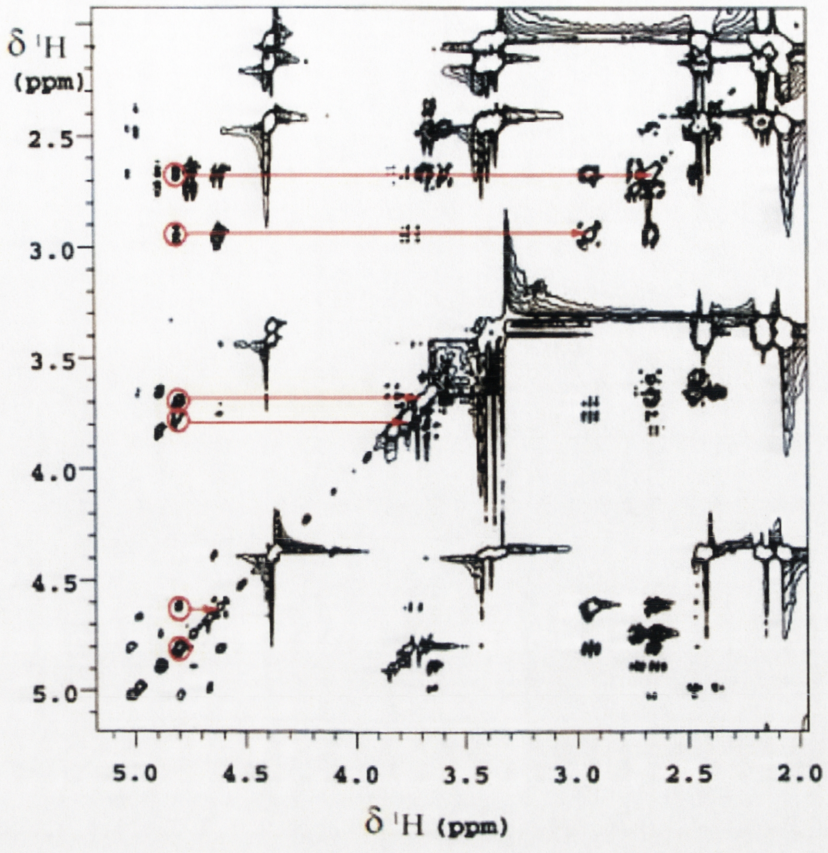

Figure 2.9: TOCSY NMR spectrum of the products from reaction of proline (**29**)

The products from reaction of leucine (**30**) (Figure 2.10) are distinct in the ^{1}H NMR spectrum. The methyl groups of γ-chloroleucine (**48**) appear as singlets at δ 1.6 and δ 1.7 ppm and those resonances of the methyl groups of both diastereomers of δ-chloroleucine (**49**) are only slightly shifted downfield from those of leucine (**30**). The diastereomers of δ-chloroleucine (**49**) occur in equal amounts. The above resonances were used to identify other proton resonances in each compound using correlations in the TOCSY NMR spectrum as has been described above. The products (**48**) and (**49**) account for greater than 95% of the starting material consumed.

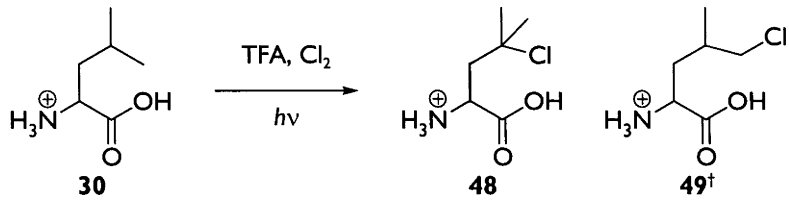

†Both diastereomers produced

Compound	^{1}H NMR Resonances (δ ppm) αH	βH	γH	δH	εH
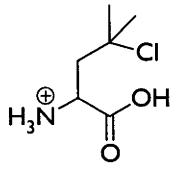 **48**	4.20 dd 5 Hz 6 Hz	2.57 dd 5 Hz 15 Hz 2.32 dd 6 Hz 15 Hz	N/A	1.60 s† 1.75 s†	
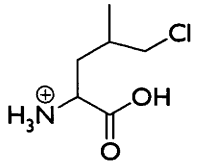 **49**	4.00 t 7 Hz	2.03 m	2.17 m	1.11 d 6.5 Hz† 1.12 d 6 Hz† 3.58 m	

Figure 2.10: Reaction of leucine (**30**) and NMR data of the products (**48**) and (**49**)

There are six products from the reaction of lysine (**21**) (Figure 2.11). This results in a complicated ^{1}H NMR spectrum as many of the resonances for various methylene groups appear as coincident multiplets. However, both the α-proton and ε-proton resonances are fairly distinct, and the further the chlorine is from these protons the further upfield the resonance occurs. With this in mind, the TOCSY spectrum of the mixture of diastereomers of β-chlorolysine (**50**), γ-chlorolysine (**22**) and δ-chlorolysine (**51**) is fairly easily deconvoluted. Each pair of diastereomers occurs as an equal mixture. The products (**22**), (**50**) and (**51**) account for greater than 95% of the starting material consumed.

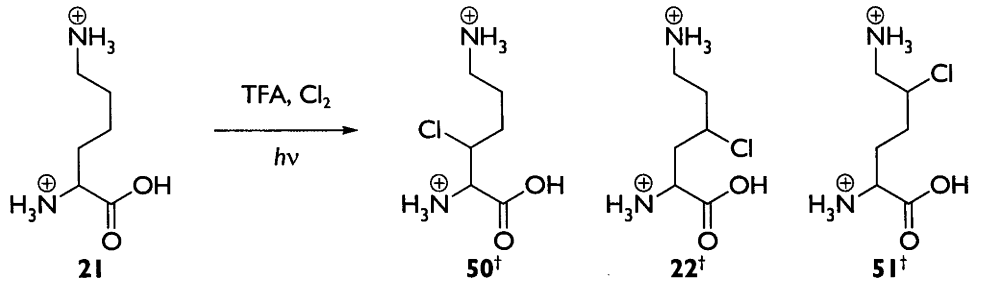

21 **50**† **22**† **51**†

†Both diastereomers produced

Compound	¹H NMR Resonances (δ ppm)				
	αH	βH	γH	δH	εH
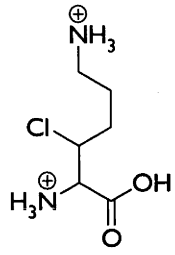 **50**	4.42 m	4.20 m*	2.46 m	2.30 m	~ 2.95 m*
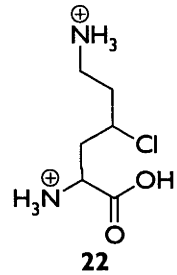 **22**	4.25 m*	2.48 m	3.23 m*	2.20 m*	3.14 m*
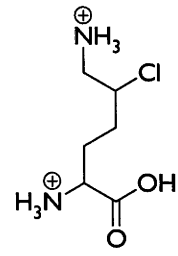 **51**	4.03 t 6 Hz	2.20 m*	2.10 m*	3.42 m	3.23 m*

*Discrete resonance not detected in 1D ¹H NMR spectrum

Figure 2.11: Reaction of lysine (**21**) and NMR data of the products (**22**), (**50**) and (**51**)

The identification of the products from the reaction of phenylalanine (**28**) (Figure 2.12) is quite simple. The resonances of the α- and β-protons of β-chlorophenylalanine (**52**) are distinct, however this is one of the few cases where the formation of diastereomers does not occur in equal amounts (in this case a 9:1 mixture is produced).

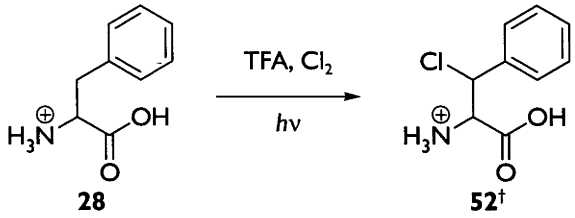

28 **52**†

†Both diastereomers produced

Compound	^{1}H NMR Resonances (δ ppm)				
	αH	βH	γH	δH	εH
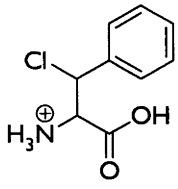	4.50 d 4 Hz† minor	5.58 d 4 Hz† minor			
	4.45 d 6 Hz† major	5.63 d 6 Hz† major			

52

Figure 2.12: Reaction of phenylalanine (**28**) and NMR data of the products (**52**)

Ornithine (**23**) is structurally similar to lysine (**21**), however the shorter side chain means that, when it reacts (Figure 2.13), the ^{1}H NMR spectrum of the product mixture was noticeably less complicated. In a similar manner to that used with lysine (**21**), the shifts of the α- and δ-protons and those geminal to chlorine can by used to unambiguously assign the resonances due to both β-chloroornithine (**53**) and γ-chloroornithine (**24**). Both (**24**) and (**53**) are produced as equal mixtures of diastereomers. The products (**24**) and (**53**) account for greater than 95% of the starting material consumed.

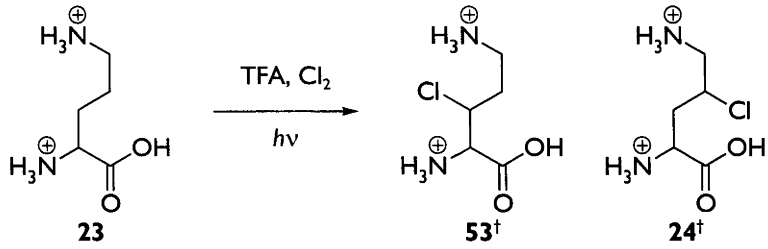

23 **53**† **24**†

†Both diastereomers produced

Compound	¹H NMR Resonances (δ ppm) αH	βH	γH	δH	εH
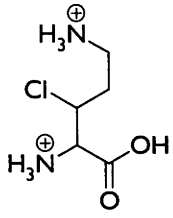 **53**	4.50 d 6.4 Hz†	4.25 m*	2.16 m	3.30 m*	
	4.51 d 6.5 Hz†				
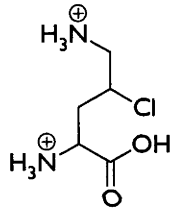 **24**	4.25 dd 4 Hz 6.5 Hz†	2.36 m†	3.21 m*	3.50 d 3.5 Hz†	
	4.22 dd 3.5 Hz 7 Hz†	2.51 m†		3.46 d 3.5 Hz†	

*Discrete resonance not detected in 1D ¹H NMR spectrum

Figure 2.13: Reaction of ornithine (**23**) and NMR data of the products (**24**) and (**53**)

α-Aminobutyric acid (**15**) forms both the diastereomeric α-amino-β-chlorobutyric acid (**16**) and α-amino-γ-chlorobutyric acid (**17**) when chlorinated (Figure 2.14). The ¹H NMR spectrum of this mixture, like those of most of the smaller amino acids, is relatively simple. As was the case with phenylalanine (**28**), the diastereomers of the β-chlorinated product (**16**) are not produced in equal amounts (in this case, a 40:60 ratio is formed).

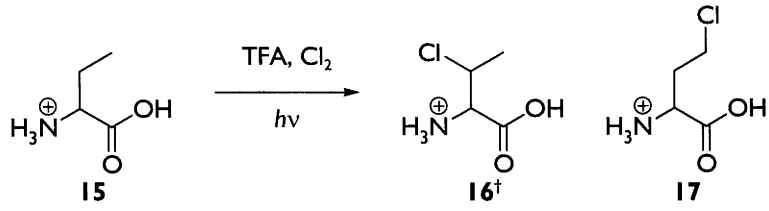

†Both diastereomers produced

Compound	^{1}H NMR Resonances (δ ppm)				
	αH	βH	γH	δH	εH
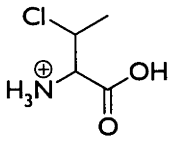 **16**	4.19 d, 3 Hz† major 4.23 d, 2 Hz† minor	4.04 m	1.42 d, 7 Hz		
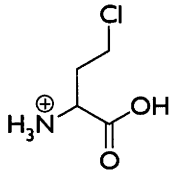 **17**	4.12 t, 6 Hz	2.25 m 2.22 m	3.54 m		

Figure 2.14: Reaction of α-aminobutyric acid (**15**) and NMR data of the products (**16**) and (**17**)

From the reaction of norvaline (**38**) (Figure 2.15), TOCSY analysis only shows three products. The shifts of the methyl resonances clearly identify the diastereomers of γ-chloronorvaline (**54**) which occur in an equal mixture of the two. The other product is δ-chloronorvaline (**55**). No β-chlorinated compound was observed. The products (**54**) and (**55**) account for greater than 95% of the starting material consumed.

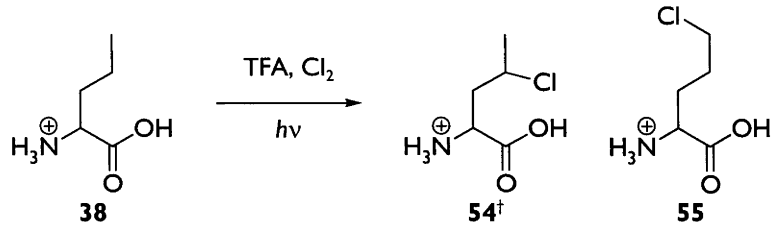

†Both diastereomers produced

Compound	¹H NMR Resonances (δ ppm) αH	βH	γH	δH	εH
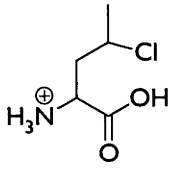 54	4.09 m	2.20 m	4.05 m	1.21 d 6 Hz† 1.23 d 6 Hz†	
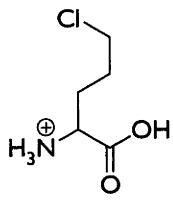 55	3.78 dd 6 Hz 6.5 Hz	1.65 m	1.85 m	3.40 t 6 Hz	

Figure 2.15: Reaction of norvaline (**38**) and NMR data of the products (**54**) and (**55**)

For the reaction of norleucine (**39**) (Figure 2.16), the ^{1}H NMR spectrum of the product mixture is slightly more complicated than that of norvaline (**38**), as there are a greater number of methylene resonances which have similar chemical shifts, and two pairs of diastereomers are produced, so there are a large number of coincident signals. Despite this, the TOCSY spectrum enables the chemical shifts of overlapping resonances to be identified and the ^{1}H resonances of each compound can be assigned. The products, γ-chloronorleucine (**56**), δ-chloronorleucine (**57**) and ε-chloronorleucine (**58**) can in this way be identified using the TOCSY methodology, despite having a rather ambiguous ^{1}H spectrum. The products (**56-58**) account for greater than 85% of the starting material consumed.

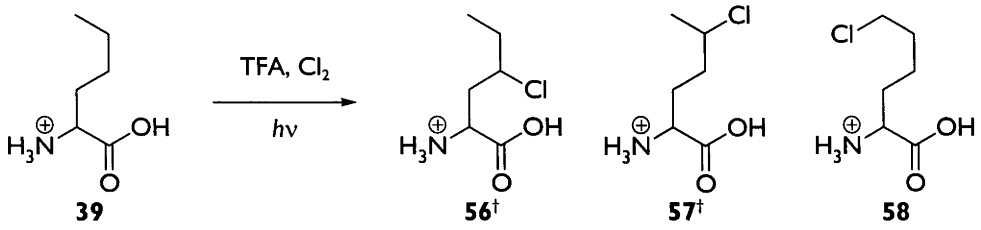

39 **56**† **57**† **58**

†Both diastereomers produced

Compound	¹H NMR Resonances (δ ppm) αH	βH	γH	δH	εH
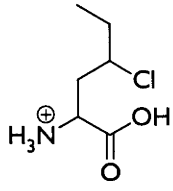 **56**	4.20 m	~ 2.45 m*† ~ 2.25 m*†	3.79 m	~ 1.90 m* ~ 1.75 m*	1.08 t 7 Hz† 1.09 t 7 Hz†
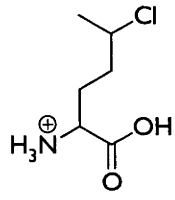 **57**	~ 4.10 m*	~ 2.20 m* ~ 2.00 m*	~ 1.90 m*	~ 4.00 m*	1.52 d 6.5 Hz
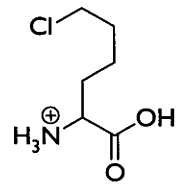 **58**	~ 4.00 m*	~ 1.90 m*	~ 1.80 m*	1.62 m	3.59 t 6 Hz

*Discrete resonance not detected in 1D ¹H NMR spectrum

Figure 2.16: Reaction of norleucine (**39**) and NMR data of the products (**56-58**)

Only one product forms from the chlorination of *tert*-leucine (**40**) (Figure 2.17). However, each methyl group of the product, γ-chloro-*tert*-leucine (**59**), has a separate resonance, presumably due to hindered rotation of the *tert*-butyl group.

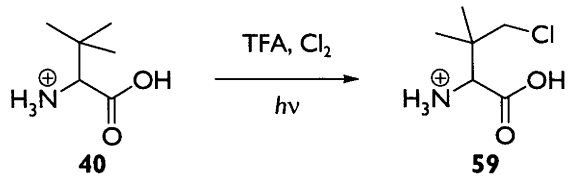

40 59

Compound	^{1}H NMR Resonances (δ ppm)				
	αH	βH	γH	δH	εH
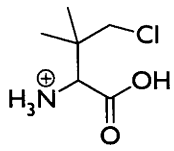	4.19 s	N/A	1.23 s 1.29 s 3.57 s		

59

Figure 2.17: Reaction of *tert*-leucine (**40**) and NMR data of the product (**59**)

Homophenylalanine (**41**), like phenylalanine (**28**), only shows the two diastereomeric benzylic products (γ-chlorohomophenylalanine (**60**) (Figure 2.18)). The diastereomers are formed in equal amounts. The products (**60**) account for at least 95% of the starting material consumed.

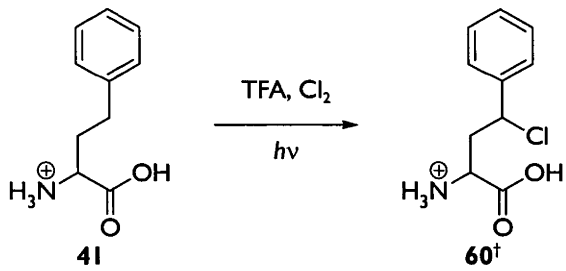

41 60†

†Both diastereomers produced

Compound	^{1}H NMR Resonances (δ ppm)				
	αH	βH	γH	δH	εH
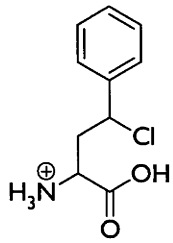	4.12 dd 6.5 Hz 7 Hz†	2.57 m† 2.49 ddd 5 Hz 8 Hz 15 Hz	5.19 dd 5.5 Hz 10 Hz†		
	4.03 dd 5 Hz 8 Hz†	2.82 m†	5.30 dd 6 Hz 8 Hz†		

41

Figure 2.18: Reaction of homophenylalanine (**41**) and NMR data of the product (**60**)

2.2 Formation of Diastereomers

A number of the amino acids (**12**), (**13**), (**15**), (**18**), (**21**), (**23**), (**25**), (**28-31**) and (**37-41**) reacted to give diastereomers. When a hydrogen atom is abstracted from an sp^3 hybridised carbon, the newly formed radical centre is essentially planar, and the reaction with chlorine can occur on either face of the radical (Figure 2.19). Consequently diastereomers of the chlorinated compounds can often form.

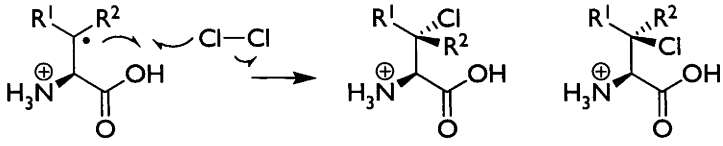

Figure 2.19: Reaction of a β-centred amino acid radical with chlorine

In general the proportions of each of the diastereomers are approximately equal. However, in the case of phenylalanine (**28**), the diastereoselectivity is quite significant.

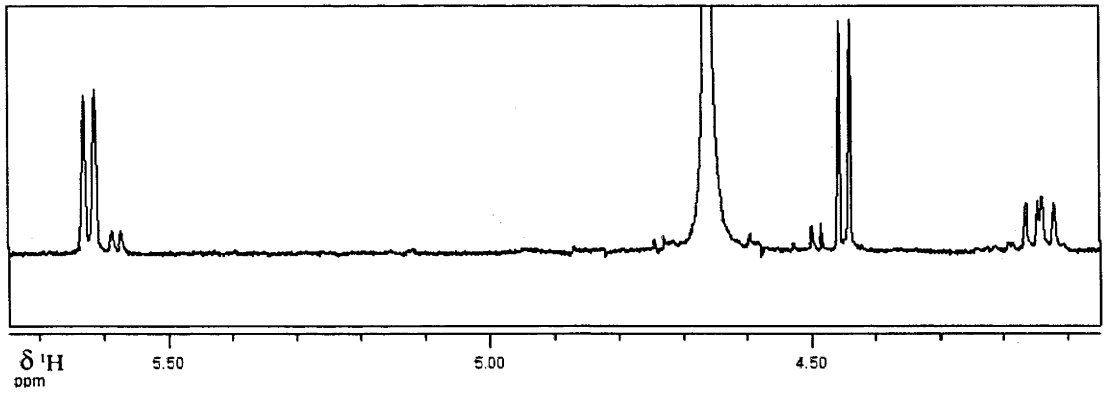

Figure 2.20: Partial ^{1}H NMR spectrum of the products of chlorination of phenylalanine (**28**)

Figure 2.20 shows a portion of the ^{1}H NMR spectrum of the products of radical chlorination of phenylalanine (**28**), between δ 4.0 and δ 5.8 ppm. The peaks at ~δ 4.1 ppm are the resonances due to the α-proton of phenylalanine (**28**). The two sets of peaks at ~δ 4.5 and ~δ 5.6 ppm are those of the α- and β-protons of β-chlorophenylalanine (**52**), respectively. The integrals of these peaks (approximately 9:1) indicate that there is a distinct diastereoselectivity (80% *d.e.*).

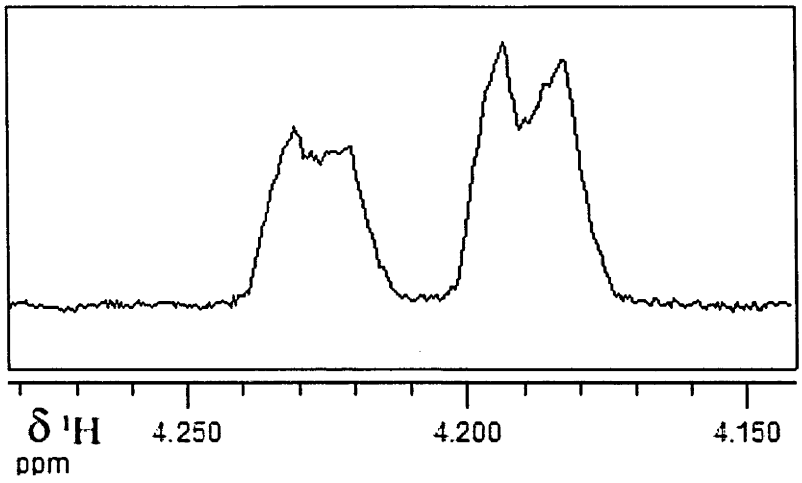

Figure 2.21: Partial ^{1}H NMR spectrum showing the α-proton resonances of α-amino-β-chlorobutyric acid (**16**)

α-Aminobutyric acid (**15**) is another amino acid which showed a degree of diastereoselectivity. In the above diagram (Figure 2.21), the α-proton resonances due to the diastereomers of α-amino-β-chlorobutyric acid (**16**) are shown. Integration of the resonances show the diastereomers were formed in a 40:60 ratio (20% *d.e.*).

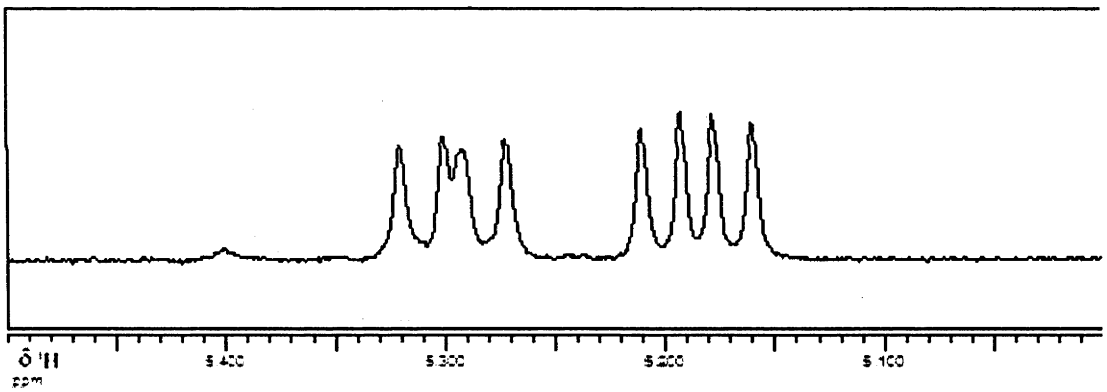

Figure 2.22: Partial ^{1}H NMR spectrum showing the γ-proton resonances of γ-chlorohomophenylalanine (**41**)

The above portion of the ^{1}H NMR spectrum of the products of reaction of homophenylalanine (**41**) (Figure 2.22) shows the γ-proton resonances of γ-chloro-homophenylalanine (**60**). The integrals of these peaks show a difference of less than 2%, which is small enough to be considered within the margin of error for the measurement. When the results of the reaction of phenylalanine (**28**) and homophenylalanine (**41**) are compared, it can be seen that the facial selectivity due to the chiral α-centre does not extend to the γ-position. Despite some degree of

diastereoselectivity that is shown in a minor number of the reactions of the amino acids (**12**), (**13**), (**15**), (**18**), (**21**), (**23**), (**25**), (**28-31**) and (**37-41**), no information can be obtained on the stereoselectivity of the hydrogen abstraction step from the presence (or lack thereof) of diastereoselectivity in the products formed, as the reactions proceed through achiral intermediates. As a result, in the following analysis all diastereotopic hydrogens are assumed to have equal reactivity.

2.3 Product Distribution

Once the identities of the products formed from the chlorination of the amino acids (**12**), (**13**), (**15**), (**18**), (**21**), (**23**), (**25**), (**28-31**) and (**37-41**) were known, the proportion of each product was relatively easily calculated by integrating resonances in the ^{1}H NMR spectra of the product mixtures. The product distribution illustrates the reactivity of each position within an amino acid. Glycine (**12**), alanine (**13**), aspartic acid (**37**) and glutamic acid (**18**) do not show chlorinated products and so were excluded from this analysis. For the remaining amino acids (**15**), (**21**), (**23**), (**25**), (**28-31**) and (**38-41**), no α-chlorinated products were observed and the corrected product yields are in general over 95% so it can be assumed that very little if any α-hydrogen abstraction is occurring. The percentages of each product formed are consistent over repeated experiments. The percentage of each product observed is tabulated below (Figure 2.24). A value of zero (0) indicates that no product was observed. The percentage of reacted starting material observed as products, and the accuracy of the integration of the NMR spectra mean that the accuracy of the figures obtained is likely to be ±5%.

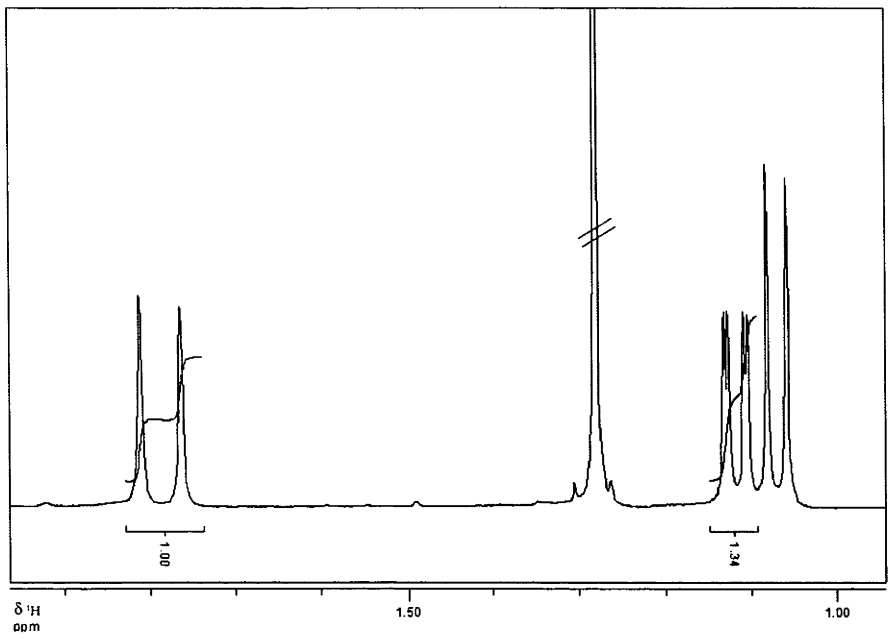

Figure 2.23: Partial ^{1}H NMR spectrum of the products of chlorination of valine (**25**)

As an example of this analysis, shown above (Figure 2.23) is the methyl region of the ^{1}H NMR spectrum of the products from the chlorination of valine (**25**). The two singlets at ~δ 1.8 ppm are the methyl resonances of β-chlorovaline (**26**), while the two doublets at ~δ 1.1 ppm are those of the unchlorinated methyl resonances of the diastereomers of γ-chlorovaline (**27**). The doublet to the right of those is due to unreacted valine (**25**). From the above spectrum the reactivity of each position can be determined.

$$\% \text{ of } \beta\text{-chlorovaline (26) formed} = \frac{1.00/6}{(1.00/6)+(1.34/3)} \times 100 = 27\%$$

$$\% \text{ of } \gamma\text{-chlorovaline (27) formed} = \frac{1.34/3}{(1.00/6)+(1.34/3)} \times 100 = 73\%$$

Starting Amino Acid	Percent reaction at each position			
	β	γ	δ	ε
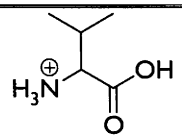 **25**	27	73		
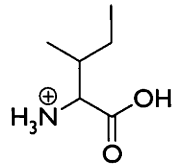 **31**	16	38 (CH_2) 6 (CH_3)	40	
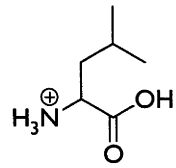 **30**	0	29	71	
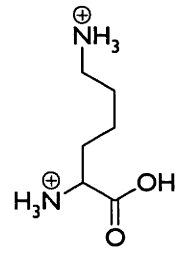 **21**	29	50	21	0
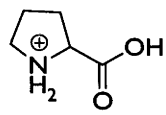 **29**	32	68	0	
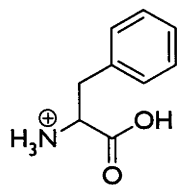 **28**	100			
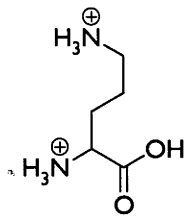 **23**	47	53	0	

Figure 2.24: Percentage reaction at each position for the amino acids **(15)**, **(21)**, **(23)**, **(25)**, **(28-31)** and **(38-41)**

Starting Amino Acid	Percent reaction at each position			
	β	γ	δ	ε
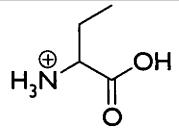 **15**	25	75		
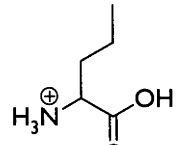 **38**	0	40	60	
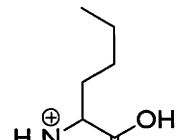 **39**	0	17	43	40
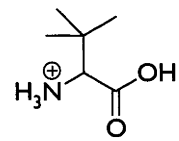 **40**	-	100		
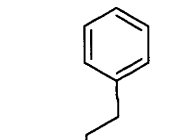 **41**	0	100		

Figure 2.24 *cont.*: Percentage reaction at each position for the amino acids (**15**), (**21**), (**23**), (**25**), (**28-31**) and (**38-41**)

From the results tabulated above (Figure 2.24) it can be seen that there is a tendency for reaction at positions further along the side chains (see, for example α-aminobutyric acid (**15**), norvaline (**38**) and norleucine (**39**)). The major exception to this is for the amino acids with amino functionality at both ends of the side chain (*i.e.*, lysine (**21**), ornithine (**23**) and proline (**29**)), where reaction occurs at more central positions.

To quantify these effects, the reactivity of each of the amino acids (**12**), (**13**), (**15**), (**18**), (**21**), (**23**), (**25**), (**28-31**) and (**37-41**) was compared, both at the molecular level, as well as the reactivity of each hydrogen towards abstraction.

2.4 Relative Rates of Reaction

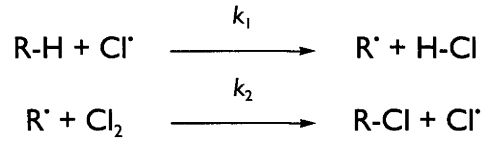

Figure 2.25: Chain propagation steps of radical chlorination

The two steps above (Figure 2.25) are the chain propagation steps for the chlorination reaction. As the overall rate of reaction is dependent on factors such as chlorine concentration, radical concentration, light intensity and the rates of radical chain termination reactions, the absolute rates of chlorination are extremely difficult to determine. However, competitive experiments can be performed where two hydrogen atom abstraction reactions are compared (Figure 2.26), which allows determination of the relative rate at which each hydrogen atom abstraction is occurring.

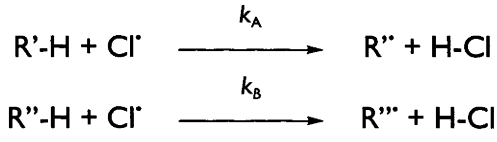

Figure 2.26: Competitive hydrogen atom abstraction reactions

Thus, the ratio of the rates of hydrogen abstraction (or the relative rates of reaction) can be determined. The hydrogen abstraction step is rate limiting, therefore the formation of chlorinated products is directly related to the formation of the corresponding alkyl radicals, and so the formation of radicals from hydrogen atom abstraction can be measured by determination of the amount of each chlorinated product formed.

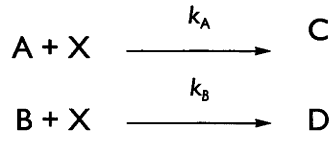

Figure 2.27: Generic competitive reactions

For a general competitive reaction (Figure 2.27), the relative rates of reaction, or k_{rel}, can be determined by comparing the concentrations of A and B over the period of reaction (*i.e.*, from $t = 0$ to $t = x$). This is done using the formula below (Figure 2.28).[132]

$$k_{rel} = \frac{\ln\left(\frac{[A]_X}{[A]_0}\right)}{\ln\left(\frac{[B]_X}{[B]_0}\right)}$$

Figure 2.28: Determination of k_{rel} for a generic competitive reaction

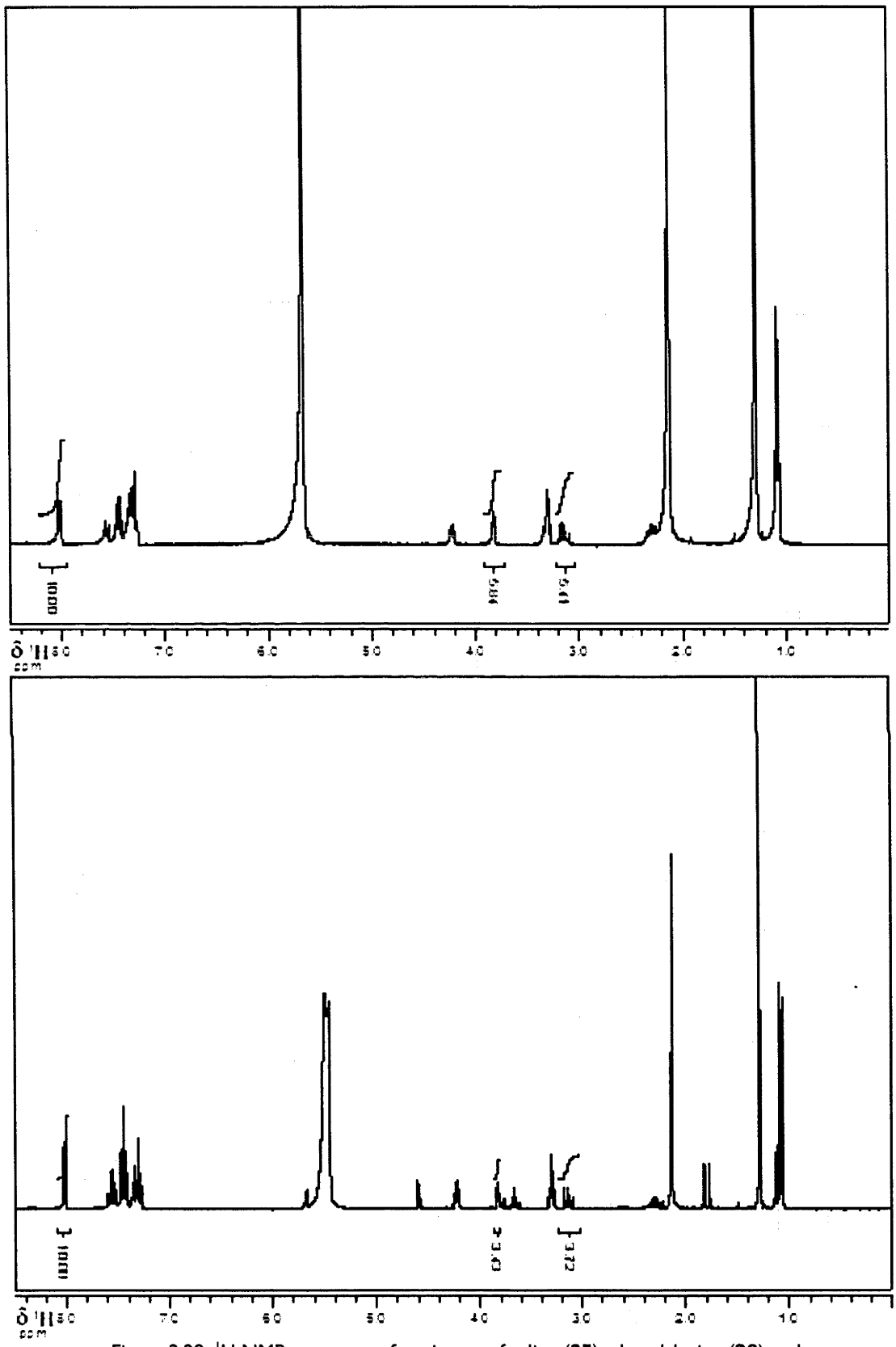

Figure 2.29: ^{1}H NMR spectrum of a mixture of valine (**25**), phenylalanine (**28**) and benzoic acid, before (top) and after (above) reaction with chlorine.

For a representative example of the determination of k_{rel}, in Figure 2.29 are ^{1}H NMR spectra used to determine k_{rel} values of valine (**25**) and phenylalanine (**28**). The resonances at ~δ 8 ppm are of those from benzoic acid (specifically the *ortho*-protons), and these can be used as the reference for which the integral is set to 10.00. Now, because the spectra are referenced against benzoic acid, the integrals of the other compounds are proportional to their concentrations. The integrals for valine (**25**) (the α-proton resonance at ~δ 3.9 ppm) and phenylalanine (**28**) (a benzylic proton resonance at ~δ 3.1 ppm) can then be used in the formula below (Figure 2.30) to obtain the k_{rel} of valine (**25**) compared to phenylalanine (**28**).

$$k_{rel} = \frac{\ln\left(\frac{Val_X}{Val_0}\right)}{\ln\left(\frac{Phe_X}{Phe_0}\right)} = \frac{\ln\left(\frac{3.43}{5.84}\right)}{\ln\left(\frac{3.72}{5.41}\right)} = \frac{-0.53}{-0.37} \approx 1.4$$

Figure 2.30: Determination of k_{rel} for the reaction of valine (**25**) and phenylalanine (**28**)

Because of the high total yields of identified products, a similar process can be used which analyses the amounts of products formed (rather than starting materials consumed). The results obtained in this way are very similar to those derived from consumption of starting materials.

The same process as above can be followed to determine the k_{rel} of norvaline (**38**) relative to phenylalanine (**28**) (Figures 2.31, 2.32). As with the example above, benzoic acid is used as the reference. The integrals for norvaline (**38**) (the δ-proton resonance at ~δ 1.0 ppm) and phenylalanine (**28**) (a benzylic proton resonance at ~δ 3.1 ppm) can be used in the same manner as before.

$$k_{rel} = \frac{\ln\left(\frac{Nva_X}{Nva_0}\right)}{\ln\left(\frac{Phe_X}{Phe_0}\right)} = \frac{\ln\left(\frac{4.33}{6.56}\right)}{\ln\left(\frac{1.86}{2.21}\right)} = \frac{-0.41}{-0.17} \approx 2.4$$

Figure 2.31: Determination of k_{rel} for the reaction of norvaline (**38**) and phenylalanine (**28**)

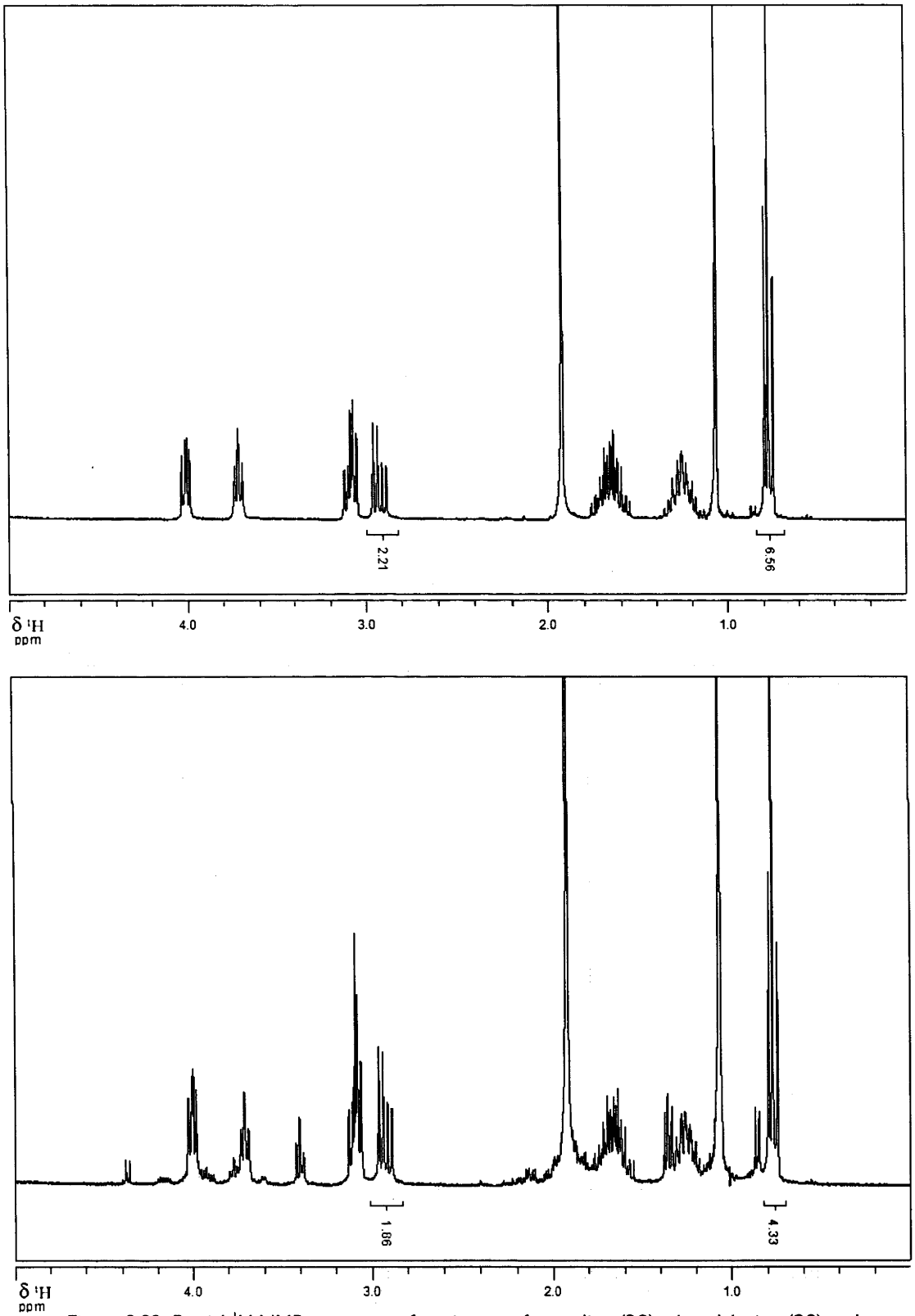

Figure 2.32: Partial ^{1}H NMR spectrum of a mixture of norvaline (**38**), phenylalanine (**28**) and benzoic acid, before (top) and after (above) reaction with chlorine

The k_{rel} values for the range of amino acids (**12**), (**13**), (**15**), (**18**), (**21**), (**23**), (**25**), (**28-31**) and (**37-41**) were thus determined in the manner described above and are shown

in Figure 2.33. The reactivity of all the amino acids (**12**), (**13**), (**15**), (**18**), (**21**), (**23**), (**25**), (**29-31**) and (**37-41**) was compared against phenylalanine (**28**), and so the k_{rel} for the reaction of phenylalanine (**28**) has been arbitrarily set to 1.0. To ensure accuracy, amino acids that showed particularly high reactivity were also compared against homophenylalanine (**41**), and those that showed particularly low reactivity were compared against α-aminobutyric acid (**15**). Repeat experiments demonstrated the consistency of the results obtained (at least within ±10%).

Amino Acid	k_{rel}	Amino Acid	k_{rel}
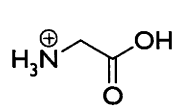 **12**	0.1	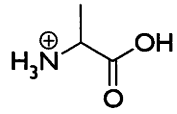 **13**	0.1
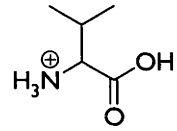 **25**	1.4	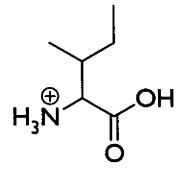 **31**	4.4
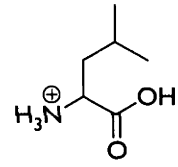 **30**	18	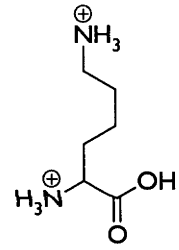 **21**	5.2
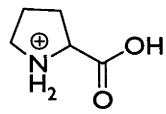 **29**	0.24	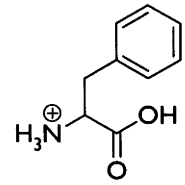 **28**	1.0
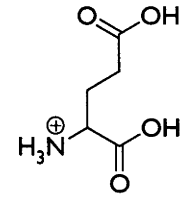 **18**	≤ 0.02	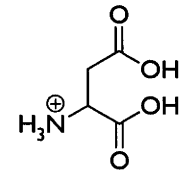 **37**	≤ 0.01
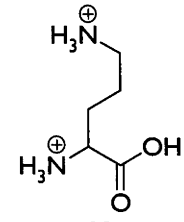 **23**	2.8	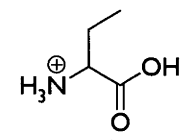 **15**	0.4

Figure 2.33: Relative rates of reaction for the amino acids (**12**), (**13**), (**15**), (**18**), (**21**), (**23**), (**25**), (**28-31**) and (**37-41**)

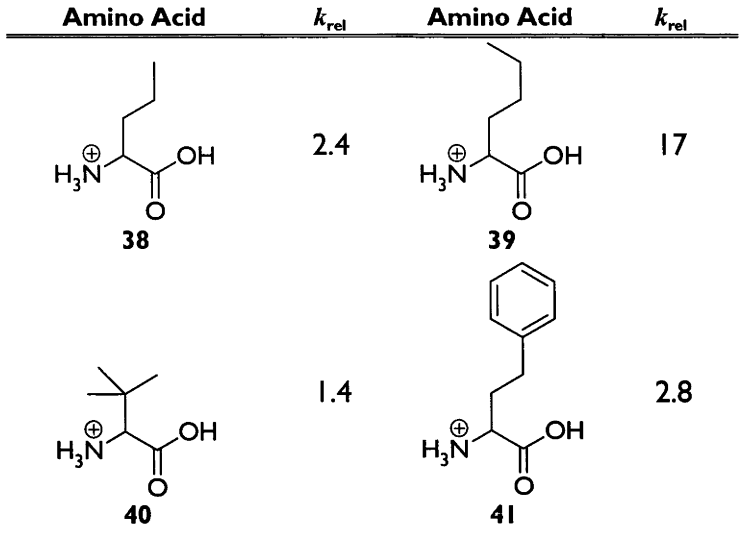

Figure 2.33 *cont.*: Relative rates of reaction for the amino acids (**12**), (**13**), (**15**), (**18**), (**21**), (**23**), (**25**), (**28-31**) and (**37-41**)

The relative rates of reaction (Figure 2.33) show a large range of reactivity between amino acids (at least three orders of magnitude). The fastest reacting amino acids, leucine (**30**) and norleucine (**39**), are those with the longest side chains. The side-chain functionalised amino acids (**18**), (**21**), (**23**) and (**37**) tend to have slower reaction rates.

2.5 Reactivity per Hydrogen

While the relative reaction rates are informative, they do not allow an explanation of the magnitude of the reactivity, or the factors which control it. Calculating a per hydrogen reactivity (k_{rel}^{H}) provides both an internal and external correlation between hydrogens, or a relative rate of abstraction for each type of hydrogen to provide the information desired.

Within the limits of detection, hydrogen atom abstraction from phenylalanine (**28**) occurs at the β-position and given the k_{rel} of phenylalanine is 1.0, and that there are two β-hydrogens, the relative reactivity per hydrogen is then:

Reactivity (k_{rel}^{H}) of the β-hydrogens of phenylalanine (**28**) = 1.0 / 2 = 0.50

The k_{rel} of valine (**25**) has been determined to be 1.4, and the percentage of each product formed is known. The reactivity at each position is thus:

Reactivity of valine (**25**) at the β-position = 1.4 x 0.27 = 0.38

Reactivity of valine (**25**) at the γ-position = 1.4 x 0.73 = 1.0

As there is only one hydrogen at the β-position:

k_{rel}^{H} of the β-hydrogen of valine (**25**) = 0.38 / 1 = 0.38

and as there are six hydrogens at the γ position:

k_{rel}^{H} of each of the γ-hydrogens of valine (**25**) = 1.0 / 6 = 0.17

In an identical manner to that used for valine (**25**), the reactivity of the various hydrogens of proline (**29**) can be assigned. The k_{rel} of proline is 0.24, and the reactivity at each position is then:

Reactivity of proline (**29**) at the β-position = 0.24 x 0.32 = 0.077

Reactivity of proline (**29**) at the γ-position = 0.24 x 0.68 = 0.16

Then, as there are two hydrogens at each of these positions:

k_{rel}^{H} of each of the β-hydrogens of proline (**29**) = 0.077 / 2 = 0.039

k_{rel}^{H} of each of the γ-hydrogens of proline (**29**) = 0.16 / 2 = 0.080

Determined in an analogous manner, the k_{rel}^{H} values for the compounds studied (**12**), (**13**), (**15**), (**18**), (**21**), (**23**), (**25**), (**28-31**) and (**37-41**) calculated to two significant figures are tabulated below (Figure 2.34). Glycine (**12**), alanine (**13**), aspartic acid (**37**) and glutamic acid (**18**) show very small rates and no products are detected, therefore only the maximum possible k_{rel}^{H} could be determined. For all the other amino acids, (**15**), (**21**), (**23**), (**25**), (**28-31**) and (**38-41**), the values are likely to be accurate, at least within a factor of two. This assessment is based on both the high yields of identified products formed and reliability of the compound reaction rates, as demonstrated by repeat experiments and cross correlations, which were used to determine the k_{rel}^{H} values. The accuracy of the k_{rel}^{H} values is therefore quite high in the context that the values range over approximately three orders of magnitude.

Amino Acid	Reactivity per hydrogen (k_{rel}^{H}) at each position				
	α	β	γ	δ	ε
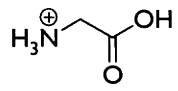 **12**	≤ 0.05				
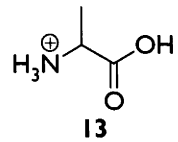 **13**	≤ 0.10	≤ 0.03			
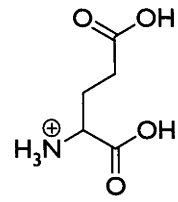 **18**	≤ 0.02	≤ 0.01	≤ 0.01		
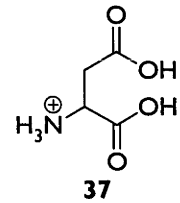 **37**	≤ 0.01	≤0.005			
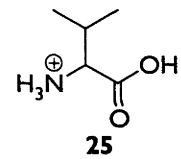 **25**	0	0.38	0.17		
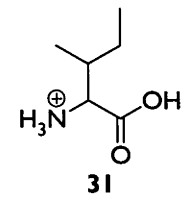 **31**	0	0.70	0.84 (CH_2) 0.09 (CH_3)	0.59	
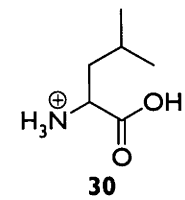 **30**	0	0	5.2	2.1	
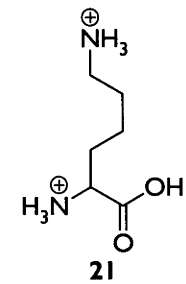 **21**	0	0.75	1.3	0.55	0

Figure 2.34: Reactivity of the various hydrogens k_{rel}^{H} for the amino acids **(12)**, **(13)**, **(15)**, **(18)**, **(21)**, **(23)**, **(25)**, **(28-31)** and **(37-41)**

Amino Acid	Reactivity per hydrogen (k_{rel}^{H}) at each position				
	α	β	γ	δ	ε
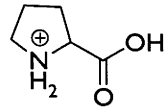 **29**	0	0.039	0.080	0	
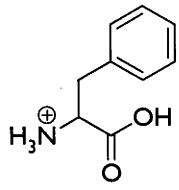 **28**	0	0.50			
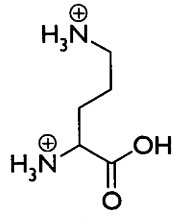 **23**	0	0.66	0.74	0	
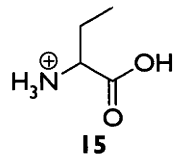 **15**	0	0.05	0.10		
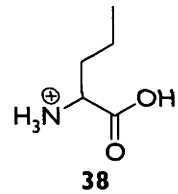 **38**	0	0	0.48	0.48	
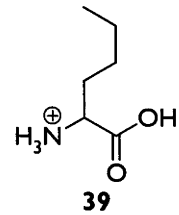 **39**	0	0	1.4	3.7	2.3
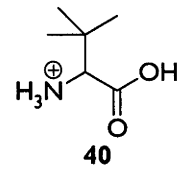 **40**	0	-	0.16		
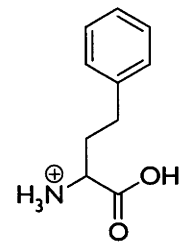 **41**	0	0	1.4		

Figure 2.34 *cont.*: Reactivity of the various hydrogens k_{rel}^{H} for the amino acids **(12)**, **(13)**, **(15)**, **(18)**, **(21)**, **(23)**, **(25)**, **(28-31)** and **(37-41)**

Above, the apparent higher reactivity at positions further along amino acid side chains was noted. The combined reactivity at the β- and γ-positions of norvaline (**38**) was 40% of the total reactivity, but the combined reactivity of the β- and γ-positions of norleucine (**39**) was only 17% of the total reactivity with the remainder occurring further out on the side-chain (Figure 2.24). The higher reactivity of positions further along the side-chains is now also demonstrated by the k_{rel}^{H} values. Again, with the examples of norvaline (**38**) and norleucine (**39**) (Figure 2.34), the reactivity (k_{rel}^{H}) of the hydrogens on the terminal methyl of each of these amino acids, at the δ- and ε-positions is 0.48 and 2.3, respectively.

2.6 Average Per Hydrogen Reactivity

It can be seen that the NH_3^+ and COOH groups of the amino acids (**12**), (**13**), (**15**), (**18**), (**21**), (**23**), (**25**), (**28-31**) and (**37-41**) deactivate adjacent positions. In Figure 2.34 the protonated amino groups on the side-chains of lysine (**21**) and ornithine (**23**) and in the ring of proline (**29**) cause deactivation of the hydrogens adjacent to them and no reaction at these positions is detected. The carboxylic acid groups of the side-chains of glutamic acid (**18**) and aspartic acid (**37**) cause deactivation to the point where the k_{rel}^{H} values of the ω-methylenes in these compounds are negligible, at ≤ 0.01 and ≤ 0.005, respectively. The magnitude of this deactivation is obvious when the k_{rel}^{H} values of glutamic acid (**18**) and aspartic acid (**37**) are compared to those of norvaline (**38**) and α-aminobutyric acid (**15**), which have k_{rel}^{H} values for the ω-methylenes of 0.48 and 0.10, respectively. The combined deactivating effect of the α-substituents appears to be greater than that of either single substituent as there is a tendency for reaction to be faster further along the side-chain away from the α-centre. For example ornithine (**23**) in Figure 2.34 shows slightly greater reactivity (k_{rel}^{H}) at the γ-position (0.74) compared to the β-position (0.66).

The amino acids (**12**), (**13**), (**15**), (**25**), (**28**), (**30**), (**31**) and (**38-41**) that contain alkyl and benzylic side-chains only have deactivating groups at the α-position. They form a large set of compounds with similar structures, therefore information about the reactivity of the hydrogens at each position on the side-chains can be obtained by comparison of their k_{rel}^{H} values.

Position	Reactivity per hydrogen (k_{rel}^{H})			
	Methyl	Methylene	Methine	Benzylic
α	-	≤ 0.05	≤ 0.10	-
β	≤ 0.03	≤ 0.05	0.38 0.70	0.5
γ	0.09 0.10 0.16 0.17	0.48 0.84 1.4	5.2	1.4
δ	0.48 0.59 2.1	3.7		
ε	2.3			

Figure 2.35: Reactivity per hydrogen (k_{rel}^{H}) of the amino acids **(12)**, **(13)**, **(15)**, **(25)**, **(28)**, **(30)**, **(31)** and **(38-41)**

In Figure 2.35, the k_{rel}^{H} values for the amino acids **(12)**, **(13)**, **(15)**, **(25)**, **(28)**, **(30)**, **(31)** and **(38-41)** with alkyl side-chains and benzylic side chains have been tabulated. In many instances multiple amino acids have k_{rel}^{H} values for a given type of hydrogen at a given position and so they can be compared. The two examples of β-methine hydrogens have k_{rel}^{H} values within a factor of two, as do the four cases of the γ-methyl hydrogens. The three examples of γ-methylene hydrogens have k_{rel}^{H} values within a factor of three and the three cases of δ-methyl hydrogens have k_{rel}^{H} values within a factor of 4.5. The k_{rel}^{H} values for the range of amino acids **(12)**, **(13)**, **(15)**, **(25)**, **(28)**, **(30)**, **(31)** and **(38-41)** vary over more than two orders of magnitude and so variations of the measured k_{rel}^{H} values are relatively small. An average value for each type of hydrogen can therefore be determined and a table of these average k_{rel}^{H} values can be constructed (Figure 2.36).

Position	Average reactivity per hydrogen			
	Methyl	Methylene	Methine	Benzyl
α	-	≤ 0.05	≤ 0.10	-
β	≤ 0.03	≤ 0.05	0.54	0.5
γ	0.13	0.91	5.2	1.4
δ	1.1	3.7		
ε	2.3			

Figure 2.36: Average k_{rel}^{H} values for various types of hydrogens

When compiled into a table, the trends become distinct. As expected, the reactivity is greater if the radical generated is tertiary rather than secondary or primary. For example the k_{rel}^{H} of a γ-hydrogen increases from 0.13 for a methyl hydrogen, to 0.91 for a methylene hydrogen to 5.2 for a methine hydrogen. This can be explained by the differences in stability of such radicals, which is attributed to hyper-conjugative effects and relief of steric compression.

More important however is the increase in rate as the radical centre formed is more distant from the α-centre. Comparing the reactivity of methyl hydrogens, the difference in reactivity for those at the γ-position relative to the β-position is an increase by a more than a factor of four. The difference in reactivity for the hydrogens at the δ-position compared to the γ-position is again an increase by almost an order of magnitude. The increase in reactivity between hydrogens at the ε-position and the δ-position is slight. For the methylene hydrogens the difference in reactivity between the α- and β-positions and the γ-position is more than an order of magnitude, and the difference in reactivity between hydrogens at the γ-position and the δ-position is an increase by a factor of four. For the methine hydrogens the difference in reactivity between the α- and β-positions is at least a factor of five and the difference in reactivity between the β- and γ-positions is an increase by almost an order of magnitude. The difference in reactivity of the benzylic hydrogens at the β- and γ-positions is a factor of three. The results observed are indicative of a polar effect, where the deactivating effect is strongest nearby, and less so at more distal positions.

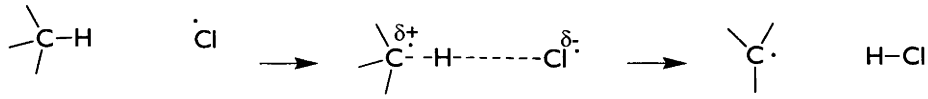

Figure 2.37: The transition state of the abstraction of a hydrogen atom by chlorine radical

In Figure 2.37 the transition state of the hydrogen atom abstraction is depicted. Due to the electrophilic and reactive nature of the chlorine radical, the transition state causes the formation of a partial positive charge and little radical character on the carbon from where the hydrogen atom is abstracted. As a result of this phenomenon, the degree to which a positive charge can form on the carbon has a greater effect on the reaction rate than the stability of the product radical. The inductively electron-withdrawing nature of the protonated amino and carboxyl groups results in the carbons situated further away being more able to allow the formation of the partial positive charge. With such a polar effect, it would be expected that the effect would diminish with distance, and for it to reach a point where no effect is seen. This would manifest as the rate not increasing further as the distance from the polar group continued to increase. It is likely that any polar effect felt at the ε-position is negligible, and this is reflected in the k_{rel}^{H} values of the δ- and ε-methyl hydrogens (Figure 2.35) which are in the same range. Polar effects such as that observed in these reactions have been described in detail in both substituted alkanes and carboxylic acids by Russel and coworkers,[77] and they show similar reactivity patterns to those seen with these reactions of amino acids, such as increased reaction at positions further away from polar groups (Figures 2.38 and 2.39).

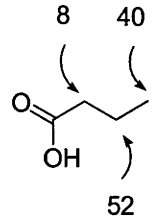

Figure 2.38: Percentage chlorination of *n*-butanoic acid at each position.
Conditions: Cl_2, CCl_4, 20 °C[77]

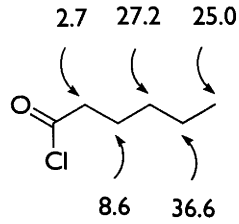

Figure 2.39: Percentage chlorination of *n*-hexanoyl chloride at each position. Conditions: $(CH_3)_2NHCl^+$, Fe, 25 °C [77]

The work described in this chapter has thus shown that not only do polar effects control the position of hydrogen atom abstraction by chlorine radicals from amino acids, but the magnitude of the reactivity has been measured by comparison of the reactivity of a range of amino acids and this, for the first time, allows the polar effect in amino acids to be quantified.

Chapter 3: Results and Discussion

Hydrogen Atom Transfer from *N*-Acetylamino Acids to Chlorine

In addition to the reactions of free amino acids, the reactions of *N*-acetylamino acids with chlorine were investigated. *N*-Acetylamino acids were of interest as models of amino acid residues in peptides and proteins. As before, chlorination was studied as a way to assess the susceptibility of *N*-acetylamino acids and therefore peptides and proteins to hydrogen atom transfer.

The choice of *N*-acetylamino acids on which to study the effect of chlorine radical-facilitated hydrogen atom abstraction was determined by the same factors as for the free amino acids (**12**), (**13**), (**15**), (**18**), (**21**), (**23**), (**25**), (**28-31**) and (**37-41**), and so the analogous set of *N*-acetylamino acids (**61-76**) was selected.

As for free amino acids, excluding *N*-acetylglycine (**61**), all *N*-acetyl-α-amino acids have at least one chiral centre. In general, the *S*-isomers were selected for the experiments, due to their availability. As with the free amino acids (**13**), (**15**), (**18**), (**21**), (**23**), (**25**), (**28-31**) and (**37-41**), the chirality of the acetamides (**62-76**) at the α-centre is not of great importance and therefore chirality is not depicted in the structures. *N*-Acetylisoleucine (**64**) was used as the (2*S*,3*S*)-form.

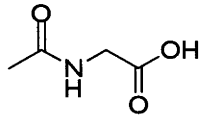

61

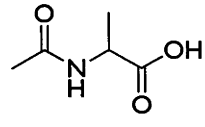

62

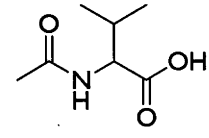

63

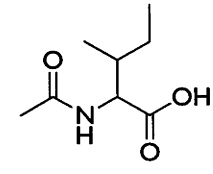

64

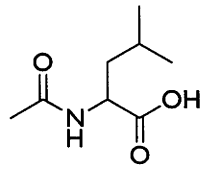

65

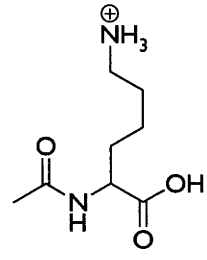

66

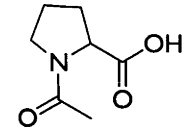

67

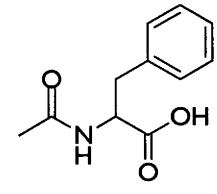

68

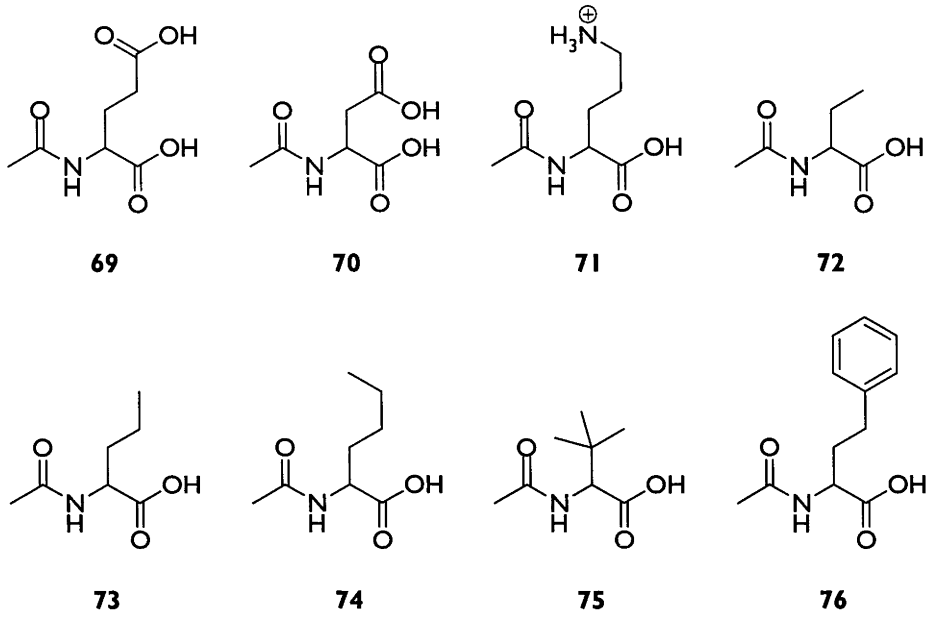

69 70 71 72

73 74 75 76

3.1 Reaction Products

The reactions of the *N*-acetylamino acids (**61-76**) were studied under the same conditions as for the free amino acids (**12**), (**13**), (**15**), (**18**), (**21**), (**23**), (**25**), (**28-31**) and (**37-41**). Under the acidic conditions the carboxyl and side chain amino groups of the acetamides (**61-76**) may be assumed to be protonated. The extent of substrate reaction was generally kept relatively low to obtain good yields of mono-chlorinated products. The products were identified by direct analysis of crude reaction mixtures, after concentration under reduced pressure, using ^{1}H and 2D TOCSY NMR experiments. Comparison to the products from reaction of the free amino acids (**12**), (**13**), (**15**), (**18**), (**21**), (**23**), (**25**), (**28-31**) and (**37-41**) aided identification. Benzoic acid was again used as an inert standard to determine the yields of the products and ascertain if they accounted for the amounts of the starting amino acids (**61-76**) that had reacted.

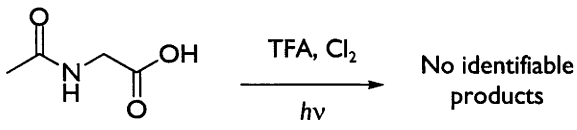

61

Figure 3.1: Reaction of *N*-acetylglycine (**61**)

N-Acetylglycine (**61**), like free glycine (**12**), gave no observable products when treated using the conditions described in the previous chapter (Figure 3.1). In the presence of benzoic acid as an internal standard *N*-acetylglycine (**61**) slowly reacted. It is likely that the mechanisms for the decomposition of glycine (**12**) and its *N*-acetylated analogue (**61**) are similar, probably involving reactions at the α-centres.

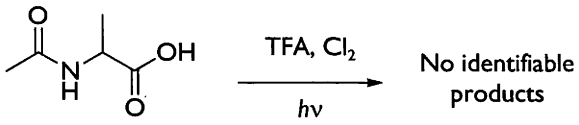

62

Figure 3.2: Reaction of *N*-acetylalanine (**62**)

N-Acetylalanine (**62**), as with *N*-acetylglycine (**61**), slowly reacts as demonstrated by the disappearance of the starting material, but again there is no evidence of reaction at the β-position (Figure 3.2). Instead, a process similar to what occurs with glycine (**12**) and alanine (**13**) is likely to be involved.

N-Acetylaspartic acid (**70**) doesnot show any discrete products (Figure 3.3) and, as with free aspartic acid (**37**), when the mass balance during the reaction is monitored, it is seen that no discernable reaction occurs.

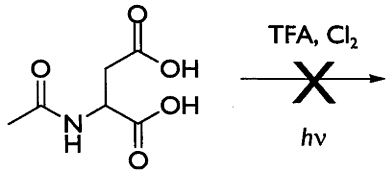

70

Figure 3.3: Reaction of *N*-acetylaspartic acid (**70**)

Upon chlorination of *N*-acetylglutamic acid (**69**) (Figure 3.4) *N*-acetyl-β-chloroglutamic acid (**77**) and *N*-acetyl-γ-chloroglutamic acid (**78**) are formed, the former as a 57:43 mixture of diastereomers. No diastereoselectivity is seen with the γ-chlorinated product (**78**). The yields of the chloride (**77**) and (**78**) account for at least 95% of the reacted starting material.

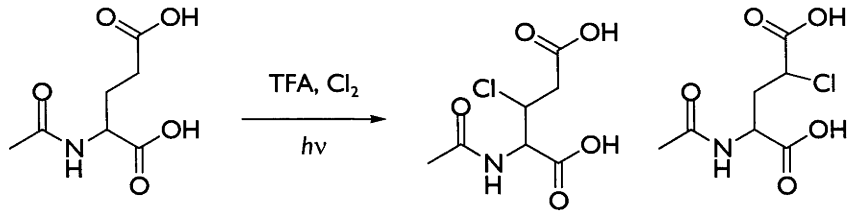

69 **77**† **78**†

†Both diastereomers produced

Compound	¹H NMR Resonances (δ ppm)				
	αH	βH	γH	δH	εH
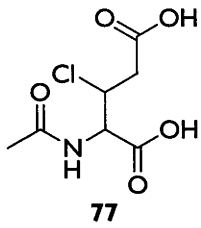 **77**	4.86 d 4.5 Hz†	4.60 m†	2.70 dd 8 Hz 17 Hz† 2.84 dd 6 Hz 17 Hz†		
	5.10 d 2.5 Hz†	4.93 m†	2.87 dd 10 Hz 17 Hz† 2.98 dd 4 Hz 17 Hz†		
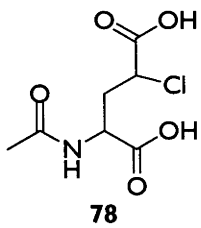 **78**	4.56 dd 5 Hz 8 Hz†	2.25 m* 2.64 m*	4.37 dd 6.5 Hz 8.5 Hz†		
	4.67*†	2.17 m* 2.41 m*	4.48 dd 6.5 Hz 7 Hz†		

*Discrete resonance not detected in 1D ¹H NMR spectrum

Figure 3.4: Reaction of *N*-acetylglutamic acid (**69**) and NMR data of the products (**77**) and (**78**)

N-Acetylvaline (**63**), when chlorinated, produces three products which are clearly identifiable by ¹H NMR spectroscopy (Figure 3.5), *N*-acetyl-β-chlorovaline (**79**), and the diastereomers of *N*-acetyl-γ-chlorovaline (**80**), which are produced in a 50:50 mixture. The yields of the chlorides (**79**) and (**80**) account for all the reacted starting material. The chemical shifts of the side-chain methyl resonances for the three products are diagnostic. The acetyl resonances for all compounds are coincident at ~δ 2 ppm, not only in this case, but for all products formed from chlorination of the acetylated amino acids (**61-76**) and so are ignored for identification purposes. Because of the high yield

of identified products (>95%) it is likely that non-specific decomposition analogous to that occurring for glycine (**12**) and *N*-acetylglycine (**61**) does not happen in this case.

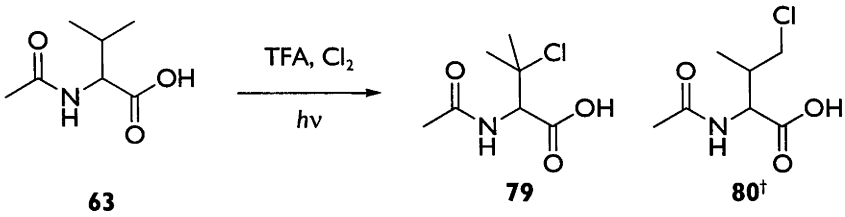

63 **79** **80**†

†Both diastereomers produced

Compound	¹H NMR Resonances (δ ppm)				
	αH	βH	γH	δH	εH
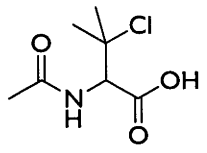 **79**	4.73 s	N/A	1.74 s 1.65 s		
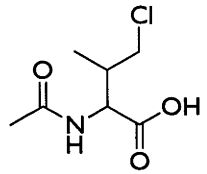 **80**	4.53 d 6 Hz† 4.80 d 4 Hz†	2.30 m† 2.47 m†	1.05 d 7 Hz† 1.10 d 7 Hz† 3.45 m† 3.55 m†		

Figure 3.5: Reaction of *N*-acetylvaline (**63**) and NMR data of the products (**79**) and (**80**)

TOCSY NMR experiments were again used to help identify resonances belonging to chlorinated products. Figure 3.6, a TOCSY spectrum of the products from the chlorination of *N*-acetylvaline (**63**), shows the resonances due to one diastereomer of *N*-acetyl-γ-chlorovaline (**80**) highlighted.

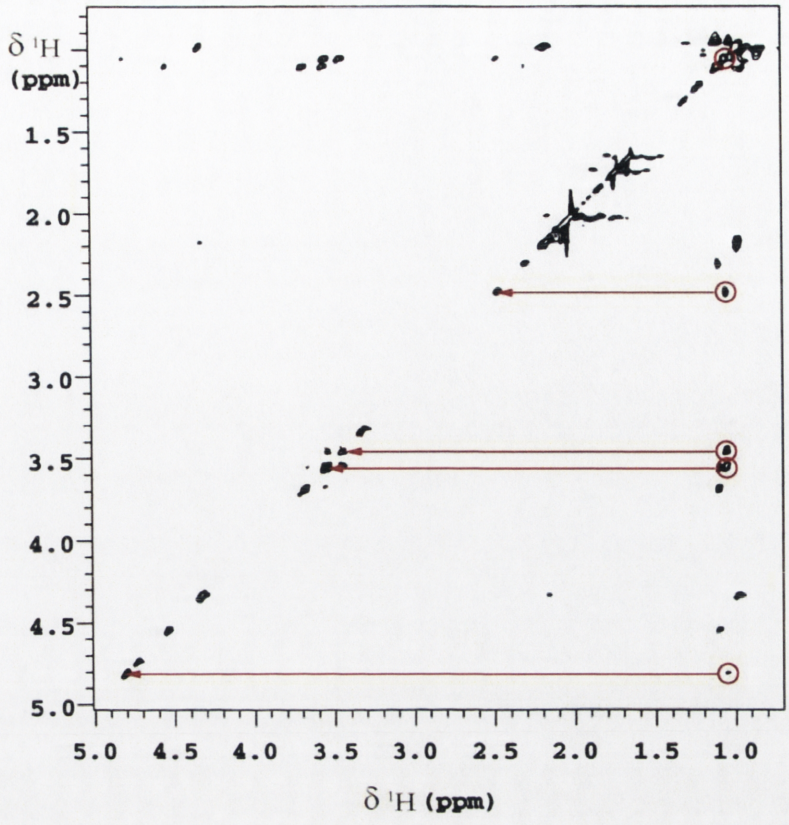

Figure 3.6: TOCSY NMR spectrum of the products from reaction of *N*-acetylvaline (**63**)

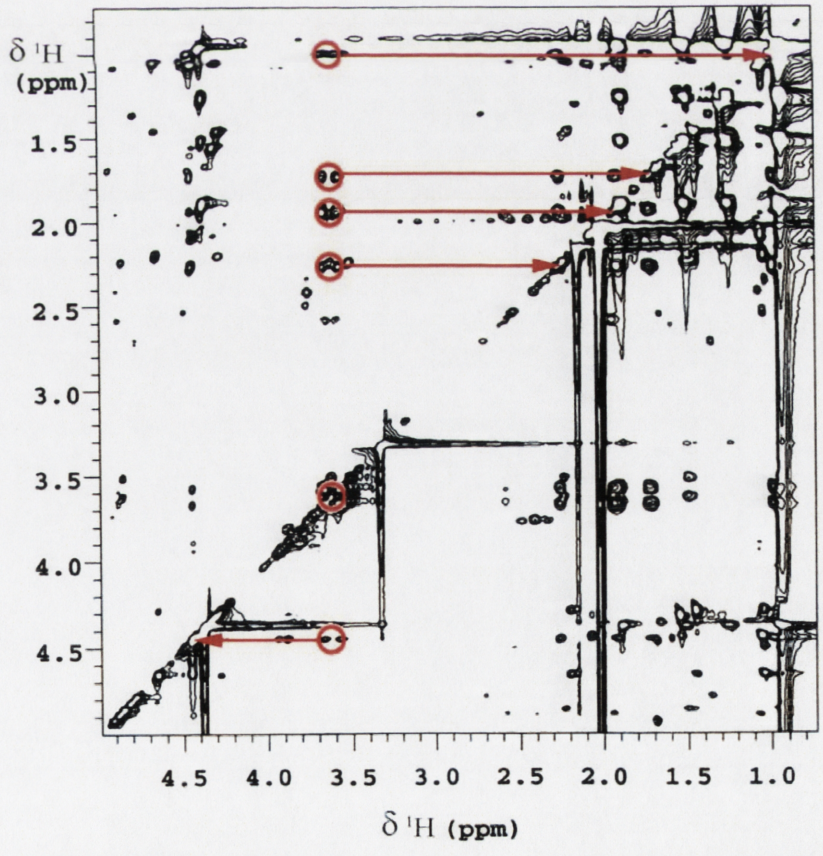

Figure 3.7: TOCSY NMR spectrum of the products from reaction of *N*-acetylisoleucine (**64**)

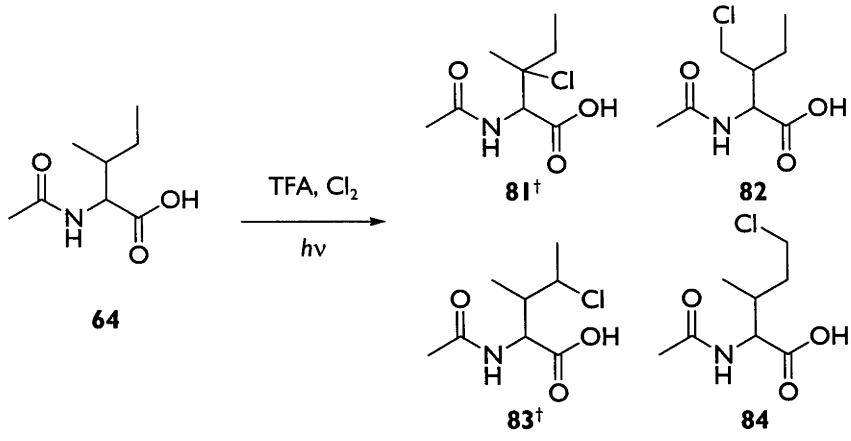

†Both diastereomers produced

Compound	^{1}H NMR Resonances (δ ppm)				
	αH	βH	γH	δH	εH
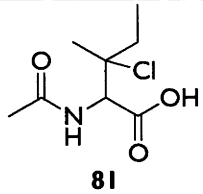 **81**	4.85 s† 4.86 s†	N/A	2.5 m* 1.57 s† 1.61 s†	0.95*	
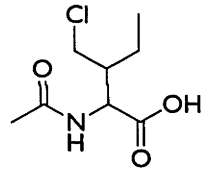 **82**	4.77 d 3 Hz	2.2 m*	1.33 m* 4.47 m*	1.03*	
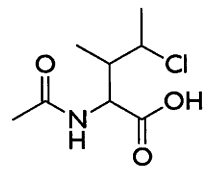 **83**	4.62 d 7 Hz† 4.30*†	2.07 m*† 2.20 m*†	1.03 d 6.5 Hz† 1.05 d 7 Hz† 4.27 m† 4.39 m†	1.47*	
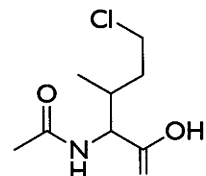 **84**	4.43 d 5 Hz	2.23 m*	0.98 d 7 Hz 1.94 m* 1.74 m*	3.6*	

*Discrete resonance not detected in 1D ^{1}H NMR spectrum

Figure 3.8: Reaction of *N*-acetylisoleucine (**64**) and NMR data of the products (**81-84**)

The identification of products from the chlorination of *N*-acetylisoleucine (**64**) (Figure 3.8) is much simpler than was the case with free isoleucine (**31**) because TOCSY experiments can be used to identify each group of resonances and comparisons between resonances of analogous hydrogens in the products from the free and *N*-acetylated amino acids (**31**) and (**64**) can be made. The TOCSY spectrum (Figure 3.7) shows six separate spin systems that are similar to those which occur with the products from free isoleucine (**31**). The main difference in the ^{1}H NMR spectra of the products of reaction of isoleucine (**31**) and *N*-acetylisoleucine (**64**) is a shift downfield of the resonances of the α-protons of the latter. The diastereomers of the chlorides (**81**) and (**83**) occur in equal amounts, and the products (**81-84**) account for all the reacted starting material. Above is the TOCSY spectrum of the products of reaction of *N*-acetylisoleucine (**64**) (Figure 3.7). The resonances which have been assigned to *N*-acetyl-δ-chloroisoleucine (**84**) are indicated in red.

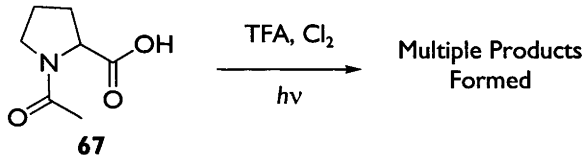

67

Figure 3.9: Reaction of *N*-acetylproline (**67**)

The resonances in the ^{1}H NMR spectra of the products of reaction of *N*-acetylproline (**67**) (Figure 3.9) are irreducibly complex. In part, this can be attributed to the presence of *cis* and *trans* isomers of the amide moiety, which is peculiar to the proline derivative (**67**) as the only secondary amide studied in this work.

The resonances in the ^{1}H NMR spectrum of the products from the chlorination of *N*-acetylleucine (**65**) (Figure 3.10) are similar to those from the chlorination of leucine (**30**). The methyl resonances are again diagnostic, with singlets attributable to *N*-acetyl-γ-chloroleucine (**85**) at approximately δ 1.6 ppm and sets of doublets attributable to *N*-acetyl-δ-chloroleucine (**86**) at ~δ 1.0 ppm. Both diastereomers of the latter compound are seen, and appear in equal amounts.

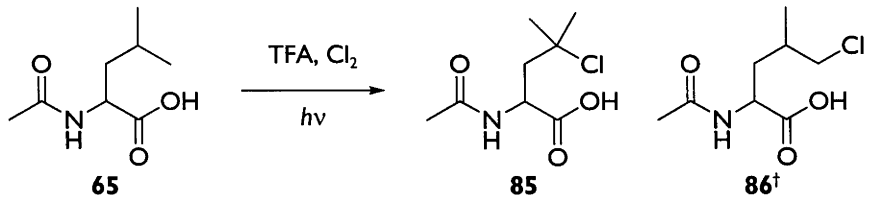

†Both diastereomers produced

Compound	^{1}H NMR Resonances (δ ppm)				
	αH	βH	γH	δH	εH
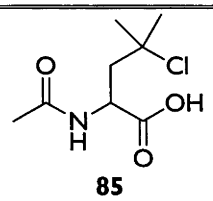 **85**	4.68 dd 3 Hz 9 Hz	2.42 dd 3 Hz 15 Hz 2.07*	N/A	1.59 s 1.61 s	
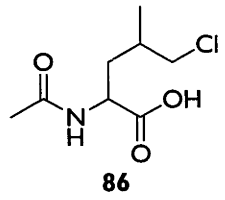 **86**	4.46*	1.80 m*	2.00 m*	1.03 d 6.5 Hz† 1.06 d 6.5 Hz† 3.51 d 5 Hz† 3.54 d 4.5 Hz†	

*Discrete resonance not detected in 1D ^{1}H NMR spectrum

Figure 3.10: Reaction of N-acetylleucine (**65**) and NMR data of the products (**85**) and (**86**)

There are six products from the reaction of N^{α}-acetyllysine (**66**) (Figure 3.11), one of which has resonances largely coincident with N^{α}-acetyllysine (**66**) in the ^{1}H NMR spectrum of the reaction mixture. The products have been assigned based largely on the shifts of the α-proton resonances, as the closer the chlorine is to the α-position, the further downfield the α-proton resonance occurs. The other resonances for each compound are consistent with what would be expected. In this way both diastereomers of N^{α}-acetyl-β-chlorolysine (**87**), N^{α}-acetyl-γ-chlorolysine (**88**) and N^{α}-acetyl-δ-chlorolysine (**89**) are assigned. Each pair of diastereomers occurs as an equal mixture. The products (**87**)-(**89**) account for more than 95% of the starting material consumed.

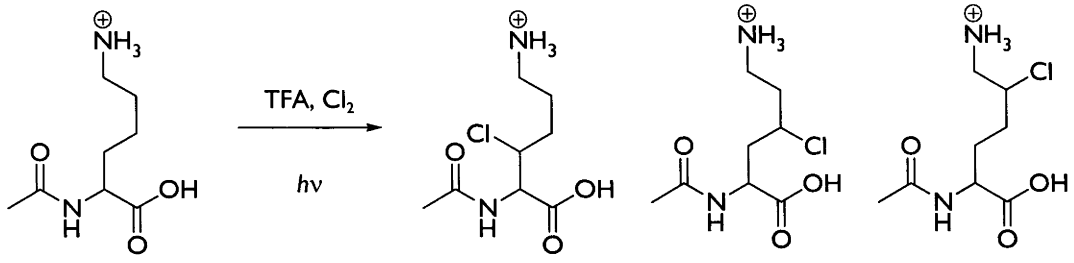

66 **87**† **88**† **89**†

†Both diastereomers produced

Compound	¹H NMR Resonances (δ ppm) αH	βH	γH	δH	εH
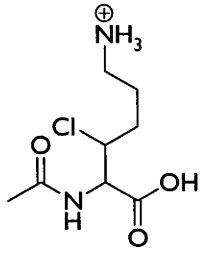 **87**	4.83 d 5 Hz†	4.24 m†	1.80 m*†	2.00 m*	2.90 m*†
	5.00 d 3 Hz†	4.57 m*†	2.00 m*†		2.96 m*†
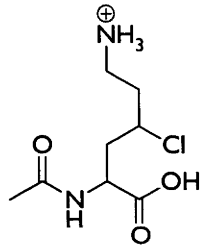 **88**	4.68 dd 3 Hz 11 Hz†	2.21 m*†	4.11 m*†	2.00 m*†	3.15 m*†
	4.62 dd 6 Hz 7.5 Hz†	2.35 m*†	4.14 m*†	2.14 m*†	3.16 m*†
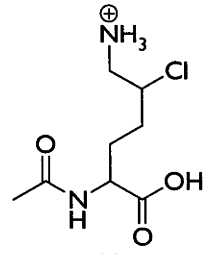 **89**	4.45 m*	2.0 m*	1.89 m*	4.21 m*	3.13 m*†
	4.39 m*				3.35 m*†

*Discrete resonance not detected in 1D ¹H NMR spectrum

Figure 3.11: Reaction of N^{α}-acetyllysine (**66**) and NMR data of the products (**87-89**)

One product from reaction of *N*-acetylphenylalanine (**68**) (Figure 3.12) can be detected. There is no spectral evidence for a second non-coincident diastereomer of *N*-acetyl-β-chlorophenylalanine (**90**). Either the resonances for both diastereomers of *N*-acetyl-β-chlorophenylalanine (**90**) are coincident in the ¹H NMR spectra or only one diastereomer is formed. At least 95% of the starting material is accounted for by the identified product (**90**).

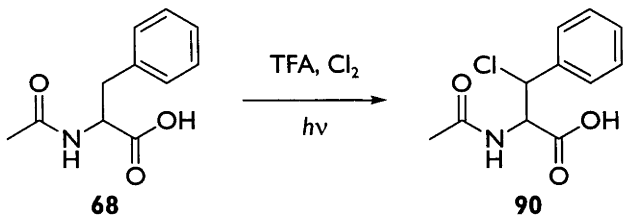

68 **90**

Compound	^{1}H NMR Resonances (δ ppm)				
	αH	βH	γH	δH	εH
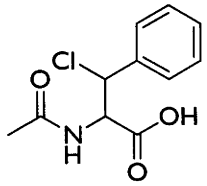 **90**	5.13 d 5 Hz	5.60 d 5 Hz			

Figure 3.12: Reaction of *N*-acetylphenylalanine (**68**) and NMR data of the product (**90**)

N^{α}-Acetylornithine (**71**), when reacted as in Figure 3.13, forms four products that can be detected in the ^{1}H NMR spectrum. These have been assigned as both diastereomers of N^{α}-acetyl-β-chloroornithine (**91**) and N^{α}-acetyl-γ-chloroornithine (**92**). As for N^{α}-acetyllysine (**66**), the proximity of the α-protons to the chlorine, and the resultant shifts of their resonances are used to identify the products. Both the chlorides, (**91**) and (**92**), are produced as equal mixtures of diastereomers. The products (**91**) and (**92**) account for all of the starting material consumed.

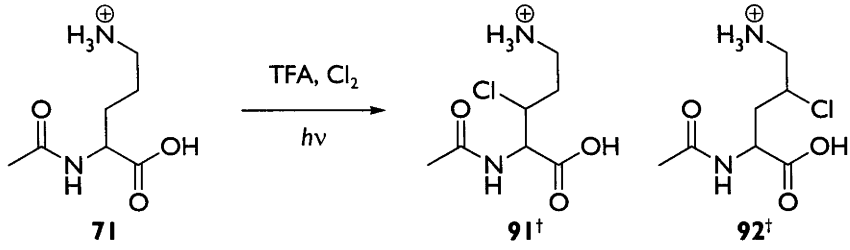

71 **91**† **92**†

†Both diastereomers produced

Compound	^{1}H NMR Resonances (δ ppm)				
	αH	βH	γH	δH	εH
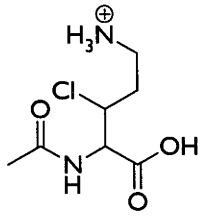 **91**	4.82 d 5 Hz†	4.76 m*†	2.33 m*†	3.17 m*†	
	5.03 d 2.5 Hz†	4.37 m*†	2.36 m*†	3.19 m*†	
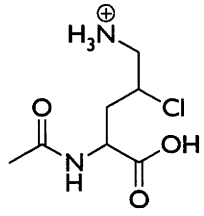 **92**	4.67 m*†	2.36 m*†	4.29 m*†	3.43 m*†	
	4.70 m*†	2.48 m*†	4.41 m*†	3.52 m*†	

*Discrete resonance not detected in 1D ^{1}H NMR spectrum

Figure 3.13: Reaction of N^{α}-acetylornithine (**71**) and NMR data of the products (**91**) and (**92**)

The products of chlorination of *N*-acetyl-α-aminobutyric acid (**72**) are both the diastereomers *N*-acetyl-α-amino-β-chlorobutyric acid (**93**) and *N*-acetyl-α-amino-γ-chlorobutyric acid (**94**) (Figure 3.14). As for α-aminobutyric acid (**15**), the diastereomers of the *N*-acetyl-α-amino-β-chlorobutyric acid (**93**) are produced in an approximately 40:60 ratio. The products (**93**) and (**94**) account for more than 90% of the reacted starting material.

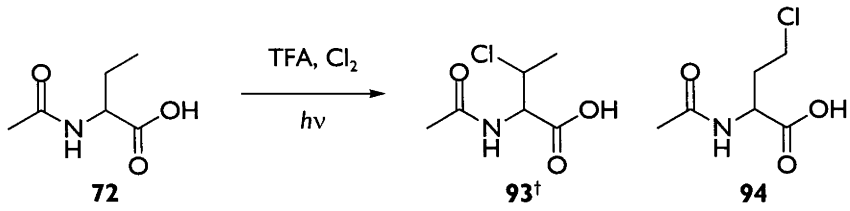

†Both diastereomers produced

Compound	^{1}H NMR Resonances (δ ppm) αH	βH	γH	δH	εH
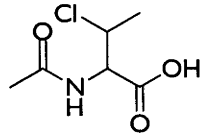 **93**	4.77 d, 5 Hz† minor 4.87 d, 3 Hz† major	3.61 m*†	1.48 d, 7 Hz† major 1.56 d, 7 Hz† minor		
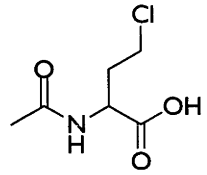 **94**	4.57 dd, 5 Hz, 10 Hz	2.12 m* 2.29 m*	3.66 m*		

*Discrete resonance not detected in 1D ^{1}H NMR spectrum

Figure 3.14: Reaction of *N*-acetyl-α-aminobutyric acid (**72**) and NMR data of the products (**93**) and (**94**)

The chlorination of *N*-acetylnorvaline (**73**) (Figure 3.15) results in three identifiable products, equal amounts of the diastereomers of *N*-acetyl-γ-chloronorvaline (**95**), and *N*-acetyl-δ-chloronorvaline (**96**). These products, like those from the chlorination of norvaline (**38**), can be identified by the chemical shifts of the terminal methyl groups. No β-chlorinated compound was detected. The products (**95**) and (**96**) account for 90% of the starting material consumed.

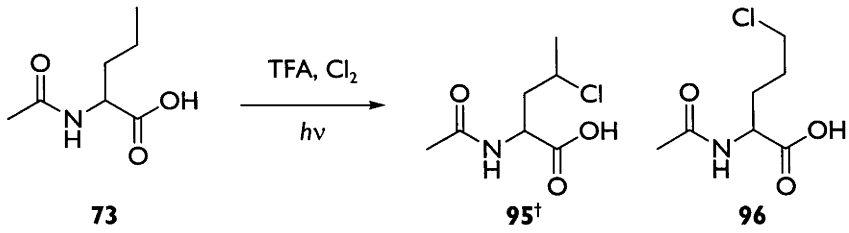

73 95† 96

†Both diastereomers produced

Compound	^{1}H NMR Resonances (δ ppm) αH	βH	γH	δH	εH
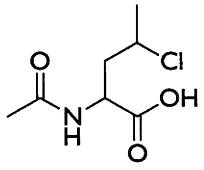 95	4.67 dd 4 Hz 11 Hz†	2.10 m*	4.12 m*†	1.55 d 6 Hz†	
	4.59 dd 6 Hz 8 Hz†		4.20 m*†	1.57 d 6 Hz†	
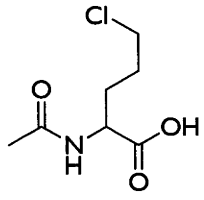 96	4.45 t 8 Hz*	1.72 m*	1.83 m*	3.61 t 6 Hz	

*Discrete resonance not detected in 1D ^{1}H NMR spectrum

Figure 3.15: Reaction of *N*-acetylnorvaline (**73**) and NMR data of the products (**95**) and (**96**)

The products from reaction of *N*-acetylnorleucine (**74**) (Figure 3.16) have been identified as the diastereomers of *N*-acetyl-γ-chloronorleucine (**97**), the diastereomers of *N*-acetyl-δ-chloronorleucine (**98**), and *N*-acetyl-ε-chloronorleucine (**99**). Similar to previous examples, the shifts due to the terminal methyl resonances of products, combined with the TOCSY spectrum of the reaction mixture can be used to assign the resonances of each product. There is no detectable amount of diastereoselectivity. The products (**97-99**) account for greater than 95% of the starting material consumed.

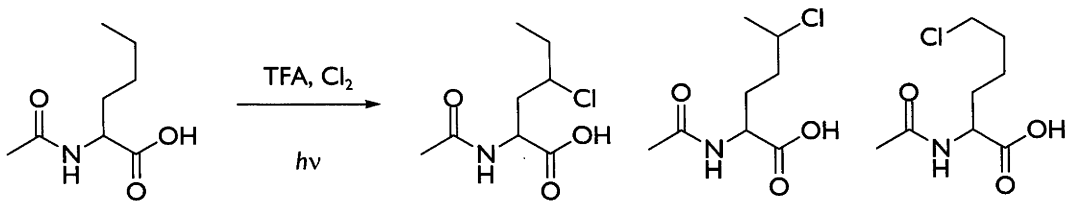

74 **97**† **98**† **99**

†Both diastereomers produced

Compound	¹H NMR Resonances (δ ppm) αH	βH	γH	δH	εH
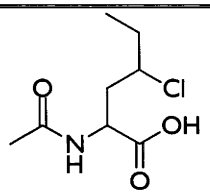 **97**	4.64 m*	2.30 m*	3.88 m*† 4.00 m*†	1.75 m*	1.04 t 7 Hz† 1.07 t 7 Hz†
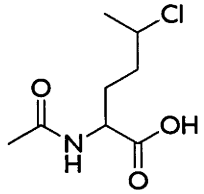 **98**	4.39 m*	2.10 m*	1.80 m*	4.07 m*	1.49 d 6.5 Hz† 1.50 d 6 Hz†
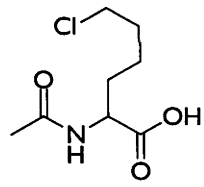 **99**	4.36 m*	1.87 m*	1.74 m*	1.54 m*	3.57 t 6.5 Hz

*Discrete resonance not detected in 1D ¹H NMR spectrum

Figure 3.16: Reaction of *N*-acetylnorleucine (**74**) and NMR data of the products (**97-99**)

The product from the chlorination of *N*-acetyl-*tert*-leucine (**75**) is *N*-acetyl-γ-chloro-*tert*-leucine (**100**) (Figure 3.17). It accounts for all the starting material consumed.

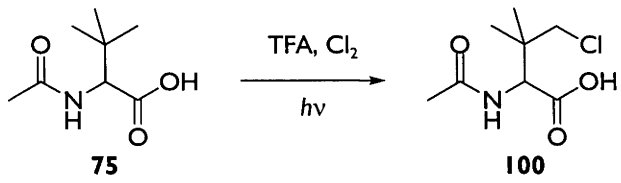

75 100

Compound	^{1}H NMR Resonances (δ ppm) αH	βH	γH	δH	εH
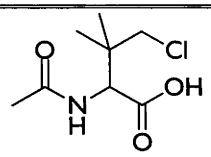 100	4.63 s	N/A	1.00 s 1.07 s 3.57 ABq		

Figure 3.17: Reaction of *N*-acetyl-*tert*-leucine (**75**) and NMR data of the product (**100**)

N-Acetylhomophenylalanine (**76**), like the other amino acids with benzylic hydrogens, only shows the diastereomeric benzylic products, *N*-acetyl-γ-chloro-homophenylalanine (**101**) (Figure 3.18). The diastereomers are formed in equal amounts. The products (**101**) account for at least 90% of the starting material consumed.

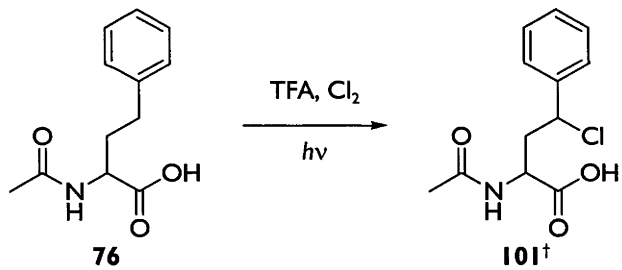

76 101†

†Both diastereomers produced

Compound	^{1}H NMR Resonances (δ ppm) αH	βH	γH	δH	εH
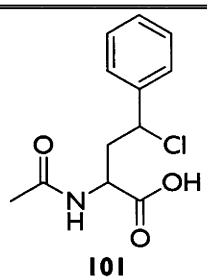 101	4.67 m*	2.18 m*	5.00 dd 4 Hz 8 Hz† 5.05 apparent t 6 Hz†		

*Discrete resonance not detected in 1D ^{1}H NMR spectrum

Figure 3.18: Reaction of *N*-acetylhomophenylalanine (**76**) and NMR data of the products (**101**)

3.2 Formation of Diastereomers

The diastereoselectivity in the chlorination of *N*-acetyl-α-aminobutyric acid (**72**), within the limits of detection, is identical to that of free α-aminobutyric acid (**15**). In both instances the diastereomers of the β-chlorinated products (**16**) and (**93**) are formed in an approximately 60:40 ratio. The other instance where diastereoselectivity occurred in the reaction of the free amino acids (**12**), (**13**), (**15**), (**18**), (**21**), (**23**), (**25**), (**28-31**) and (**37-41**) was phenylalanine (**28**). With *N*-acetylphenylalanine (**68**) only one set of resonances is seen in the ^{1}H NMR spectrum of the reaction products. Either the signals of the two diastereomers of the β-chloride (**90**) are coincident or the diastereoselectivity is very high. The latter is more likely. As was discussed in Chapter 2, the diastereoselectivity shown in the products has no correlation to the stereochemistry of the hydrogen atom abstraction reaction. Because of this, in the following discussion diastereotopic hydrogens are assumed to have equal reactivity towards abstraction.

3.3 Product Distribution

As for the free amino acids (**12**), (**13**), (**15**), (**18**), (**21**), (**23**), (**25**), (**28-31**) and (**37-41**), the proportion of each product from chlorination of the acetylated amino acids (**61-76**) can be determined by integrating resonances in the ^{1}H NMR spectra of the product mixtures. Compounds which do not yield identifiable products upon reaction, namely *N*-acetylglycine (**61**), *N*-acetylalanine (**62**), *N*-acetylaspartic acid (**70**) and *N*-acetylproline (**67**), are not included in this analysis. Again the high yields of identified products, in general 95% or greater, means it can be assumed that very little reaction at the α-position is occurring. The percentages of each product formed are consistent over repeated experiments and so can be considered relatively precise. The percentage of each product observed is tabulated in Figure 3.19, below. The accuracy of the figures is likely to be within 5% due to the accuracy of the integration of the NMR spectra and because the reactivity seen is accounted for by the products observed.

Starting Amino Acid	Percent reaction at each position			
	β	γ	δ	ε
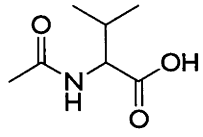 **63**	25	75		
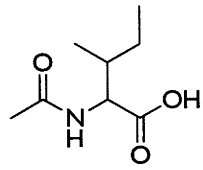 **64**	12	16 (CH_3) 39 (CH_2)	32	
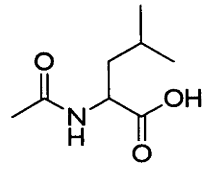 **65**	0	49	51	
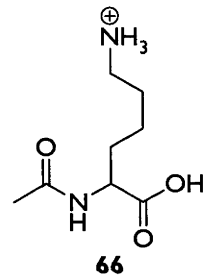 **66**	20	64	16	0
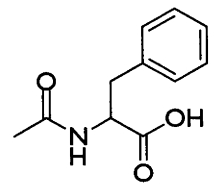 **68**	100			
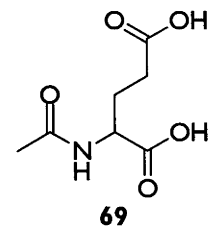 **69**	83	17		

Figure 3.19: Percentage reaction at each position for the *N*-acetylamino acids **(63-66)**, **(68)**, **(69)** and **(71-76)**

Starting Amino Acid	Percent reaction at each position			
	β	γ	δ	ε
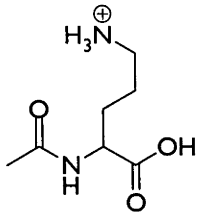 **71**	44	56	0	
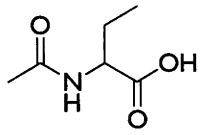 **72**	32	68		
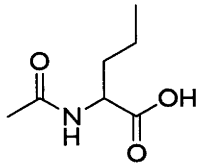 **73**	0	66	44	
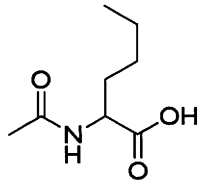 **74**	0	28	45	27
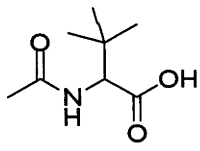 **75**	N/A	100		
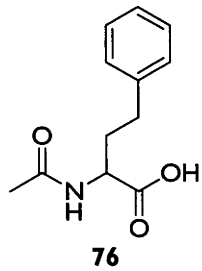 **76**	0	100		

Figure 3.19 *cont.*: Percentage reaction at each position for the *N*-acetylamino acids **(63-66)**, **(68)**, **(69)** and **(71-76)**

3.4 Relative Rates of Reaction

As in the previous chapter, a relative rate of hydrogen abstraction (k_{rel}) can be determined by examining the relative amounts of starting material consumed or chlorinated products formed. This allows the direct comparison of the reactivity of the *N*-acetylamino acids (**61-71**). The experimental methodology used to determine the relative rates of reaction, or k_{rel}, for the *N*-acetylamino acids (**61-71**) is identical to that which was used to determine the k_{rel} values of the free amino acids (**12**), (**13**), (**15**), (**18**), (**21**), (**23**), (**25**), (**28-31**) and (**37-41**). To aid comparison, phenylalanine (**28**) rather than *N*-acetylphenylalanine (**68**) was used as the standard against which the *N*-acetylated amino acids (**61-71**) were tested; however values obtained from competitive reactions using other amino acids as the standard are consistent with these values.

Thus the k_{rel} values for the *N*-acetylamino acids (**61-71**) below (Figure 3.20) are measured on the same scale as those for the free amino acids ((**12**), (**13**), (**15**), (**18**), (**21**), (**23**), (**25**), (**28-31**) and (**37-41**).

N-Acetylamino Acid	k_{rel}	*N*-Acetylamino Acid	k_{rel}
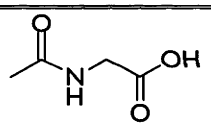 **61**	0.4	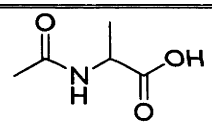 **62**	0.1
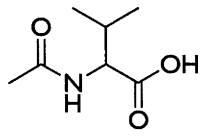 **63**	3.5	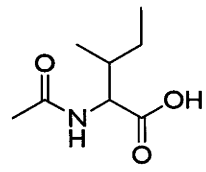 **64**	6.6
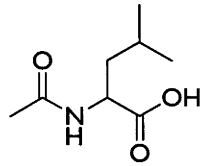 **65**	19	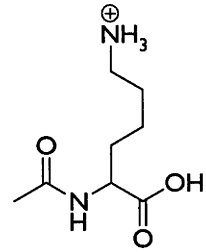 **66**	2.7

Figure 3.20: Relative rates of reaction for the *N*-acetylamino acids (**61-76**)

N-Acetylamino Acid	k_{rel}	N-Acetylamino Acid	k_{rel}
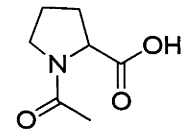 **67**	0.5	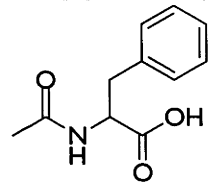 **68**	7.9
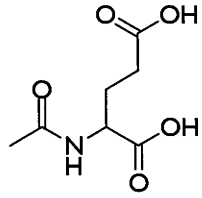 **69**	0.2	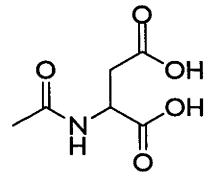 **70**	≤ 0.01
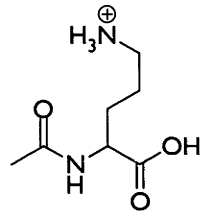 **71**	0.6	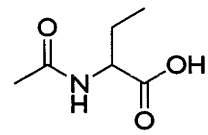 **72**	2.2
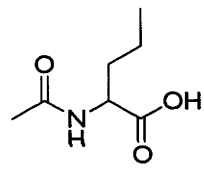 **73**	11	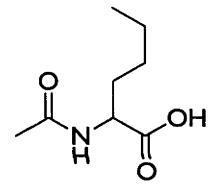 **74**	22
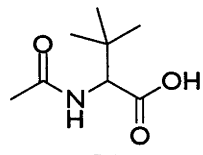 **75**	4.5	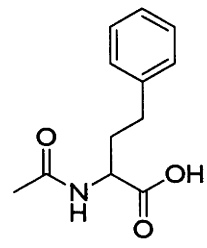 **76**	10

Figure 3.20 *cont.*: Relative rates of reaction for the *N*-acetylamino acids (**61-76**)

Like the free amino acids (**12**), (**13**), (**15**), (**18**), (**21**), (**23**), (**25**), (**28-31**) and (**37-41**) discussed in Chapter 2, the relative rates of reaction of the *N*-acetylamino acids (**61-76**) (Figure 3.20) vary over a large range of more than three orders of magnitude. The fastest reacting acetamides, as seen with the free amino acids (**12**), (**13**), (**15**), (**18**), (**21**), (**23**), (**25**), (**28-31**) and (**37-41**), tend to be those with longer, non-polar side-chains such as *N*-acetylleucine (**65**) and *N*-acetylnorleucine (**74**) while those with polar, functionalised side-chains, such as *N*-acetylglutamic acid (**69**) and *N*-acetylornithine (**71**), tend to have slower reaction rates.

3.5 Reactivity per Hydrogen

As for the free amino acids (**12**), (**13**), (**15**), (**18**), (**21**), (**23**), (**25**), (**28-31**) and (**37-41**), the magnitude of reaction can be further investigated by calculating the reactivity per hydrogen, or k_{rel}^{H}, which allows correlation between hydrogens within the *N*-acetylamino acids (**61-76**) and an absolute correlation between hydrogens in different compounds. Determined in the same manner as the k_{rel}^{H} values of the free amino acids (**12**), (**13**), (**15**), (**18**), (**21**), (**23**), (**25**), (**28-31**) and (**37-41**) the k_{rel}^{H} values for the *N*-acetylamino acids (**61-76**) are tabulated below (Figure 3.21). As *N*-acetylglycine (**61**), *N*-acetylalanine (**62**), and *N*-acetylaspartic acid (**70**) either have very small reaction rates and do not give identified reaction products only maximum k_{rel}^{H} values were calculated in these cases. For all the other *N*-acetylamino acids (**63-66**), (**68**), (**69**) and (**71-76**) the values are likely to be accurate to within at least a factor of two, due to the same reasons as for the free amino acids (**12**), (**13**), (**15**), (**18**), (**21**), (**23**), (**25**), (**28-31**) and (**37-41**). The accuracy of the k_{rel}^{H} values is again high relative to the overall variation in the reactivity of the *N*-acetylamino acids (**63-66**), (**68**), (**69**) and (**71-76**) (over three orders of magnitude).

The reactions of the acetamides (**61-76**) tend to be faster at positions further from the α-centre. See, for example, the k_{rel}^{H} values of the terminal methyl groups of *N*-acetylalanine (**62**) (≤0.03), *N*-acetyl-α-aminobutyric acid (**72**), (0.50) and *N*-acetylnorleucine (**74**) (2.0). For the *N*-acetylamino acids with functionalised side-chains the rate of abstraction is the greatest for hydrogens nearer the centre of the side-chain. For *N*-acetyllysine (**66**) no reaction is observed at the α- and ε-positions, the reactivity at the β- and δ-positions is 0.27 and 0.22, respectively, and the reactivity at the γ-position is 0.86. For glutamic acid the reactivity at the α- and γ-positions is 0 and 0.02, respectively and the reactivity at the β-position is 0.08.

The similarity of the reactivity patterns between both the free (**12**), (**13**), (**15**), (**18**), (**21**), (**23**), (**25**), (**28-31**) and (**37-41**) and *N*-acetylated (**61-76**) amino acids is obvious. The k_{rel}^{H} values tend to be of a similar magnitude. For example, the k_{rel}^{H} values of the γ-methyl hydrogens of valine (**25**) are 0.17, and for *N*-acetylvaline (**63**) are 0.44. The k_{rel}^{H} value for the γ-methine hydrogen of leucine (**30**) is 5.2, and for *N*-acetylleucine (**65**) is 9.3. Although the measured k_{rel}^{H} values of the *N*-acetylated compounds are consistently higher than those of the free amino acids, this may not be significant. The exception to

this pattern is for ornithine (**23**) and lysine (**21**) where the k_{rel}^{H} values of the acetylated compounds (**71** and **66**) are noticeably lower than the free amino acids, but again this may not be of significance.

N-Acetylamino Acid	Reactivity per hydrogen (k_{rel}^{H}) at each position				
	α	β	γ	δ	ε
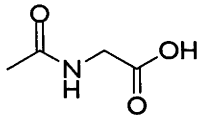 **61**	≤0.20				
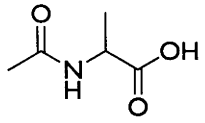 **62**	≤0.10	≤0.03			
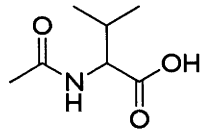 **63**	0	0.88	0.44		
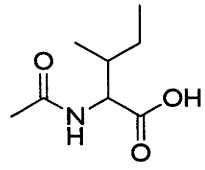 **64**	0	0.80	0.35 (CH_3) 1.3 (CH_2)	0.70	
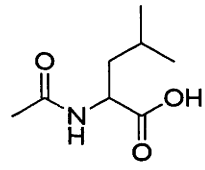 **65**	0	0	9.3	1.6	
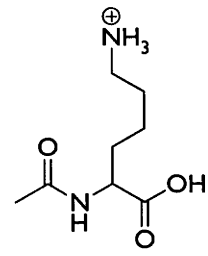 **66**	0	0.27	0.86	0.22	0
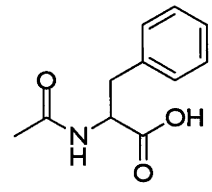 **68**	0	4.0			
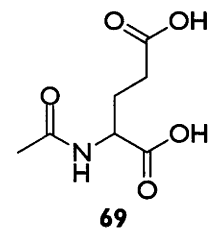 **69**	0	0.08	0.02		

Figure 3.21: Reactivity of the various hydrogens k_{rel}^{H} for the *N*-acetylamino acids (**61-66**) and (**68-76**)

N-Acetylamino Acid	Reactivity per hydrogen (k_{rel}^{H}) at each position				
	α	β	γ	δ	ε
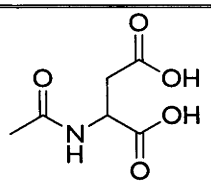 **70**	≤0.01	≤0.005			
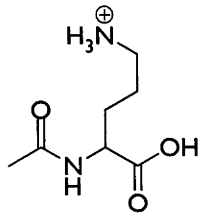 **71**	0	0.13	0.17	0	
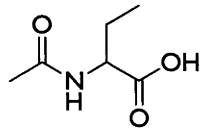 **72**	0	0.35	0.50		
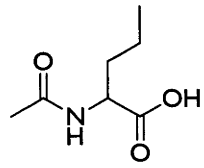 **73**	0	0	3.6	1.6	
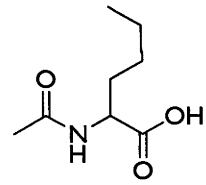 **74**	0	0	3.1	5.0	2.0
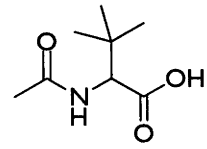 **75**	0	-	0.50		
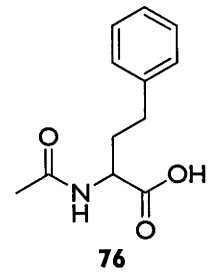 **76**	0	0	5.0		

Figure 3.21 *cont.*: Reactivity of the various hydrogens k_{rel}^{H} for the *N*-acetylamino acids (**61-66**) and (**68-76**)

The k_{rel}^{H} values suggest that the amide functionality in the *N*-acetylamino acids (**61-76**) is deactivating hydrogen abstraction in a similar manner to that which the protonated amino functionality does in the free amino acids (**12**), (**13**), (**15**), (**18**), (**21**), (**23**), (**25**), (**28-31**) and (**37-41**). For all of the *N*-acetylamino acids (**62-76**) excluding *N*-acetylglycine (**61**), the amount of reaction at the α-centre is negligible. For *N*-acetylglycine (**61**), the amount of reaction is appreciably higher, although it is not definitive that the reaction occurring is hydrogen atom abstraction at the α-centre.

3.6 Average Reactivity Per Hydrogen

The amides (**61-65**), (**68**) and (**72-76**) contain only alkyl side-chains that have deactivating groups at the α-position. They, like the analogous amino acids (**12**), (**13**), (**15**), (**18**), (**21**), (**23**), (**25**), (**28-31**) and (**37-41**) in the previous chapter, form a collection of compounds with similar structures, and again information about the reactivity of the hydrogens at each position on the side-chains can be obtained by comparison of their k_{rel}^{H} values. The process undertaken in Chapter 2, whereby the k_{rel}^{H} values of amino acids that only contained deactivating functional groups at the α-centre were compared, can be repeated for the *N*-acetylamino acids (**61-65**), (**68**) and (**72-76**).

Position	Reactivity per hydrogen (k_{rel}^{H})			
	Methyl	Methylene	Methine	Benzylic
α	-	≤ 0.20	≤ 0.10	-
β	≤ 0.03	≤ 0.35	0.80 0.88	4.0
γ	0.35 0.44 0.50 0.50	1.3 3.1 3.6	9.3	5.0
δ	0.70 1.6 1.6	5.0		
ε	2.0			

Figure 3.22: Reactivity per hydrogen (k_{rel}^{H}) of the amino acids (**61-65**), (**68**) and (**72-76**)

In Figure 3.22, the k_{rel}^{H} values of amino acids without deactivating functional groups on their side-chains (**61-65**), (**68**) and (**72-76**) are tabulated. The two cases of β-methine hydrogens have k_{rel}^{H} values are within 10 percent, and the four examples of the γ-methyl hydrogens have k_{rel}^{H} values within a factor of two. The three examples of γ-methylene hydrogens have k_{rel}^{H} values within a factor of three, and the three instances of δ-methyl hydrogens have k_{rel}^{H} values within a factor of two. As the k_{rel}^{H} values for the *N*-acetylamino acids that are being compared (**61-65**), (**68**) and (**72-76**) vary in reactivity over a factor of more than 100, it can be concluded that the variation in k_{rel}^{H} values between hydrogens of a given type (less than a factor of three) are relatively small. An average value for each type of hydrogen can be determined and a table of these average k_{rel}^{H} values can be constructed (Figure 3.23).

Position	Average reactivity per hydrogen			
	Methyl	Methylene	Methine	Benzyl
α	-	≤ 0.20	≤ 0.10	-
β	≤ 0.03	≤ 0.35	0.84	4.0
γ	0.45	2.6	9.3	5.0
δ	1.3	5.0		
ε	2.0			

Figure 3.23: Average k_{rel}^{H} values for various types of hydrogens in *N*-acetylamino acids

For the *N*-acetylamino acids (**61-65**), (**68**) and (**72-76**) (Figure 3.23), there is an increase in reactivity from γ-methyl hydrogens (0.45) to γ-methylene hydrogens (2.6) to γ-methine hydrogens (9.3) which is consistent with the difference in stability of the generated radicals. This trend is shown for the β- and δ-hydrogens also. For each type of hydrogen there is an increase in reactivity as the distance from the α-centre is increased. For example, on comparison of the reactivity of the methyl hydrogens, it can be shown that the reactivity of those at the γ-position relative to those at the β-position is increased by more than an order of magnitude. The reactivity for the hydrogens at the δ-position compared to those at the γ-position is higher a factor of three. The reactivity of hydrogens at the δ-position compared to those at the ε-position is greater by around 65 percent. For the methylene hydrogens the reactivity

of the γ-position compared to the α- and β-positions is increased by a factor of seven, and the reactivity of hydrogens at the δ-position compared to those at the γ-position is greater by almost a factor of two. For the methine hydrogens the reactivity of the β-position compared to the α-position is faster by a factor of eight and the difference in reactivity between the γ- and β-positions more than a factor of seven. The difference in reactivity of the benzylic hydrogens at the γ- position compared to the β-positions slight increase.

Position	Average reactivity per hydrogen			
	Methyl	Methylene	Methine	Benzyl
α	-	≤ 0.05	≤ 0.10	-
β	≤ 0.03	≤ 0.05	0.54	0.5
γ	0.13	0.91	5.2	1.4
δ	1.1	3.7		
ε	2.3			

Figure 3.24: Average k_{rel}^{H} values for various types of hydrogens in free amino acids

It can be seen that the table of average k_{rel}^{H} values for the *N*-acetylamino acids (**61-65**), (**68**) and (**72-76**) (Figure 3.23) shows the same trends as the table for the free amino acids (**12**), (**13**), (**15**), (**25**), (**28**), (**30**), (**31**) and (**38-40**) (Figure 3.24). This suggests that these results are also indicative of a polar effect.

The explanation of this effect is the same for both the free (**12**), (**13**), (**15**), (**18**), (**21**), (**23**), (**25**), (**28-31**) and (**37-41**) and *N*-acetylated amino acids (**61-76**). The amide group, while being π-electron donating which would in theory stabilise a radical at the α-centre, is inductively electron withdrawing. This would, like the protonated amine in the free amino acids (**12**), (**13**), (**15**), (**18**), (**21**), (**23**), (**25**), (**28-31**) and (**37-41**), effect carbons situated further away by reducing the ease of formation of partial positive charges which are required by the transition state. As with the free amino acids (**12**), (**13**), (**15**), (**18**), (**21**), (**23**), (**25**), (**28-31**) and (**37-41**), it would be expected that the effect would diminish with distance, and for it to reach a point where no effect is seen, and this is consistent with the k_{rel}^{H} values for the δ- and ε-methyl hydrogens (Figure 3.23) which are relatively close in reactivity. Based on the similarity of the k_{rel}^{H} values

for the ε-methyl hydrogens in both series of compounds it is not likely that the polar effect extends to the ε-position for either free or *N*-acetylamino acids.

The work described in this chapter has shown that a polar effect qualitatively identical to that shown in Chapter 2 appears to operate in *N*-acetylamino acids (**61-76**) which controls the position of hydrogen atom abstraction by chlorine radicals. The magnitude of the reactivity of the *N*-acetylamino acids (**61-76**) has been quantified and compared to that of the free amino acids.

Chapter 4: Results and Discussion

Regioselective Hydrogen Atom Transfer from Peptides to Chlorine

In Chapters 2 and 3, the predictability of k_{rel}^{H} values between amino acids and *N*-acetyl-amino acids was noted. This suggests that for a given amino acid or peptide, the regioselectivity of hydrogen abstraction can be calculated by comparing the rate of abstraction of a particular hydrogen with the sum of the rates of hydrogen abstraction for the whole system. For any simple peptide, the reactivities of free amino acids (as described in Chapter 2) serve as a model for the reactivity of the *N*-terminal residue and the reactivities of *N*-acetylamino acids (as described in Chapter 3) serve as models for the central and *C*-terminal amino acids.

The first tripeptide selected to test this hypothesis was glycylalanylphenylalanine (**102**). In this molecule the reactivity at the benzylic position would be expected to dominate. The regioselectivity of reaction can be predicted by comparing the k_{rel}^{H} values for these hydrogens with the sum of the k_{rel}^{H} values of each of the hydrogen types taken from Figures 2.36 and 3.23 (Figure 4.1).

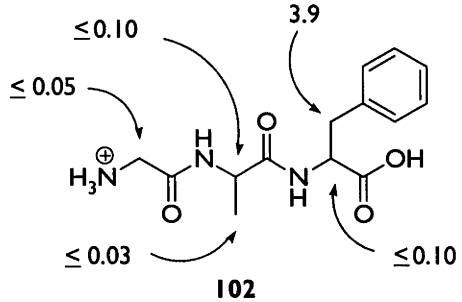

102

Regioselectivity of reaction at the benzylic position ≥ 95%

$$= \frac{2 \times 3.9 \times 100}{(2 \times \leq 0.05) + \leq 0.10 + (3 \times \leq 0.03) + \leq 0.10 + (2 \times 3.9)}$$

Figure 4.1: k_{rel}^{H} values and calculated regioselectivity for the reaction of the tripeptide (**102**)

From the calculation in Figure 4.1, we can therefore predict that at least 95% of the hydrogen abstraction should occur at the β-position of the phenylalanine residue.

The second tripeptide selected was phenylalanylhomophenylalanylalanine (**103**). This peptide has the possibility of reacting at more than one benzylic position. However,

from the k_{rel}^{H} values it can be determined that more than 83% of the chlorination should occur at the benzylic position on the homophenylalanine residue (Figure 4.2).

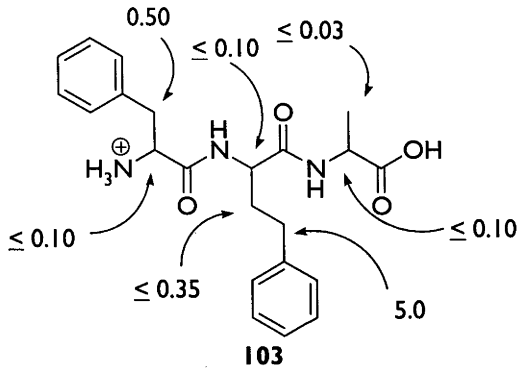

103

Regioselectivity of reaction at the γ-benzylic position ≥ 83%

$$= \frac{2 \times 5.0 \times 100}{\leq 0.10 + (2 \times 0.50) + \leq 0.10 + (2 \times \leq 0.35) + (2 \times 5.0) + \leq 0.10 + (3 \times \leq 0.03)}$$

Figure 4.2: k_{rel}^{H} values and calculated regioselectivity for the reaction of the tripeptide (**103**)

The third tripeptide selected was phenylalanylleucylalanine (**104**). In this peptide, based on the results in Chapters 2 and 3, the reactivity of hydrogens on the long alkyl side-chain would somewhat anomalously be predicted to be more reactive than those at the benzylic position.

From the knowledge of k_{rel}^{H} values, it can be predicted that around 48% of the hydrogen abstraction should take place at the tertiary γ-position (Figure 4.3). It can also be predicted by using an analogous calculation that a similar amount (41%) of δ-chlorination would also occur (Figure 4.3).

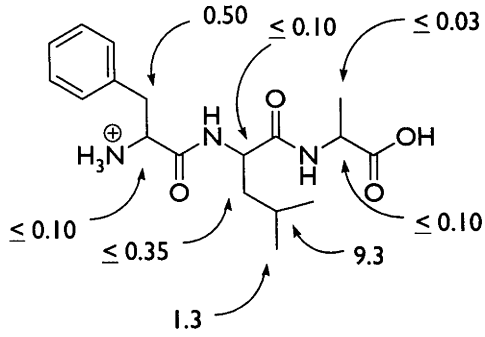

104

Regioselectivity of reaction at the γ-position of the leucine residue ≥ 48%

$$= \frac{9.3 \times 100}{\leq 0.10 + (2 \times 0.50) + \leq 0.10 + (2 \times \leq 0.35) + 9.3 + (6 \times 1.3) + \leq 0.10 + (3 \times \leq 0.03)}$$

Regioselectivity of reaction at the δ-position of the leucine residue ≥ 41%

$$= \frac{6 \times 1.3 \times 100}{\leq 0.10 + (2 \times 0.50) + \leq 0.10 + (2 \times \leq 0.35) + 9.3 + (6 \times 1.3) + \leq 0.10 + (3 \times \leq 0.03)}$$

Figure 4.3: k_{rel}^{H} values and calculated regioselectivity for the reaction of the tripeptide (**104**)

The final tripeptide selected for this study was *N*-(α-aminobutanoyl)-norvalylalanine (**105**) (Figure 4.4) which contains three residues with different length *n*-alkyl side-chains; the alanine residue has one carbon in the side chain, the norvaline residue, three, and the α-aminobutyric acid residue, two. Calculations suggest that the reactivity of hydrogens on longer side-chains should dominate over hydrogen abstraction reactions on shorter side-chains.

From the k_{rel}^{H} values that have been determined, it is predicted that more than 50% of the chlorination should occur at the γ-position on the norvaline residue. Based on the same methodology, it can be calculated that at least 37% of the δ-chlorinated product would be expected to be formed.

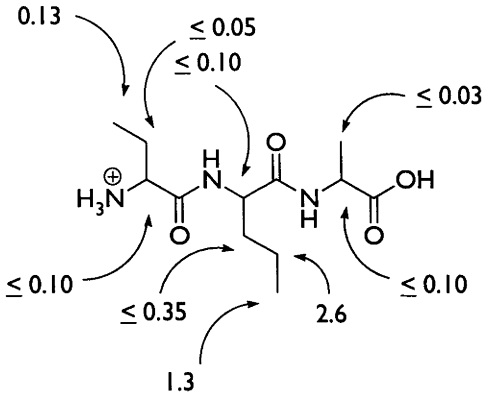

105

Regioselectivity of reaction at the γ-position of the norvaline residue ≥ 50%

$$= \frac{2 \times 2.6 \times 100}{\leq 0.10 + (2 \times \leq 0.05) + 0.13 + \leq 0.10 + (2 \times \leq 0.35) + (2 \times 2.6) + (3 \times 1.3) + \leq 0.10 + (3 \times \leq 0.03)}$$

Regioselectivity of reaction at the δ-position of the norvaline residue ≥ 37%

$$= \frac{3 \times 1.3 \times 100}{\leq 0.10 + (2 \times \leq 0.05) + 0.13 + \leq 0.10 + (2 \times \leq 0.35) + (2 \times 2.6) + (3 \times 1.3) + \leq 0.10 + (3 \times \leq 0.03)}$$

Figure 4.4: k_{rel}^{H} values and calculated regioselectivity for the reaction of the tripeptide (**105**)

The tripeptides (**102-105**) studied were either commercially available or synthesised to order using solid phase peptide syntheses. Details are given in the Experimental. All peptides used were homochiral, with each residue except glycine having the *S*-stereochemistry at the α-centre.

To gauge their level of reactivity towards chlorination a suitable compound that would be expected to have a similar reactivity was selected, and used to determine the correct period of reaction. The most obvious candidates for these studies were the *N*-acetyl derivatives of the fastest reacting residues in each of the peptides (**102-105**). To determine the conditions for reaction of 100 mg of the peptides (**102-105**), an equimolar amount of the appropriate *N*-acetylamino acid, (**68**), (**76**), (**65**) or (**73**), was chlorinated until around 50% of the starting material had reacted. These experiments showed that depending on the peptide (**102-105**), between 0.5 and 1.5 minutes was required.

The requirement for incomplete reaction has been noted before. Kollonitsch *et al.*,[109] reported that a clean product was best obtained when 0.7-0.8 mole equivalents of Cl_2 were used.

With the approximate length of reaction time for the peptides (**102-105**) determined, a solution of 100 mg of each in trifluoroacetic acid (~5 mL) saturated with Cl_2 was irradiated with a 300 W sunlamp for the required time period. Details are provided in the Experimental. The solutions were then purged of chlorine with nitrogen and the solvent removed under reduced pressure.

The ^{1}H NMR spectrum of the crude reaction mixture of chlorinated glycylphenylalanyl-phenylalanine (**102**) shows chlorination at the β-position of the phenylalanine residue. This is evidenced by the distinct doublet resonances at ~δ4.5 and 5.0 ppm which have very similar chemical shifts to the α- and β-proton resonances of *N*-acetyl-β-chlorophenylalanine (**90**). There was no evidence for chlorination occurring at any other position. The product (**106**) was isolated using semi-preparative HPLC and a 52% isolated yield was obtained, or 78% corrected yield based on recovered starting material. As the starting peptide (**102**) is homochiral, the product (**106**) can possibly exist as two diastereomers. The ^{1}H NMR spectrum suggests, however, that only one stereoisomer is formed, as was the case with *N*-acetylphenylalanine (**68**).

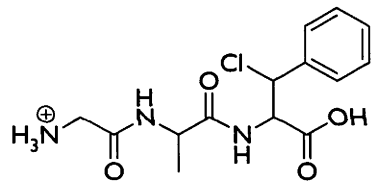

106

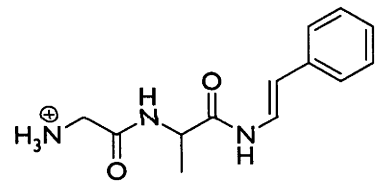

107

Glycylalanyl-*β*-chlorophenylalanine (**106**) is unstable, and quantitative conversion to the corresponding phenyleneamide (**107**) occurred on standing in solution at room temperature over several days. This is evidenced by the disappearance of the characteristic resonances of the β-chlorophenylalanine residue, specifically the α- and β-proton resonances as described above, and the appearance of resonances typical of an alkene at ~δ6.3 and 7.4 ppm. The *trans*-stereochemistry of the eneamide (**107**) is demonstrated by the coupling for the alkenyl protons of 14 Hz.

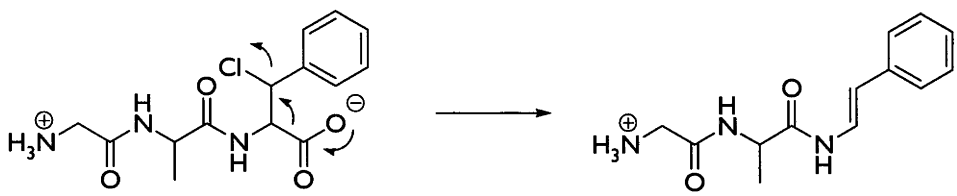

106 **107**

Figure 4.5: Conversion of the chloride (**106**) to the eneamide (**107**)

The elimination could proceed by any of a number of possible mechanisms, the most likely being illustrated in Figure 4.5, whereby the peptide decarboxylates, with subsequent or simultaneous loss of chloride.

Chlorination of the second peptide (**103**) occurred at the γ-position of the homophenylalanine residue as evidenced from the ^{1}H NMR spectrum of the major product (**108**) with a doublet of doublets at ~δ5.0 ppm typical of the γ-benzylic hydrogen. The resonances due to the β-protons of the phenylalanine residue are still present confirming that the product is not the β-benzylic chlorinated regioisomer. Semi-preparative HPLC was used to isolate the product (**108**) in a 54% yield, or 69% corrected yield after taking into account recovered starting material. Only one set of resonances was seen in the ^{1}H NMR spectrum, although is seems likely that the chloride (**108**) is a mixture of diastereomers.

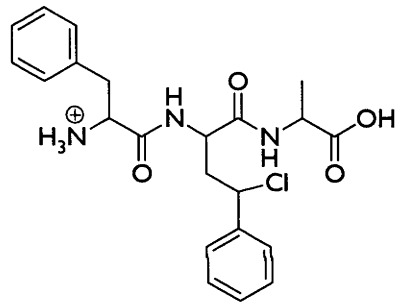

108

It can be seen from the ^{1}H NMR spectrum of the product mixture that chlorination of the third peptide (**104**), using the conditions identified with *N*-acetylleucine (**65**), occurred at both the γ- and δ-positions of the leucine residue as shown by the respectively diagnostic singlet methyl resonance at ~δ1.5 ppm and pair of doublet chloromethylene resonances at ~δ3.6 ppm. Semi-preparative HPLC was used to isolate phenylalanyl-γ-chloroleucylalanine (**109**), in a 15% yield, or 44% after taking into account recovered starting material. Other products formed were not isolated, however, the ^{1}H NMR spectrum of the crude product mixture showed that the chlorides (**109**) and (**110**) were produced in approximately equal amounts, the latter as a 1:1 mixture of diastereomers. No significant amounts of other products were apparent in the spectrum.

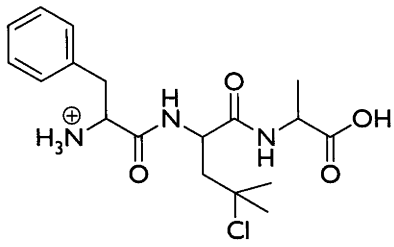

109

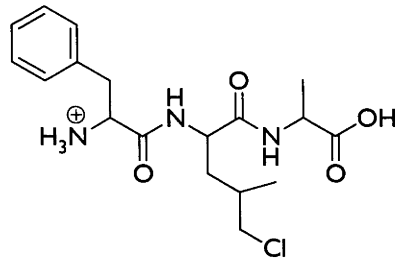

110

Analysis of the mixture from chlorination of *N*-(α-aminobutanoyl)-norvalylalanine (**105**) indicated that chlorination occurred at the γ- and δ-positions of the norvaline residue. Isolation of these products was again performed using semi-preparative HPLC to give *N*-(α-aminobutanoyl)-γ-chloronorvalylalanine (**111**) in a 9% yield, or 29% yield based on recovered starting material, and *N*-(α-aminobutanoyl)-δ-chloronorvalylalanine (**112**) in an 8% yield, or 27% yield based on recovered starting material. The ^{1}H NMR spectrum of *N*-(α-aminobutanoyl)-γ-chloronorvalylalanine (**111**) shows that each diastereomer is formed in equal amounts, which was determined by examination of the resonances of the β-methyl hydrogens of the alanine residues. The ^{1}H NMR spectrum of *N*-(α-aminobutanoyl)-δ-chloronorvalylalanine (**112**) shows resonances analogous to those of *N*-acetyl-δ-chloronorvaline (**96**) and is completely consistent with the assigned structure. No significant amounts of other products were apparent in the spectrum of the crude product.

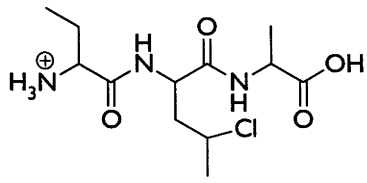

111

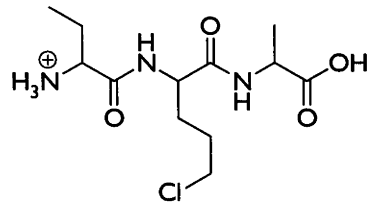

112

As summarised in Figure 4.6, in all cases the major products of chlorination of the peptides (**102-105**) were correctly predicted. The corrected yields were all reasonably close to those predicted. The differences are likely to be largely due to product loss during the isolation process rather than significant differences in the reactivity to what was expected. These examples demonstrate that the k_{rel}^{H} data from Chapters 2 and 3 is sufficiently accurate as to be used to predict the regioselectivity of chlorination of small peptides.

Peptide	Isolated Product (Calculated Yield / Isolated Yield / Corrected Yield)
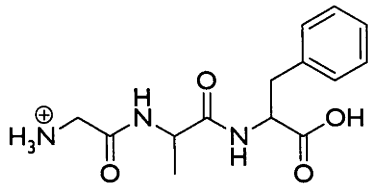 **102**	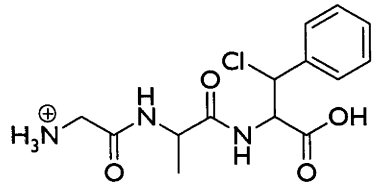 **106** 95% / 52% / 78%
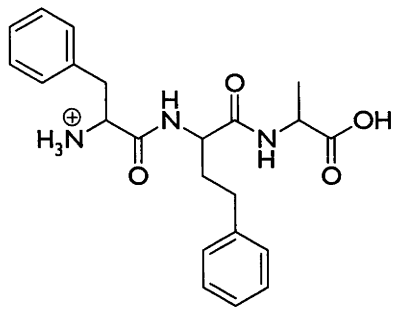 **103**	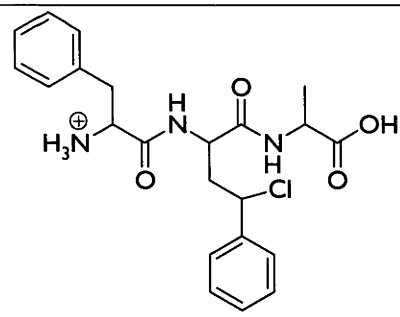 **108** 83% / 54% / 69%
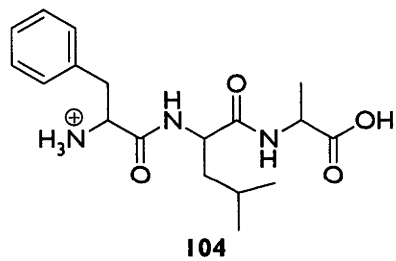 **104**	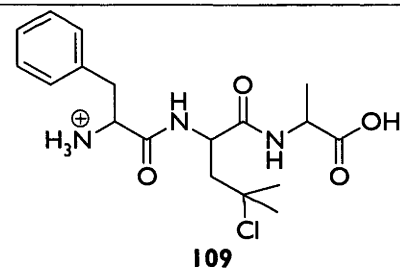 **109** 48% / 15% / 44%
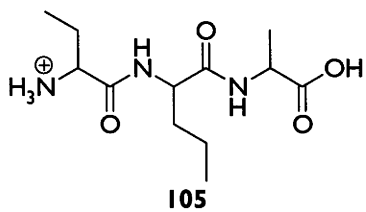 **105**	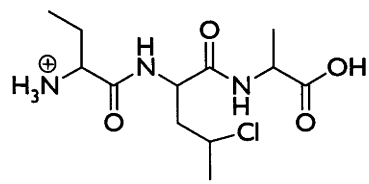 **111** 50% / 9% / 29% 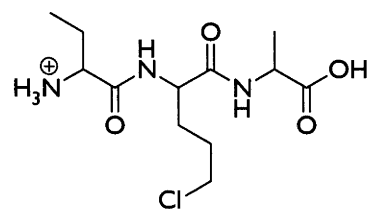 **112** 37% / 8% / 27%

Figure 4.6: Predicted, isolated and corrected yields of the products from chlorination of the peptides (**102-105**)

Chapter 5: Results and Discussion

Radical Stabilisation and its Affect on Reaction Rate

It has been shown in Chapters 2 and 3 that when the site of hydrogen abstraction is further from the α-centre, the reactivity per hydrogen increases. In the work described in this Chapter, the relationship between radical stability and rate, and the presence or absence of a polar effect in the transition state is investigated. The contribution of the stability of the radical generated to the reactivity of the hydrogen abstraction reaction was determined by calculating Radical Stabilisation Energies (RSEs). The RSEs are, as discussed in the Introduction, determined from differences in bond dissociation energies (BDEs). The BDEs were calculated at the RB3-LYP/6-311+G(3df,2p)//UB3-LYP/6-31G(d) level of theory and are listed in Figures 5.1 and 5.2 for various C-H bonds in free amino acids and *N*-acetylated amino acids, respectively. If a polar effect did not exist in these systems it would be expected that there would be a strong correlation between the rate of reaction (which is related to the activation energy) and the stability of the formed radical (which is related to the change in enthalpy of the reaction). In the presence of a polar effect a disparity between the k_{rel}^{H} values and the RSE values would be seen.

Resultant Radical	Bond Dissociation Energy (kJ mol^{-1})	Resultant Radical	Bond Dissociation Energy (kJ mol^{-1})
$^{\bullet}CH_3$	428.8	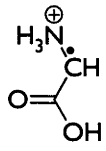	413.3
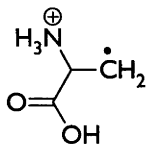	421.0	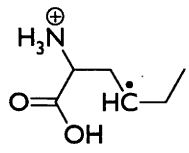	388.2
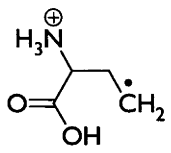	409.5	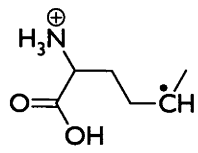	373.8
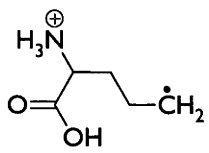	400.6	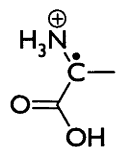	383.6

Figure 5.1: Bond Dissociation Energies (BDEs) for a range of C-H bonds in free amino acids

Resultant Radical	Bond Dissociation Energy (kJ mol^{-1})	Resultant Radical	Bond Dissociation Energy (kJ mol^{-1})
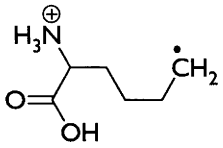	400.0	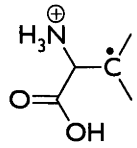	377.4
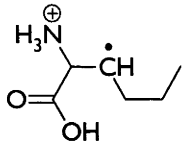	396.0	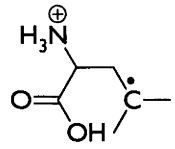	371.5

Figure 5.1 *cont.*: Bond Dissociation Energies (BDEs) for a range of C-H bonds in free amino acids

Resultant Radical	Bond Dissociation Energy (kJ mol^{-1})	Resultant Radical	Bond Dissociation Energy (kJ mol^{-1})
$^{\bullet}CH_3$	428.8	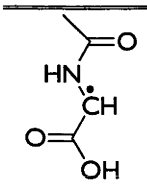	327.8
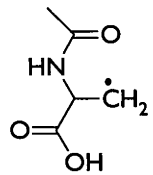	416.1	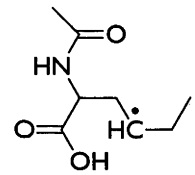	397.0
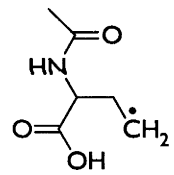	409.9	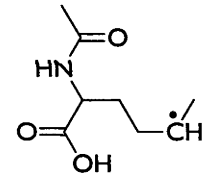	396.2
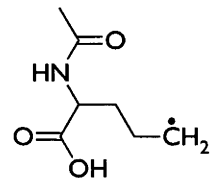	412.5	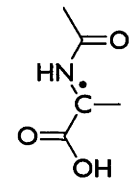	348.7
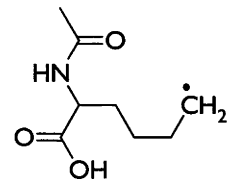	412.0	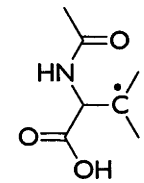	381.0
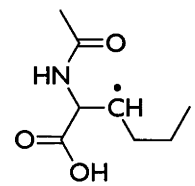	401.0	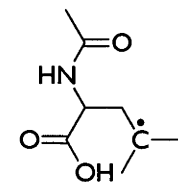	375.7

Figure 5.2: Bond Dissociation Energies (BDEs) for a range of C-H bonds in *N*-acetylamino acids

Tables which compare the RSEs and k_{rel}^{H}, Figures 5.3 and 5.4, can thus be easily generated using the data in Figures 5.1 and 2.36, and 5.2 and 3.23, respectively.

Position	Methyl		Methylene		Methine	
	RSE kJ mol^{-1}	k_{rel}^{H}	RSE kJ mol^{-1}	k_{rel}^{H}	RSE kJ mol^{-1}	k_{rel}^{H}
α	-	-	15.5	≤ 0.05	45.2	≤ 0.10
β	7.8	≤ 0.03	32.8	≤ 0.05	51.4	0.54
γ	19.3	0.13	40.6	0.91	57.3	5.2
δ	28.2	1.1	55.0	3.7		
ε	28.8	2.3				

Figure 5.3: Radical Stabilisation Energies (RSEs) for free amino acid radicals, and the corresponding k_{rel}^{H} values of the abstraction reactions

Position	Methyl		Methylene		Methine	
	RSE kJ mol^{-1}	k_{rel}^{H}	RSE kJ mol^{-1}	k_{rel}^{H}	RSE kJ mol^{-1}	k_{rel}^{H}
α	-	-	101.0	≤ 0.20	80.1	≤ 0.10
β	12.7	≤ 0.03	27.8	≤ 0.35	47.8	0.84
γ	18.9	0.45	31.8	2.6	53.1	9.3
δ	16.3	1.3	32.6	5.0		
ε	16.8	2.0				

Figure 5.4: Radical Stabilisation Energies (RSEs) for *N*-acetylamino acid radicals, and the corresponding k_{rel}^{H} values of the abstraction reactions

If the RSEs and k_{rel}^{H} values of the γ-position of free amino acids in Figure 5.3 are compared, it can be seen that there is an increase in RSE between primary (19.3 kJ mol^{-1}), secondary (40.6 kJ mol^{-1}) and tertiary (57.3 kJ mol^{-1}) radicals. This correlates to the increase in k_{rel}^{H} between primary (0.13), secondary (0.91) and tertiary (5.2) hydrogens. This is also seen in the RSEs and k_{rel}^{H} values for the γ-position of *N*-acetylamino acids (Figure 5.4), with RSE values for the primary, secondary and tertiary

radicals of 18.9 kJ mol^{-1}, 31.8 kJ mol^{-1}, 53.1 kJ mol^{-1}, respectively, and k_{rel}^{H} values of the primary, secondary and tertiary hydrogens of 0.45, 2.6 and 9.3, respectively.

If the data for the β-positions are compared against these values, however, the RSEs and k_{rel}^{H} values do not correlate. The RSE for the β-methylene derived radical in the free amino acid is 32.8 kJ mol^{-1}. This value lies between the RSEs of the γ-methyl derived radical (19.3 kJ mol^{-1}) and the γ-methylene derived radical (40.6 kJ mol^{-1}) so it might be expected that the k_{rel}^{H} value would also lie between the corresponding two (*i.e.*, between 0.13 and 0.91). However, the k_{rel}^{H} for a β-methylene hydrogen is ≤0.05. This also occurs for the analogous situation in the *N*-acetylated compounds. In this case it would be expected that the β-methylene k_{rel}^{H} value would lie between those of the γ-methyl (0.45) and γ-methylene (2.6), rather than have the measured value of ≤0.35. The k_{rel}^{H} values for the β-methine hydrogens are also noticeably lower than expected when analysed in the same manner.

The data for the α-positions can be analysed in a similar fashion. The RSE for the α-methine radical in the free amino acid is 45.2 kJ mol^{-1}. This value is between the RSEs of the γ-methylene (40.6 kJ mol^{-1}) and γ-methine (57.3 kJ mol^{-1}) radicals. If there was a direct correlation between RSE and k_{rel}^{H} it would be expected that the k_{rel}^{H} of an α-methine hydrogen would be between 0.91 and 5.2, however it is ≤0.10. For the *N*-acetylated compounds the disparity is even more pronounced. The RSEs for the α-methylene and α-methine radicals are 101.0 and 80.1 kJ mol^{-1}, respectively. These are the largest RSE values of all those calculated by a substantial amount. No other radical studied here has an RSE over 60 kJ mol^{-1}. If a direct correlation between RSE and k_{rel}^{H} existed the k_{rel}^{H} values for these positions would be well over 10.0 whereas in reality the reactivity as these positions is negligible.

As was stated earlier, a transition state effect, such as a polar effect, would be associated with a disparity between the k_{rel}^{H} and RSE values. Thus it is seen that there is a significant effect at both the α- and β-positions in both free and *N*-acetylated amino acids. The effect in the free amino acids appears to be stronger, since for positions that have similar RSE values for both free and *N*-acetylated compounds, such as the γ-methyl position (18.9 kJ mol^{-1} for the *N*-acetylated compound and 19.3 kJ mol^{-1} for the free amino acid), the k_{rel}^{H} values for the *N*-acetylated compounds are noticeably larger (0.45 compared to 0.13).

It should be noted that the effect of solvent is a factor that has not been investigated in this study. RSEs are based on gas phase calculations, therefore effects associated with solvation may be affecting the radical stabilities. This is likely to be particularly relevant for the protonated compounds. However, calculations which use a continuum to model water (PCM) do not show any significant changes for the BDEs of alanine (**13**) and α-aminobutyric acid (**15**), altering them by only 0.2 and 0.5 kJ mol^{-1}, respectively.

When *n*-pentane is used as a model for long-chain alkanes the RSEs for $^{\bullet}CH_2(CH_2)_3CH_3$ and $CH_3CH_2{}^{\bullet}CHCH_2CH_3$ are calculated to be 18.4 kJ mol^{-1} and 34.4 kJ mol^{-1}, respectively. These values agree well with the RSEs of the *N*-acetylamino acids with the longer side chains. However, they differ significantly from the RSEs of the protonated amino acids, which suggests that the protonated amine is effecting radical stability on amino acids with longer side-chains. The higher RSE values suggest that there is an increase in the stability due to the interaction with the protonated amino group.

Such an interaction can be demonstrated; below (Figure 5.5) is a graphical representation of the lowest energy conformer found for the δ-centred radical of norvaline (**38**) that has been used to compute the RSEs and BDEs. It can be seen that for this radical there is an apparent interaction of an N–H bond with the radical centre.

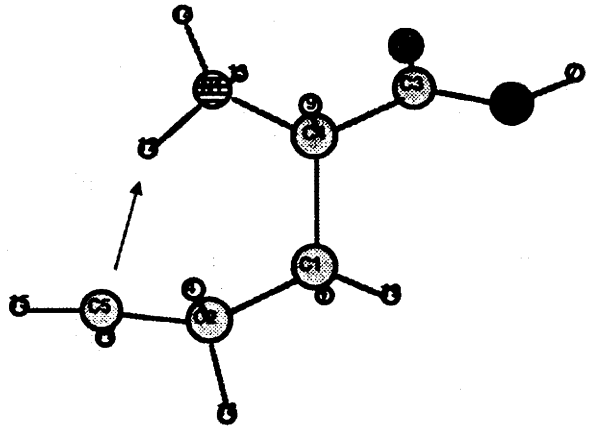

Figure 5.5: Lowest energy conformation for the δ-centred radical of norvaline (**38**)

To obtain more information about such interactions, the energy for the following process was examined (RB3-LYP/6-311+G(3df,2p)//UB3-LYP/6-31G(d)):

$$CH_3CH_2^{\bullet} + {}^{\oplus}NH_3CH_2COOH \rightarrow CH_3CH_2^{\bullet}\cdots\cdots H^{\oplus}NH_2CH_2COOH$$

The resultant interaction energy for $CH_3CH_2^{\bullet}\cdots\cdots H^{\oplus}NH_2CH_2COOH$ is –37.5 kJ mol^{-1}. Thus, if analogous interactions are occurring in the radicals of protonated amino acids we would expect the stability to increase by up to 37.5 kJ mol^{-1}. This is qualitatively consistent with the calculated RSEs in the protonated amino acids being about 15 kJ mol^{-1} higher than the long-chain estimate of 18 kJ mol^{-1}, but quantitatively the effect is smaller. It is possible that this is due to the conformational distortions that are required in attempting to achieve the optimum interaction. Comparisons of the distances between the radical centres and the nitrogen-attached hydrogens in the model systems and the protonated amino acids show that the interactions in the model system are slightly shorter than in the protonated amino acid radicals, which possibly indicates stronger interactions.

The RSEs calculated for the various hydrogen types for conformations of protonated and *N*-acetyl amino acids in which the alkyl side chain is in an extended chain conformation are more consistent with what is expected for radicals on an alkyl chain as the chain is lengthened. That is, they are converging towards similar values and these values are similar to those obtained for an isolated extended alkyl chain. This shows that in the absence of the interaction of the protonated amine and the radical centre and associated conformational strain, the RSEs of the terminal methyl of protonated amino acids converge to approximately 15 kJ mol^{-1}. However, it would be expected that the protonated amino acids will assume the lower-energy folded conformations and the RSEs will converge to the higher value of approximately 30 kJ mol^{-1}, at least in the gas phase.

In previous Chapters, the chlorination of both free amino acids and the acetylated analogues have been shown to be affected by a strong polar effect, which has been quantified. The stabilities of the corresponding radicals have now been calculated, and the lack of correlation between the RSEs and k_{rel}^{H} values, particularly at the α-centres is highly suggestive of a polar effect operating. These results indicate that the energy of the transition state does not reflect that of the resultant radical and that other factors control the rate of abstraction for hydrogens at positions nearer to the α-centre. This

behaviour is consistent with that expected for highly reactive electrophilic radicals, such as the chlorine radical.

Chapter 6: Results and Discussion

Hydrogen Atom Transfer from Amino Acids and *N*-Acetylamino Acids to Oxygen-Centred Radicals

As a complement to the chlorination studies it was decided to investigate the reactions of amino acids and peptides with oxygen centred radicals as hydrogen abstracting species. Such systems are chemically more similar to those found biologically. Water was used for the same reason. It was anticipated that an oxygen-centred radical would abstract a hydrogen from an amino acid, and the resulting radical would subsequently react with triplet oxygen, forming the corresponding peroxyl radical, which would then give rise to the corresponding hydroperoxide (Figure 6.1).

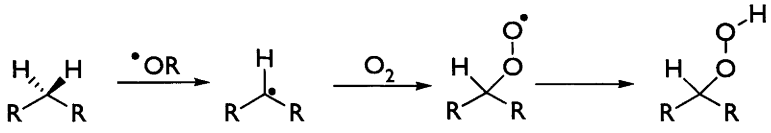

Figure 6.1: Formation of hydroperoxides via radical oxidation

The reactivity of compounds could thus be monitored by observation of products in an analogous manner to that described in earlier chapters. It was decided to use hydrogen peroxide as the initial radical source, which would yield hydroxyl radicals upon photolysis. The oxygen-centred radicals would thus be hydroxyl radicals and the chain propagating peroxyl radicals. From these requirements, a system was developed in which amino acids were irradiated in solutions of D_2O_2 in D_2O (acidified with a small amount of TFA) in a quartz NMR tube so that the mixtures could then be studied directly using NMR techniques.

The choice of amino acids with which to study oxygen-centred radical hydrogen atom abstraction was affected by the same factors as for the chlorinations, however amino acids that contain hydroxyl groups were also suitable for the reaction conditions so serine (**113**), homoserine (**114**), and threonine (**115**) were added to the list. Phenylalanine (**28**) and homophenylalanine (**41**) proved to be unsuitable for this study as their reaction mixtures showed a peculiar discolouration, and so were excluded.

Thus, a set of seventeen compounds compromising glycine (**12**), alanine (**13**), valine (**25**), isoleucine (**31**), leucine (**30**), lysine (**21**), proline (**29**), glutamic acid (**18**), aspartic

acid (**37**), ornithine (**23**), α-aminobutyric acid (**15**), norvaline (**38**), norleucine (**39**), *tert*-leucine (**40**), serine (**113**), homoserine (**114**) and threonine (**115**). For the *N*-acetylated amino acids, the analogous series (**61-67**), (**69-75**) and (**116-118**) was selected. As for the chlorinations, the *S*-isomers of the naturally occurring amino acids were generally selected for the experiments; this is, as before, primarily due to their availability. Non-natural amino acids were used as racemates. Details are given in the Experimental. The chirality is not crucial to the experiments and so stereochemistry is not depicted in the structures.

6.1 Relative Rates of Reaction

The process used to determine the relative rates of reaction of the amino acids (**12**), (**13**), (**15**), (**18**), (**21**), (**23**), (**25**), (**29-31**), (**37-40**), and (**113-115**) and the acetamides (**61-67**), (**69-75**) and (**116-118**) was similar to that used for the chlorinations, as described in Chapters 2 and 3. Because of the unsuitability of phenylalanine (**28**), *tert*-leucine (**40**) was instead selected as the standard against which the other compounds were compared. It possesses the favourable attributes of moderate reactivity and a simple ^{1}H NMR spectrum. To determine a k_{rel} value, approximately equal amounts of two amino acids were dissolved in dilute D_2O_2 in D_2O in a quartz NMR tube. TFA (~0.05 mL) was added to lower the pH. The NMR tube was then fitted with a WILMAD® coaxial insert containing benzoic acid in TFA as a reference. A ^{1}H NMR spectrum was obtained before the sample was irradiated in a photochemical reactor fitted with 16 x 254 nm bulbs for between 20 and 60 minutes depending on the compounds, then a second NMR spectrum was obtained. From the two ^{1}H NMR spectra, values of starting materials reacted and in some cases products formed were obtained, which were used as for the chlorinations described previously. The k_{rel} for *tert*-leucine (**40**) is defined as unity. The results are summarised in Figures 6.2 and 6.3.

Amino Acid	k_{rel}	Amino Acid	k_{rel}
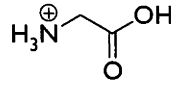 **12**	0.05	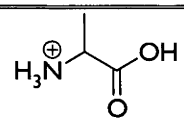 **13**	0.10
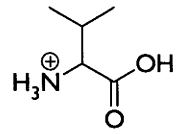 **25**	0.98	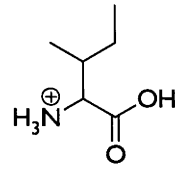 **31**	3.2
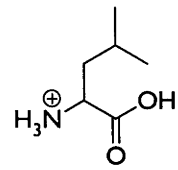 **30**	2.4	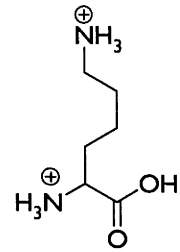 **21**	2.0
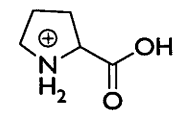 **29**	0.73	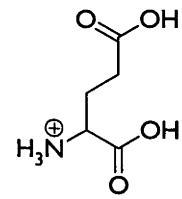 **18**	0.25
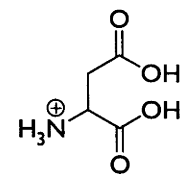 **37**	≤ 0.01	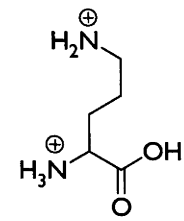 **23**	0.41
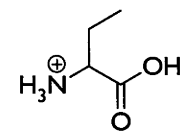 **15**	1.0	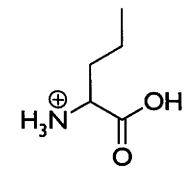 **38**	2.6
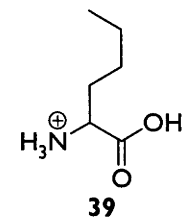 **39**	3.4	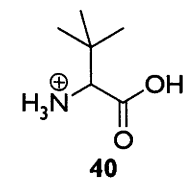 **40**	1.0

Figure 6.2: Relative rates of reaction for the amino acids

(12), **(13)**, **(15)**, **(18)**, **(21)**, **(23)**, **(25)**, **(29-31)**, **(37-40)**, and **(113-115)**

Amino Acid	k_{rel}	Amino Acid	k_{rel}
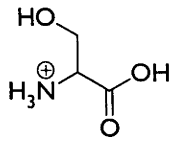 **113**	0.35	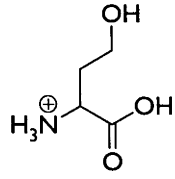 **114**	0.91
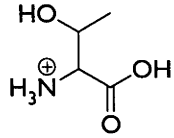 **115**	1.0		

Figure 6.2 *cont.*: Relative rates of reaction for the amino acids **(12)**, **(13)**, **(15)**, **(18)**, **(21)**, **(23)**, **(25)**, **(29-31)**, **(37-40)**, and **(113-115)**

In Figure 6.2, the general trends for the k_{rel} values for hydrogen abstraction by oxygen-centred radicals appear to be similar to those of the k_{rel} values for hydrogen abstraction by chlorine. There is a deactivation of the α- and, to some extent, β-positions. This can be seen, for example, by the low reactivity shown by glycine (**12**) (0.05) and alanine (**13**) (0.10). Functional groups on the side-chains also appear to be deactivating. This is seen in the case of aspartic acid (**37**) (≤ 0.01), glutamic acid (**18**) (0.25), ornithine (**23**) (0.41) and proline (**29**) (0.73). The most reactive amino acids appear to be those with long alkyl side-chains, such as norvaline (**38**) (2.6) and norleucine (**39**) (3.4). Lysine (**21**), which has both polar functionality and a long side-chain, has a k_{rel} of 2.0.

N-Acetylamino Acid	k_{rel}	*N*-Acetylamino Acid	k_{rel}
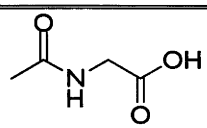 **61**	0.35	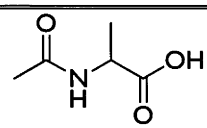 **62**	0.40
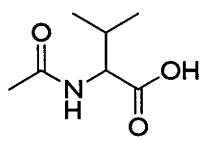 **63**	1.3	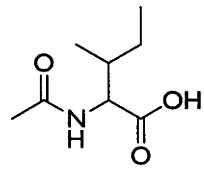 **64**	3.1

Figure 6.3: Relative rates of reaction for the *N*-acetylamino acids **(61-67)**, **(69-75)** and **(116-118)**

N-Acetylamino Acid	k_{rel}	*N*-Acetylamino Acid	k_{rel}
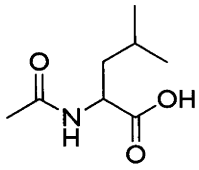 **65**	3.2	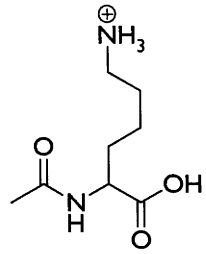 **66**	2.0
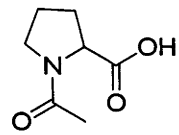 **67**	3.9	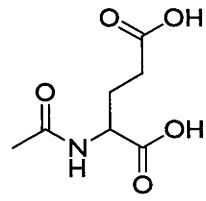 **69**	0.63
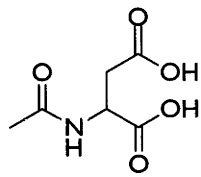 **70**	0.34	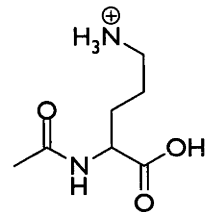 **71**	1.8
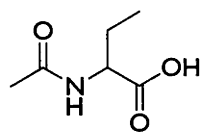 **72**	1.4	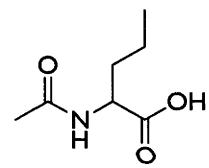 **73**	3.4
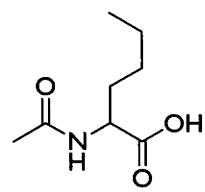 **74**	3.6	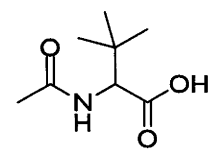 **74**	1.5
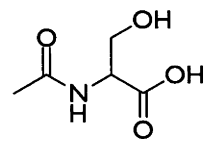 **116**	0.92	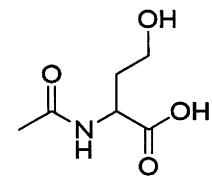 **117**	1.4
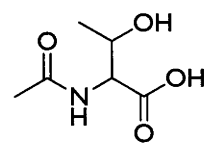 **118**	1.5		

Figure 6.3 *cont.*: Relative rates of reaction for the *N*-acetylamino acids (**61-67**), (**69-75**) and (**116-118**)

Figure 6.3 shows the k_{rel} values for hydrogen abstraction by oxygen-centred radicals for the *N*-acetylamino acids (**61-67**), (**69-75**) and (**116-118**). These values show the same trends as for the free amino acids in Figure 6.2. While the acetamides with the lowest k_{rel} values show an increased reactivity compared to that of the free analogues (*N*-acetylglycine (**61**) (0.35), *N*-acetylalanine (**62**) (0.40), *N*-acetylaspartic acid (**70**) (0.34) and *N*-acetylglutamic acid (**69**) (0.63)), the k_{rel} values are still less than 20% of those of the fastest reacting amino acids (*N*-acetylnorleucine (**74**) (3.6)). Even then, it is likely that some reaction is occurring on the acetyl group, as ESR studies have identified such radicals,[114] so it is possible that the k_{rel} values overestimate the reactivity of the amino acid core, particularly with the less reactive species and the relative reactivity of the amino acid moieties of these species is even lower.

6.2 Product Analysis and Reactivity per Hydrogen

It was not feasible to identify many of the products of these reactions of the amino acids (**12**), (**13**), (**15**), (**18**), (**21**), (**23**), (**25**), (**29-31**), (**37-40**), and (**113-115**) and the acetamides (**61-67**), (**69-75**) and (**116-118**). The product mixtures were much more complicated than those described in earlier chapters, presumably because of the general instability of the initially formed hydroperoxides and their subsequent oxidations. Therefore it was impractical to develop tables of k_{rel}^{H} values for these systems analogous to those derived for the chlorination reactions as shown in Figures 2.34 and 3.21. Nevertheless some quantitative analysis is feasible.

Serine (**113**), on reaction, produced glycine (**12**), which was identified by comparison with an authentic sample. It seems likely that this forms via aminomalonic acid (**119**), which spontaneously decarboxylates (Figure 6.4).

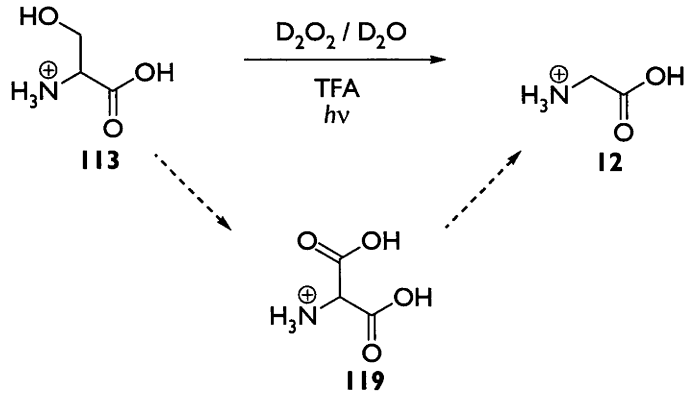

Figure 6.4: Reaction of serine (**113**)

Homoserine (**114**), on reaction, produced aspartic acid (**37**), which was identified by comparison with an authentic sample. It shows a resonance diagnostic of an ABX system in the ^{1}H NMR spectrum at δ 2.8 ppm.

On reaction of threonine (**115**), aminoacetone (**121**) is produced (Figure 6.5). Presumably this is formed through oxidation of threonine (**115**) to the ketone (**120**). It has been shown[133] that this ketone (**120**) rapidly decarboxylates with a $t_{1/2}$ of 8 minutes at pH 0, and faster at higher pH. The ^{1}H NMR spectrum of the reaction product shows two singlets at δ 3.92 and 2.41 ppm in a ratio of two to three, respectively, which are indicative of the aminoketone (**121**).

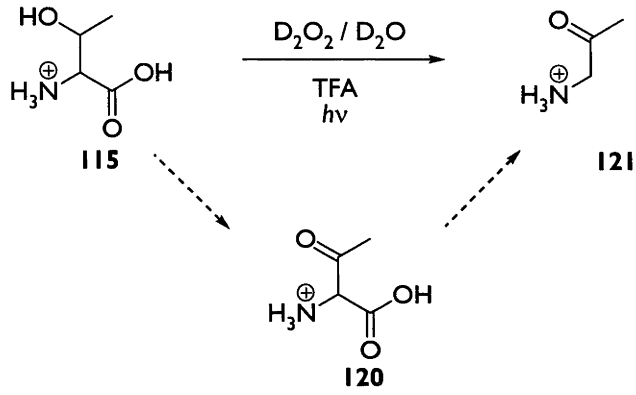

Figure 6.5: Reaction of threonine (**115**)

The reactions of the alcohols (**113-115**) detailed above indicate the types of processes that are likely to occur with the analogous hydroperoxides. In addition to the regioisomers and stereoisomers likely to be produced, deuterium hydrogen exchange is likely to occur due to aldehyde and ketone intermediates being formed, thus complicating analysis by ^{1}H NMR spectroscopy. For these reasons a full product analysis was not practical.

However, as reactions of terminal methyl groups give the corresponding carboxylic acids. Thus, on reaction of their respective terminal methyl groups alanine (**13**) produces aminomalonic acid (**119**) which decarboxylates to form glycine (**12**), α-aminobutyric acid (**15**) gives aspartic acid (**37**), norvaline (**38**) produces glutamic acid (**18**), norleucine (**39**) forms α-aminoadipic acid (**122**), valine (**25**) produces β-methylaspartic acid (**123**) and *tert*-leucine (**40**) produces β,β-dimethylaspartic acid (**124**). Each of the above products was identified by comparison with authentic samples.

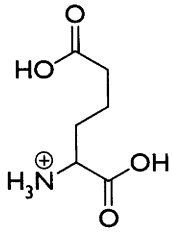

122

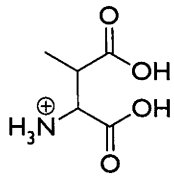

123

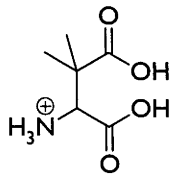

124

From the amounts of these products formed as a percentage of the total reaction, and from the k_{rel} values determined above, a k_{rel}^{H} value for each type of methyl group hydrogen can be determined (Figures 6.6, 6.7, 6.10 and 6.11). The corresponding values for the chlorinations are shown in Figures 6.8, 6.9, 6.12 and 6.13. The absolute k_{rel}^{H} values for the oxidations are not directly comparable with those for the chlorinations, having been determined for different systems with different standards, but similar trends are apparent.

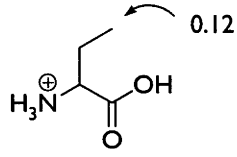

15

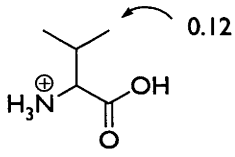

25

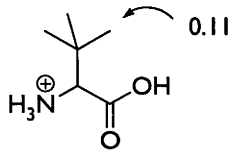

40

Figure 6.6: k_{rel}^{H} values for the γ-methyl hydrogens of the amino acids (**15**), (**25**), and (**40**) reacting with D_2O_2/D_2O

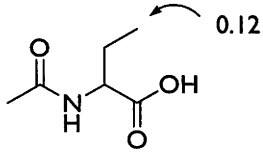

72

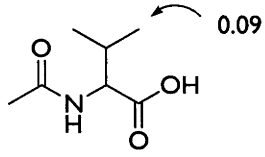

63

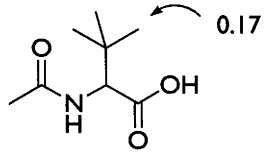

75

Figure 6.7: k_{rel}^{H} values for the γ-methyl hydrogens of the acetylamino acids (**72**), (**63**) and (**75**) reacting with D_2O_2/D_2O

The k_{rel}^{H} values of the γ-methyl hydrogens of α-aminobutyric acid (**15**), valine (**25**) and *tert*-leucine (**40**) in the reactions with deuterium peroxide (Figure 6.6) are very similar. This is all the more remarkable given that the corresponding k_{rel} values of the amino acids (**12**), (**13**), (**15**), (**18**), (**21**), (**23**), (**25**), (**29-31**), (**37-40**), and (**113-115**) vary by well over two orders of magnitude. Similar consistencies of reactivity of γ-methyl hydrogens are seen in the reactions of the acetamides (**72**), (**63**) and (**75**) with

deuterium peroxide (Figure 6.7) and in the chlorinations of the free amino acids (**15**), (**25**), and (**40**) (Figure 6.8) and the acetamides (**72**), (**63**) and (**75**) (Figure 6.9)

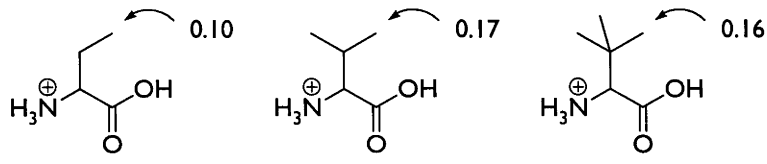

15 **25** **40**

Figure 6.8: k_{rel}^{H} values for the γ-methyl hydrogens of the amino acids (**15**), (**25**), and (**40**) reacting with chlorine

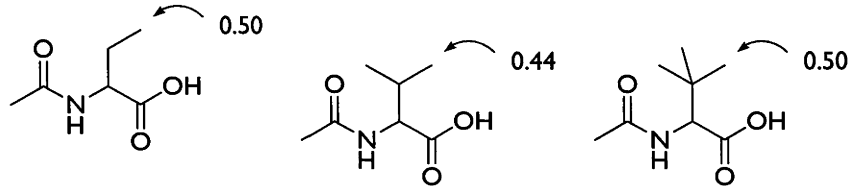

72 **63** **75**

Figure 6.9: k_{rel}^{H} values for the γ-methyl hydrogens of the acetylamino acids (**72**), (**63**) and (**75**) reacting with chlorine

Nevertheless, the k_{rel}^{H} values of the γ-methyl hydrogens of α-aminobutyric acid (**15**) and the acetamide (**72**) are consistently and significantly higher than those of the β-methyl hydrogens of alanine (**13**) and *N*-acetylalanine (**62**) in both the chlorinations and reactions with deuterium peroxide (Figures 6.10 - 6.13). This, and the low k_{rel} values for glycine (**12**), alanine (**13**), aspartic acid (**37**) and glutamic acid (**18**), and the corresponding acetamides (**61**), (**62**), (**69**) and (**72**) in each system are a measure of the deactivating effect of the protonated amino, acetamido and carboxyl groups towards hydrogen atom abstraction by electrophilic radicals.

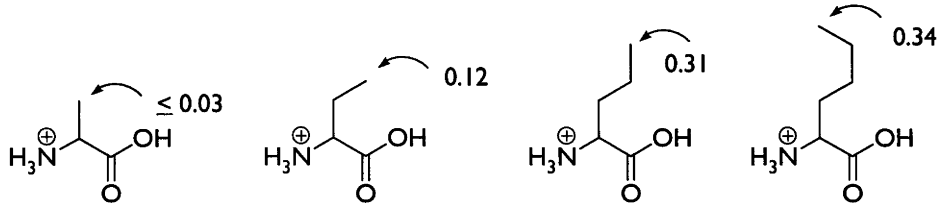

13 **15** **38** **39**

Figure 6.10: k_{rel}^{H} values for the terminal methyl hydrogens of the amino acids (**13**), (**15**), (**38**) and (**39**) reacting with D_2O_2/D_2O

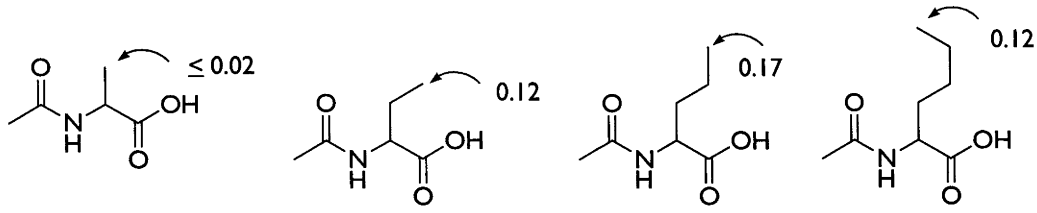

62 **72** **73** **74**

Figure 6.11: k_{rel}^{H} values for the terminal methyl hydrogens of the acetylamino acids (**62**) and (**72-74**) reacting with D_2O_2/D_2O

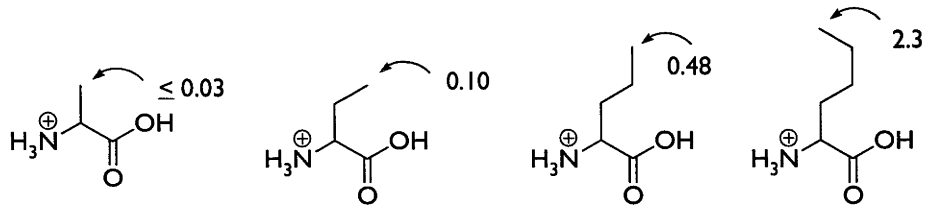

13 **15** **38** **39**

Figure 6.12: k_{rel}^{H} values for the terminal methyl hydrogens of the amino acids (**13**), (**15**), (**38**) and (**39**) reacting with chlorine

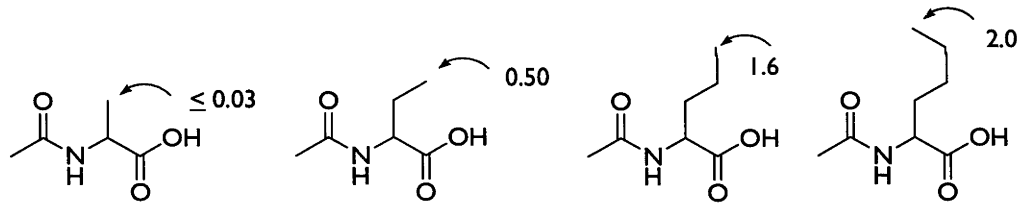

62 **72** **73** **74**

Figure 6.13: k_{rel}^{H} values for the terminal methyl hydrogens of the acetylamino acids (**62**) and (**72-74**) reacting with chlorine

The effect is greater and extends further out on the side-chains of the aliphatic amino acids with the chlorinations than with the reactions with oxygen-centred radicals, and more so with the free amino acids than with the acetamides. This is apparent from the trends in the k_{rel}^{H} values of the β-, γ-, δ and ε-methyl hydrogens summarised in Figures 6.10 - 6.13. However, even where the effect is weakest in the case of *N*-acetylamino acids reacting with oxygen-centred radicals, the effect at the β-position appears to be sufficient to reduce the reactivity of the methyl hydrogens of the alanine derivative (**62**) to less than 20% of that of the ω-methyl hydrogens of the acetamides of α-aminobutyric acid (**72**), norvaline (**73**) and norleucine (**74**) (Figure 6.11).

Chapter 7: Conclusion

In summary, a method has been developed to measure the reactivity of protonated amino acids towards hydrogen atom abstraction by chlorine. The method was used to determine the relative reactivity of the amino acids (k_{rel}), and of the various types of hydrogen within the amino acids (k_{rel}^{H}). The quantification of these values enables the magnitude of the deactivating effects caused by the α-substituents to be appreciated. The results show that hydrogen abstraction by chlorine is highly disfavoured for hydrogens at the α-, β-, and to a degree, γ-positions, and the rate of reaction is greatest for hydrogens further from the α-centre.

The same method was applied to *N*-acetylated amino acids to obtain k_{rel} and k_{rel}^{H} values. Quantification of the reactivity of these compounds illustrates that they are also affected by the deactivating effect which disfavours abstraction at the α- and β-positions. By directly comparing the k_{rel} and k_{rel}^{H} values of the protonated and *N*-acetylated amino acids, it was seen that the deactivating effect in *N*-acetylamino acids is weaker than that seen for protonated amino acids.

The k_{rel}^{H} values derived for the protonated and *N*-acetylated amino acids used to correctly predict the regioselectivity of several peptides. This establishes that the protonated and acetylated amino acids are suitable as models for the *N*- and non-terminal amino acid residues in peptides, respectively.

There was very little correlation between the rates of hydrogen atom abstraction and the calculated radical stabilisation energies of the product radicals. This illustrates that it is the not the stability of the radicals that is the primary factor controlling where hydrogen abstraction occurs. Instead, the results reflect a polar effect dominating the transition states of the abstraction reactions. In particular the protonated amino, acetamido and carboxyl groups are inductively electron-withdrawing and deactivate adjacent positions to hydrogen abstraction by electrophilic chlorine radicals.

The reactivity of both protonated and *N*-acetylated amino acids has also been determined using electrophilic oxygen-centred radicals. As expected, this system also shows a deactivation of the amino acid α-positions and other behaviours characteristic

of a polar effect. The decreased extent of deactivation seen in these systems is consistent with the lower reactivity and later transition states expected for abstractions facilitated by oxygen-centred radicals compared to abstractions by chlorine radicals.

The extent of the deactivation of the hydrogen abstraction reactions decreased from protonated amino acids with chlorine radicals to *N*-acetylamino acids with chlorine radicals to protonated amino acids with oxygen-centred radicals and to *N*-acetylated amino acids with oxygen-centred radicals. The following graphs (Figures 7.1-7.4) illustrate the relative ordering of the reactivity of amino acids for the four systems studied, where the proteinogenic amino acids are indicated by the conventional three letter codes and Nle indicates norleucine (**39**), hPh homophenylalanine (**41**), Nva norvaline (**72**), tLe *tert*-leucine (**40**), and Abu α-aminobutyric acid (**15**). The data show two main features; firstly, in all cases the most reactive compounds are those with long alkyl side-chains. Secondly, and perhaps most interestingly, in all cases the four least reactive amino acids are glycine (**12**), alanine (**13**), aspartic acid (**37**) and glutamic acid (**18**), or the corresponding acetamides (**61**,**62**,**69**,**70**).

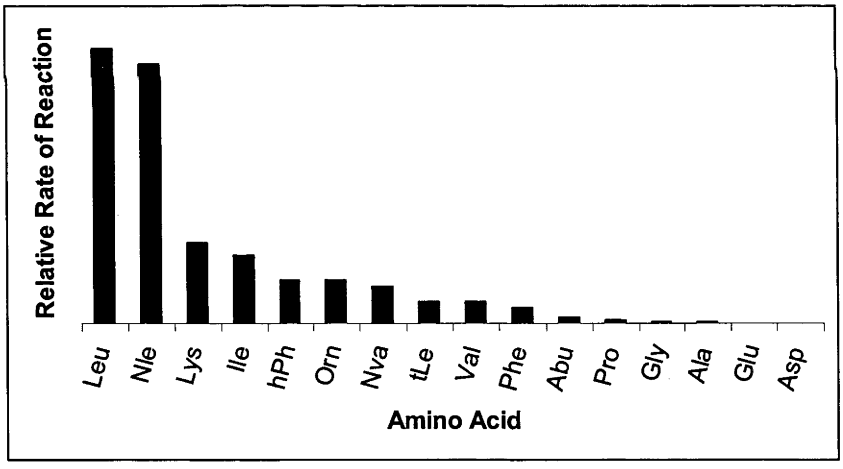

Figure 7.1: Relative rates of chlorination of protonated amino acids

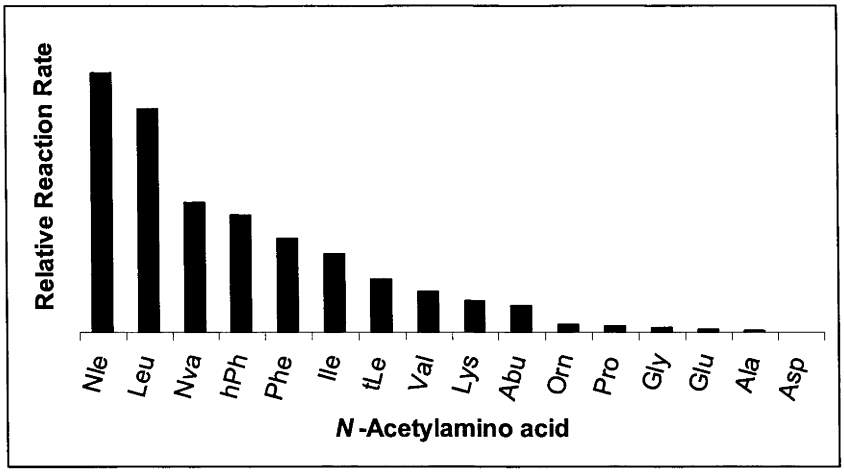

Figure 7.2: Relative rates of chlorination of *N*-acetylamino acids

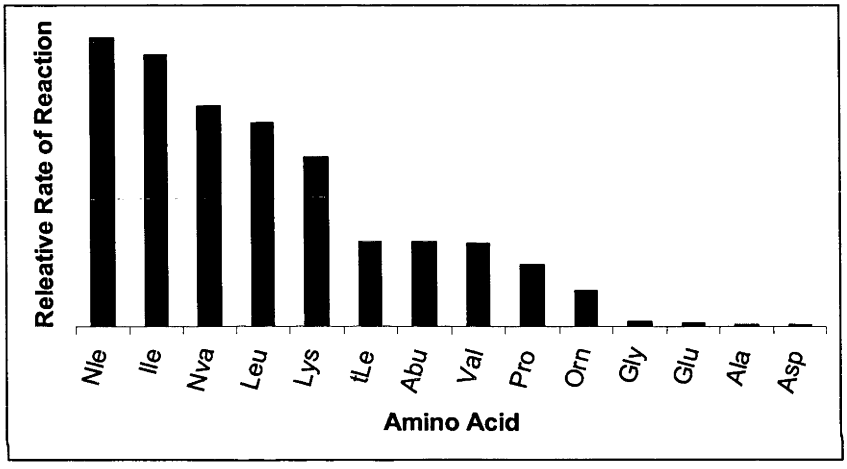

Figure 7.3: Relative rates of reaction of free amino acids with D_2O_2

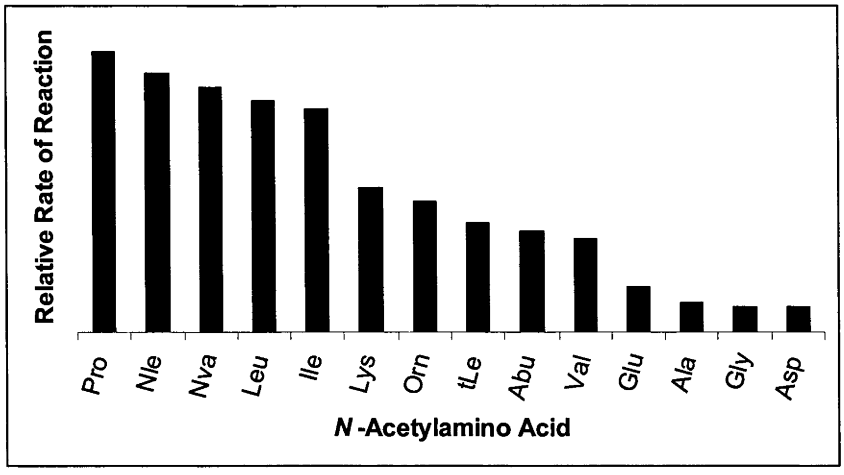

Figure 7.4: Relative rates of reaction of *N*-acetylamino acids with D_2O_2

The above results indicate that polar effects control the location of hydrogen abstraction. The obvious question raised is whether this is seen in biological systems. Isopenicillin-*N*-synthetase, which was discussed in the introduction, is an enzyme used

in the biosynthesis of β-lactam antibiotics[68-71] (Figures 7.5 and 7.6). The enzyme abstracts a hydrogen from the substrate which subsequently cyclises to form either the penicillin or cephem depending on whether the abstraction occurs in the β-position or the γ-position, respectively. In the first example (Figure 7.5), there appears to be a large preference to form the β-methylene radical over the γ-methyl radical, which are formed in a ratio of 2:1. However, in the second example (Figure 7.6), both the β-methylene radical and the γ-methylene radical can be formed and they are generated in a ratio of greater than 1:10. This appears to be quite indicative of a polar effect analogous to that seen in systems investigated in this thesis. Despite enzymes often catalysing reactions that have unfavourable thermodynamics, as it has been shown, there is an inherent advantage towards abstraction of hydrogens further along amino acid side-chains.

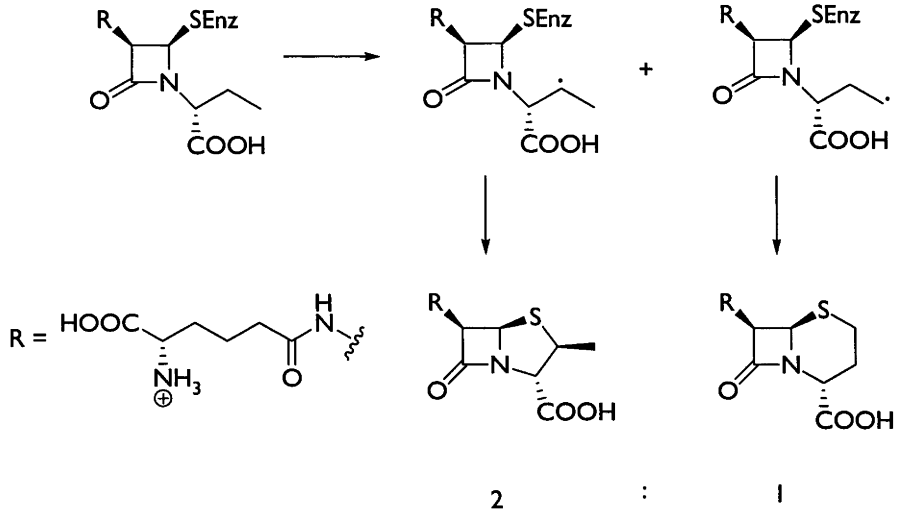

Figure 7.5: Biosynthesis of penicillin analogues derived from δ-(*L*-α-amino-adipate)-*L*-cysteine-*D*-(α-amino)-butyric acid[71]

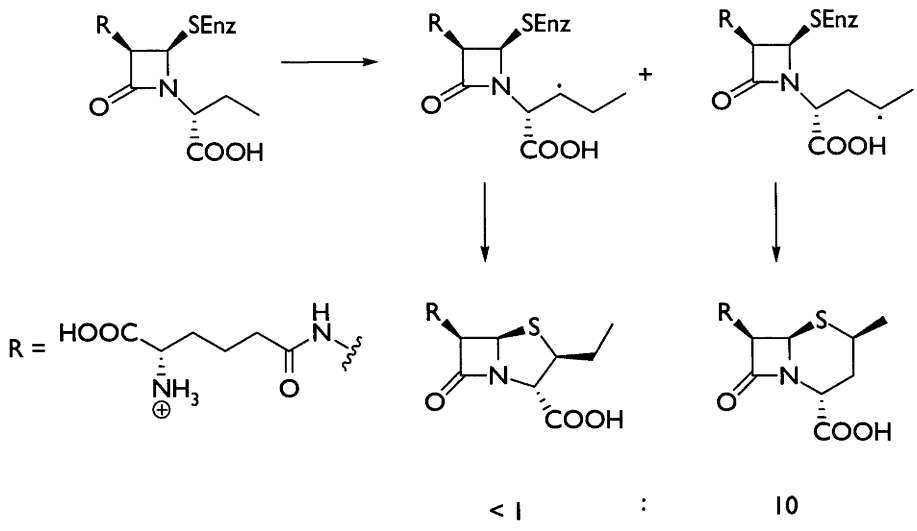

Figure 7.6: Biosynthesis of penicillin analogues derived from δ-(*L*-α-amino-adipate)-*L*-cysteine-*D*-norvaline[71]

The results in this thesis show the prevalence of side-chain hydroxylated amino acids in natural products (as illustrated in Chapter 1, Figure 1.8) are, rather than a surprise, to be expected as the ease of abstraction of hydrogens from positions on amino acid side-chains has been demonstrated to often be greater than abstraction from α-centres.

The above results indicate that peptides are a relatively inert structural motif, and that proteins made from α-amino acids are a good framework for building biological structures which can resist oxidative degradation. To further investigate the use of α-amino acids as basis of the primary structural macromolecules in biological systems the following should be investigated. A broader investigation of the k_{rel}^{H} values for abstraction by oxygen centred radicals needs to be performed. Additionally, the reactivity of other compounds found in primeval environments such as those that have been postulated to have been formed in abiotic processes such as those seen in Miller-Urey type experiments,[134] or seen in non-terrestrial sources such as the Murchison meteorite[135] should be measured in a similar manner to the α-amino acids. It is hypothesised that such compounds would have a higher reactivity towards hydrogen abstraction. This raises the question of whether the current, near universal use of α-amino acids as the basis of proteins was influenced by the generation of an oxidative atmosphere by primitive organisms, an atmosphere in which protein-like structures containing non-α-amino acids would be selected against.

Experimental

General Procedures

Nuclear Magnetic Resonance (NMR) spectra were recorded on either a Varian Inova 500 spectrometer operating at 500 MHz (^{1}H) or 125 MHz (^{13}C), or a Varian Mercury 300 spectrometer operating at 300 MHz (^{1}H). The δ values are given in parts per million, and *J* values, where determined, are given in Hz. Spectra were referenced against residual solvent. d_4-Methanol was purchased from Apollo Scientific, Ltd., d_6-dimethylsulfoxide was purchased from Cambridge Isotope Laboratories Inc. The following abbreviations have been used: s singlet, d doublet, t triplet, q quartet, m multiplet, and b broad. NMR spectra were processed using MestReC v4.7.8.0 software.

High resolution mass spectra were obtained on a Bruker Apex 4.7T FTICR-MS (Fourier Transform/Ion Cyclotron Resonance-Mass Spectroscopy) instrument. Mass spectral data are reported as the mass-to-charge ratio (*m*/z).

High Performance Liquid Chromatography was performed on a Waters Alliance Separation Module 2690 with a Waters 996 Photodiode Array Detector fitted with a Symmetry® C_{18}, 4.6 x 250 mm column. The system was controlled using Waters Millennium 32 software. Semi-preparative HPLC was performed on a SymmetryPrep 20 × 300 mm column using a Waters 510 pump with a Waters 717 Plus auto sampler, and compounds were detected using a Waters 486 Tunable Absorbance Detector. This system was controlled using the Millipore Millennium 32 software.

Photolysis was either conducted using an Osram ULTRA-VITALUX® sunlamp or a Luzchem LZC-ORG photoreactor fitted with Sankyo Denki G8TC germicidal lamps.

Trifluoroacetic acid and benzoic acid were purchased from Sigma-Aldrich Chemical Company. The sources of other chemicals used are detailed in the appropriate sections below.

Chapter 2

Glycine (**12**), *S*-alanine (**13**), *S*-valine (**25**), 2*S*,3*S*-isoleucine (**30**), *S*-leucine (**30**), *S*-lysine (**21**), *S*-proline (**29**), *S*-phenylalanine (**28**), *S*-glutamic acid (**19**), *S*-aspartic acid (**37**), *S*-ornithine (**23**), *S*-α-aminobutyric acid (**15**), *RS*-norvaline (**38**), *RS*-norleucine (**39**), *S*-*tert*-leucine (**40**) and *RS*-homophenylalanine (**41**) were purchased from Sigma-Aldrich Chemical Company and used as received.

Benzoic acid was shown to be inert towards chlorination by the following procedure: 100 mg benzoic acid was dissolved in 5 mL TFA in a quartz reaction vessel. The solution was then irradiated with a 300W broad spectrum sunlamp while it was saturated with molecular chlorine for 30 min. The solution was degassed with N_2, and then the solvent was removed under reduced pressure. ^{1}H NMR analysis showed that no detectable reaction had occured.

The amino acids (**12**), (**13**), (**15**), (**18**), (**21**), (**23**), (**25**), (**28-31**) and (**37-41**) were chlorinated using the following procedure: 100 mg of the amino acid was dissolved in 5 mL TFA. The solution was then irradiated with a 300W broad spectrum sunlamp while it was saturated with molecular chlorine for periods between 45 seconds and 20 minutes depending on the particular compound. The solution was degassed with N_2, then the solvent was removed under reduced pressure. The mixture of products was analysed using 1D and 2D ^{1}H NMR spectroscopy as described in Chapter 2.

From the reaction of valine (**25**) as above, the following products were identified:

β-chlorovaline (**26**) (27% by NMR) ^{1}H NMR (MeOH-d_4, 300 MHz): δ 1.78 (s, 3H), 1.83 (s, 3H) 4.23 (s, 1H) ppm.

γ-chlorovaline (**27**) (73% by NMR) ^{1}H NMR (MeOH-d_4, 300 MHz): δ 1.14 (d *J*=7Hz, 1.5H) and 1.13 (d *J*=7Hz, 1.5H), 2.62 (m, 0.5H) and 2.40 (m, 0.5H), 3.65 (m, 2H), 4.21 (d *J*=4Hz, 0.5H) and 4.22 (d *J*=4Hz, 0.5H) ppm.

From the reaction of isoleucine (**31**) as above, the following products were identified:

β-chloroisoleucine (**42**) (16% by NMR) ^{1}H NMR (MeOH-d_4, 300 MHz): δ 1.15 (m, 3H), 1.68 (s, 3H), 1.74 (s, 3H), 2.20 (m, 4H), 4.49 (s, 1H), 4.50 (s, 1H) ppm.

α-amino-β-(chloromethyl)pentanoic acid (**43**) (6% by NMR) ^{1}H NMR (MeOH-d_4, 300 MHz): δ 1.10 (m, 3H), 1.70 (m, 2H), 2.40 (m, 1H), 3.80 (m, 3H), 4.27 (d *J*=5Hz, 1H) ppm.

α-amino-γ-chloro-β-methylpentanoic acid (**44**) (38% by NMR) ^{1}H NMR (MeOH-d_4, 300 MHz): δ 1.09 (d *J*=7Hz, 1.5H) and 1.18 (d *J*=7Hz, 1.5H), 1.56 (d *J*=6Hz, 1.5H) and 1.60 (d *J*=6Hz, 1.5H), 2.28 (m, 1H), 3.98 (d *J*=3Hz, 0.5H) and 4.03 (d *J*=6Hz, 0.5H), 4.29 (m, 1H) ppm.

δ-chloroisoleucine (**45**) (40% by NMR) ^{1}H NMR (MeOH-d_4, 300 MHz): δ 1.07 (d *J*=7 Hz, 3H), 1.88 (m, 1H), 2.00 (m, 1H), 2.41 (m, 1H), 3.68 (m, 2H), 3.90 (m, 1H) ppm.

From the reaction of proline (**29**) as above, the following products were identified:

β-chloroproline (**46**) (32% by NMR) ^{1}H NMR (MeOH-d_4, 300 MHz): δ 2.68 (m, 1H) and 2.96 (m, 1H), 3.69 (m, 1H) and 3.78 (m, 1H), 4.66 (br, 0.5H) and 4.80 (m, 0.5H), 4.98 (m, 0.5H) and 5.02 (m, 0.5H) ppm.

γ-chloroproline (**47**) (68% by NMR) ^{1}H NMR (MeOH-d_4, 300 MHz): δ 2.64 (m, 1H) and 2.75 (m, 1H), 3.67 (m, 1H) and 3.82 (m, 1H), 4.61 (dd *J*=4Hz *J*=10Hz, 0.5H) and 4.74 (dd *J*=7Hz *J*=10Hz, 0.5H), 4.80 (m, 0.5H) and 4.89 (m, 0.5H) ppm.

From the reaction of leucine (**30**) as above, the following products were identified:

γ-chloroleucine (**48**) (29% by NMR) ^{1}H NMR (MeOH-d_4, 300 MHz): δ 1.60 (s, 3H), 1.75 (s, 1H), 2.32 (dd *J*=6Hz *J*=15Hz, 1H), 2.57 (dd *J*=5 Hz *J*=15Hz, 1H), 4.20 (dd *J*=5Hz *J*=6Hz) ppm.

δ-chloroleucine (**49**) (71% by NMR) ^{1}H NMR (MeOH-d_4, 300 MHz): δ 1.11 (d *J*=6.5Hz, 1.5H) and 1.12 (d *J*=6Hz, 1.5H), 2.03 (m, 2H), 2.17 (m, 1H), 3.58 (m, 2H), 4.00 (t *J*=7Hz, 1H) ppm.

From the reaction of lysine (**21**) as above, the following products were identified:

β-chlorolysine (**50**) (29% by NMR) ^{1}H NMR (MeOH-d_4, 300 MHz): δ 2.30 (m, 2H), 2.46 (m, 2H), 2.95 (m, 2H), 4.20 (m, 1H), 4.42 (m, 1H) ppm.

γ-chlorolysine (**22**) (50% by NMR) ^{1}H NMR (MeOH-d_4, 300 MHz): δ 2.20 (m, 2H), 2.48 (m, 2H), 3.14 (m, 2H0, 3.23 (m, 1H), 4.25 (m, 1H) ppm.

δ-chlorolysine (**51**) (21% by NMR) ^{1}H NMR (MeOH-d_4, 300 MHz): δ 2.10 (m, 2H), 2.20 (m, 2H), 3.23 (m, 2H), 3.42 (m, 1H), 4.03 (t *J*=6Hz, 1H) ppm.

From the reaction of phenylalanine (**28**) as above, the following products were identified:

β-chlorophenylalanine (**52**) (100% by NMR) ^{1}H NMR (MeOH-d_4, 300 MHz): δ 4.45 (d *J*=6Hz, 0.9H), 4.50 (d *J*=4Hz, 0.1H), 5.58 (d *J*=4Hz, 0.1H), 5.63 (d *J*=6Hz, 0.9H), 7.20 (m, 5H) ppm.

From the reaction of ornithine (**23**) as above, the following products were identified:

β-chloroornithine (**53**) (47% by NMR) ^{1}H NMR (MeOH-d_4, 300 MHz): δ 2.16 (m, 4H), 3.30 (m, 4H), 4.25 (m, 2H), 4.50 (d *J*=6.4Hz, 0.5H) and 4.51 (d *J*=6.5Hz, 0.5H) ppm.

γ-chloroornithine (**24**) (52% by NMR) ^{1}H NMR (MeOH-d_4, 300 MHz): δ 2.36 (m, 1H) and 2.51 (m, 1H), 3.21 (m, 2H), 3.50 (d *J*=3.5Hz, 1H) and 3.46 (d *J*=3.5Hz, 1H), 4.22 (dd *J*=3.5Hz *J*=7Hz, 0.5H) and 4.25 (dd *J*=4Hz *J*=6.5Hz, 0.5H) ppm.

From the reaction of α-aminobutyric acid (**15**) as above, the following products were identified:

α-amino-β-chlorobutyric acid (**16**) (25% by NMR) ^{1}H NMR (MeOH-d_4, 300 MHz): δ 1.42 (d *J*=7Hz, 3H), 4.04 (m, 1H), 4.19 (d *J*=3Hz, 0.4H) and 4.23 (d *J*=2Hz, 0.6H) ppm.

α-amino-γ-chlorobutyric acid (**17**) (75% by NMR) ^{1}H NMR (MeOH-d_4, 300 MHz): δ 2.22 (m, 1H), 2.25 (m, 1H), 3.54 (m, 2H), 4.12 (t *J*=6Hz, 1H) ppm.

From the reaction of norvaline (**38**) as above, the following products were identified:

γ-chloronorvaline (**54**) (40% by NMR) ^{1}H NMR (MeOH-d_4, 300 MHz): δ 1.21 (d *J*=6Hz, 1.5Hz) and 1.23 (d *J*=6Hz, 1.5H), 2.20 (m, 4H), 4.05 (m, 2H), 4.09 (m, 2H) ppm.

δ-chloronorvaline (**55**) (60% by NMR) ^{1}H NMR (MeOH-d_4, 300 MHz): δ 1.65 (m, 2H), 1.85 (m, 2H), 3.40 (t *J*=6Hz, 2H), 3.78 (dd *J*=6Hz *J*=6.5Hz, 1H) ppm.

From the reaction of norleucine (**39**) as above, the following products were identified:

γ-chloronorleucine (**56**) (17% by NMR) ^{1}H NMR (MeOH-d_4, 300 MHz): δ 1.08 (t *J*=7Hz, 1.5H) and 1.09 (t *J*=7Hz, 1.5H), 1.75 (m, 1H) and 1.90 (m, 1H), 2.25 (m, 1H) and 2.45 (m, 1H), 3.79 (m, 1H), 4.20 (m, 1H) ppm.

δ-chloronorleucine (**57**) (43% by NMR) ^{1}H NMR (MeOH-d_4, 300 MHz): δ 1.52 (d *J*=6.5Hz, 3H), 1.90 (m, 2H), 2.00 (m, 0.5H) and 2.20 (m, 0.5H), 4.00 (m, 1H), 4.20 (m, 1H) ppm.

ε-chloronorleucine (**58**) (40% by NMR) ^{1}H NMR (MeOH-d_4, 300 MHz): δ 1.62 (m, 2H), 1.80 (m, 2H), 1.90 (m, 2H), 3.59 (t 6Hz, 2H), 4.00 (m, 1H) ppm.

From the reaction of *tert*-leucine (**40**) as above, the following products were identified:

γ-chloro-*tert*-leucine (**59**) (100% by NMR) ^{1}H NMR (MeOH-d_4, 300 MHz): δ 1.23 (s, 3H), 1.29 (s, 3H), 3.57 (s, 2H), 4.19 (s, 1H) ppm.

From the reaction of homophenylalanine (**41**) as above, the following products were identified:

γ-chlorohomophenylalanine (**60**) (100% by NMR) ^{1}H NMR (MeOH-d_4, 300 MHz): δ 2.49 (ddd *J*=5Hz *J*=8Hz *J*=15Hz, 0.25H) and 2.57 (m, 0.25H) and 2.82 (m, 0.5H), 4.03 (dd *J*=5Hz *J*=8Hz, 0.5H) and 4.12 (dd *J*=6.5Hz *J*=7Hz, 0.5H), 5.19 (dd *J*=5.5Hz *J*=10Hz, 0.5H) and 5.30 (dd *J*=6Hz *J*=8Hz, 0.5H), 7.30 (m, 5H) ppm.

The relative rates of reaction for the amino acids (**12**), (**13**), (**15**), (**18**), (**21**), (**23**), (**25**), (**28-31**) and (**37-41**) were obtained using the following procedure: 100 mg each of two amino acids and 100 mg of benzoic acid were dissolved in 10 mL TFA. Half the solution was separated, and the solvent was removed under pressure. From this mixture the relative amounts of each of the compounds before reaction were determined using ^{1}H NMR. The remaining solution was then irradiated with a 300W broad spectrum sunlamp while it was saturated with molecular chlorine for periods between 45 seconds and 5 minutes depending on the particular compounds. The solution was degassed with N_2, then the solvent was removed under reduced pressure. From this mixture the relative amounts of each of the compounds after reaction were determined using ^{1}H NMR. The k_{rel} values were then determined as described in Chapter 2.

Competitive experiments were performed between all of the amino acids (**12**), (**13**), (**15**), (**18**), (**21**), (**23**), (**25**), (**29-31**) and (**37-41**) and phenylalanine (**28**). Additional competitive experiments against α-aminobutyric acid (**15**) were performed with glycine (**12**) and alanine (**13**). Additional competitive experiments against valine (**25**) were performed with leucine (**30**) and norleucine (**39**). The k_{rel} values obtained in this manner were consistently within 10% of the k_{rel} values determined against phenylalanine (**28**). To obtain estimates of

reproducibility, duplicate experiments were performed on glycine (**12**), alanine (**13**), leucine (**30**), norleucine (**39**), and isoleucine (**31**) and k_{rel} values were within 5% for each. Repeated determinations of product distributions for individual samples were consistently within 5%.

Chapter 3

N-acetylglycine (**61**), *S*-*N*-acetylalanine (**62**), *S*-*N*-acetylvaline (**63**), 2*S*,3*S*-*N*-acetylisoleucine (**64**), *S*-*N*-acetylleucine (**65**), *S*-N^{α}-acetyllysine (**66**), *S*-*N*-acetyl-proline (**67**), *S*-*N*-acetylphenylalanine (**68**), *S*-*N*-acetylglutamic acid (**69**), *S*-*N*-acetylaspartic acid (**70**), *S*-N^{α}-acetyl-ornithine (**71**), *S*-*N*-acetyl-α-aminobutyric acid (**72**), *RS*-*N*-acetylnorvaline (**73**), *RS*-*N*-acetylnorleucine (**74**), *S*-*N*-acetyl-*tert*-leucine (**75**) and *RS*-*N*-acetylhomophenylalanine (**76**) were purchased from Sigma-Aldrich Chemical Company and used as received.

The procedures used are identical to those for Chapter 2.

From the reaction of *N*-acetylglutamic acid (**69**) as above, the following products were identified:

N-acetyl-β-chloroglutamic acid (**77**) (83% by NMR) ^{1}H NMR (MeOH-d_4, 300 MHz): δ 2.70 (dd *J*=8Hz *J*=17Hz, 0.5H) and 2.84 (dd *J*=6Hz *J*=17Hz, 0.5H), 2.87 (dd *J*=10Hz *J*=17Hz, 0.5H) and 2.98 (dd *J*=4Hz *J*=17Hz, 0.5H), 4.60 (m, 0.5H) and 4.93 (m, 0.5H), 4.86 (d *J*=4.5Hz, 0.5H) and 5.10 (d *J*=2.5Hz, 0.5H).

N-acetyl-γ-chloroglutamic acid (**78**) (17% by NMR) ^{1}H NMR (MeOH-d_4, 300 MHz): δ 2.17 (m, 0.5H) and 2.25 (m, 0.5H) and 2.41 (m, 0.5H) and 2.64 (m, 0.5H), 4.37 (dd *J*=6.5Hz *J*=8.5Hz, 0.5H), 4.48 (dd *J*=6.5Hz, *J*=7Hz, 0.5H), 4.56 (dd *J*=5Hz *J*=8Hz, 0.5H) and 4.67 (m, 0.5H) ppm.

From the reaction of *N*-acetylvaline(**63**) as above, the following products were identified:

N-acetyl-β-chlorovaline (**79**) (25% by NMR) ^{1}H NMR (MeOH-d_4, 300 MHz): δ 1.65 (s, 3H), 1.74 (s, 3H), 4.73 (s, 1H) ppm.

N-acetyl-γ-chlorovaline (**80**) (75% by NMR) ^{1}H NMR (MeOH-d_4, 300 MHz): δ 1.05 (d *J*=7Hz, 1.5H) and 1.10 (d *J*=10Hz, 1.5H), 2.30 (m, 0.5H) and 2.47 (m, 1H), 3.45 (m, 1H) and 3.55 (m, 1H), 4.53 (d *J*=6Hz, 0.5H) and 4.80 (d *J*=4Hz, 0.5H) ppm.

From the reaction of *N*-acetylisoleucine (**64**) as above, the following products were identified:

N-acetyl-β-chloroisoleucine (**81**) (12% by NMR) ^{1}H NMR (MeOH-d_4, 300 MHz): δ 0.95 (obscured), 1.57 (s, 1.5H) and 1.61 (s, 1.5H), 2.50 (m, 2H), 4.85 (s, 0.5H) and 4.86 (s, 0.5H) ppm.

N-acetyl–α-amino-β-(chloromethyl)pentanoic acid (**82**) (16% by NMR) ^{1}H NMR (MeOH-d_4, 300 MHz): δ 1.03 (obscured), 1.33 (m, 2H), 2.20 (m, 2H), 4.47 (m 2H), 4.77 (d *J*=3H, 1H) ppm.

N-acetyl-α-amino-γ-chloro-β-methylpentanoic acid (**83**) (39% by NMR) ^{1}H NMR (MeOH-d_4, 300 MHz): δ 1.03 (d *J*=6.5Hz, 1.5H) and 1.05 (d *J*=7Hz, 1.5H), 1.47 (obscured), 2.07 (m, 0.5H) and 2.20 (m, 0.5H), 4.27 (m, 0.5H) and 4.39 (m, 0.5H), 4.30 (obscured) and 4.62 (d, *J*=7Hz, 0.5H)ppm.

N-acetyl-δ-chloroisoleucine (**84**) (32% by NMR) ^{1}H NMR (MeOH-d_4, 300 MHz): δ 0.98 (d *J*=7Hz, 3H), 1.74 (m, 1H), 1.94 (m, 1H), 2.23 (m, 1H), 3.60 (obscured), 4.43 (d *J*=5Hz, 1H) ppm.

From the reaction of *N*-acetylleucine (**65**) as above, the following products were identified:

N-acetyl-γ-chloroleucine (**85**) (49% by NMR) ^{1}H NMR (MeOH-d_4, 300 MHz): δ 1.59 (s, 3H), 1.61 (s, 3H), 2.07 (obscured), 2.42 (dd *J*=3Hz *J*=15Hz, 1H), 4.68 (dd *J*=3Hz *J*=9Hz, 1H) ppm.

N-acetyl-δ-chloroleucine (**86**) (51% by NMR) ^{1}H NMR (MeOH-d_4, 300 MHz): δ 1.03 (d *J*=6.5Hz, 1.5H) and 1.06 (d *J*=6.5Hz, 1.5H), 1.80 (m, 2H), 2.00 (m, 1H), 3.51 (d *J*=5Hz, 1H) and 3.54 (d *J*=4.5Hz, 1H), 4.46 (obscured) ppm.

From the reaction of N^{α}-acetyllysine (**66**) as above, the following products were identified:

N^{α}-acetyl-β-chlorolysine (**87**) (20% by NMR) ^{1}H NMR (MeOH-d_4, 300 MHz): δ 1.80 (m, 1H) and 2.00 (m, 3H), 2.90 (m, 1H) and 2.96 (m, 1H), 4.24 (m, 0.5H) and 4.57 (m, 0.5H), 4.83 (d *J*=5Hz, 0.5H) and 5.00 (d *J*=3Hz, 0.5H) ppm.

N^{α}-acetyl-γ-chlorolysine (**88**) (64% by NMR) ^{1}H NMR (MeOH-d_4, 300 MHz): δ 2.00 (m, 1H) and 2.14 (m, 1H), 2.21 (m, 1H) and 2.35 (m, 1H), 3.15 (m, 1H) and 3.16 (m, 1H), 4.11 (m, 0.5H) and 4.14 (m, 0.5H), 4.62 (dd *J*=6Hzm *J*=7.5Hz, 0.5H) and 4.68 (dd *J*=3Hz *J*=11Hz, 0.5H) ppm.

N^{α}-acetyl-δ-chlorolysine (**89**) (16% by NMR) ^{1}H NMR (MeOH-d_4, 300 MHz): δ 1.89 (m, 2H), 2.00 (m, 2H), 3.13 (m, 1H) and 3.35 (m, 1H), 4.21 (m, 1H), 4.39 (m, 0.5H) and 4.45 (m, 0.5H) ppm.

From the reaction of *N*-acetylphenylalanine (**68**) as above, the following products were identified:

N-acetyl-β-chlorophenylalanine (**90**) (100% by NMR) ^{1}H NMR (MeOH-d_4, 300 MHz): δ 5.13 (d *J*=5Hz, 1H), 5.60 (d *J*=5Hz, 1H), 7.13 (m, 5H) ppm.

From the reaction of N^{α}-acetylornithine (**71**) as above, the following products were identified:

N^{α}-acetyl-β-chloroornithine (**91**) (44% by NMR) ^{1}H NMR (MeOH-d_4, 300 MHz): δ 2.23 (m, 1H) and 2.36 (m, 1H), 3.17 (m, 1H) and 3.19 (m, 1H), 4.37 (m, 0.5H) and 4.76 (m, 0.5H), 4.82 (d *J*=5Hz, 0.5H) and5.03 (d *J*=2.5Hz, 0.5H) ppm.

N^{α}-acetyl-γ-chloroornthine (**92**) (56% by NMR) ^{1}H NMR (MeOH-d_4, 300 MHz): δ 2.36 (m, 1H) and 2.48 (m, 1H), 3.43 (m, 1H) and 3.52 (m, 1H), 4.29 (m, 0.5H) and 4.41 (m, 0.5H), 4.67 (m, 0.5H) and 4.70 (m, 0.5H) ppm.

From the reaction of *N*-acetyl-α-aminobutyic acid (**72**) as above, the following products were identified:

N-acetyl-α-amino-β-chlorobutyric acid (**93**) (32% by NMR) ^{1}H NMR (MeOH-d_4, 300 MHz): δ 1.48 (d *J*=7Hz, 1.8H) and 1.56 (d *J*=7Hz, 1.2H), 3.61 (m, 1H), 4.77 (d *J*=5Hz, 0.4H) and 4.87 (d *J*=3Hz, 0.6H) ppm.

N-acetyl-α-amino-γ-chlorobutyric acid (**94**) (68% by NMR) ^{1}H NMR (MeOH-d_4, 300 MHz): δ 2.12 (m, 1H), 2.29 (m, 1H), 3.66 (m, 2H), 4.57 (dd *J*=5Hz *J*=10Hz, 1H) ppm.

From the reaction of *N*-acetylnorvaline (**73**) as above, the following products were identified:

N-acetyl-γ-chloronorvaline (**95**) (66% by NMR) ^{1}H NMR (MeOH-d_4, 300 MHz): δ 1.55 (d *J*=6Hz, 1.5H) and 1.57 (d *J*=6Hz, 1.5H), 2.10 (m, 2H), 4.12 (m, 0.5H) and 4.20 (m, 0.5H), 4.59 (dd *J*=6Hz *J*=8Hz, 0.5H) and 4.67 (dd *J*=4Hz *J*=11Hz, 0.5H) ppm.

N-acetyl-δ-chloronorvaline (**96**) (44% by NMR) ^{1}H NMR (MeOH-d_4, 300 MHz): δ 1.72 (m, 2H), 1.83 (m, 2H), 3.61 (t *J*=6Hz, 2H), 4.45 (t *J*=8Hz, 1H) ppm.

From the reaction of *N*-acetylnorleucine (**74**) as above, the following products were identified:

N-acetyl-β-chloronorleucine (**97**) (28% by NMR) ^{1}H NMR (MeOH-d_4, 300 MHz): δ 1.04 (t *J*=7Hz, 1.5H) and 1.07 (t *J*=7Hz, 1.5H), 1.75 (m, 4H), 2.30 (m, 4H), 3.88 (m, 0.5H) and 4.00 (m, 0.5H), 4.64 (m, 1H) ppm.

N-acetyl-γ-chloronorleucine (**98**) (45% by NMR) ^{1}H NMR (MeOH-d_4, 300 MHz): δ 1.49 (d, *J*=6.5Hz, 1.5H) and 1.50 (d *J*=6Hz, 1.5H), 1.80 (m, 2H), 2.10 (m, 2H), 4.07 (m, 1H), 4.39 (m, 1H) ppm.

N-acetyl-δ-chloronorleucine (**99**) (27% by NMR) ^{1}H NMR (MeOH-d_4, 300 MHz): δ 1.54 (m, 2H), 1.64 (m, 2H), 1.87 (m, 2H), 3.57 (t *J*=6.5 Hz, 2H), 4.63 (m, 1H) ppm.

From the reaction of *N*-acetyl-*tert*-leucine (**75**) as above, the following products were identified:

N-acetyl-γ-chloro-*tert*-leucine (**100**) (100% by NMR) ^{1}H NMR (MeOH-d_4, 300 MHz): δ 1.00 (s, 3H), 1.07 (s, 3H), 3.57 (ABq *J*=11Hz, 2H), 4.63 (s, 1H) ppm.

From the reaction of *N*-acetyl-homophenylalanine (**76**) as above, the following products were identified:

N-acetyl-γ-chloro-homophenylalanine (**101**) (100% by NMR) ^{1}H NMR (MeOH-d_4, 300 MHz): δ 2.18 (m, 2H), 4.67 (m, 1H), 5.00 (dd *J*=4Hz *J*=8Hz, 0.5H) and 5.05 (apparent t *J*=6Hz, 0.5H) ppm.

Competitive experiments were performed between all of the acetamides (**61-67**) and (**69-76**) and phenylalanine (**68**). Additional competitive experiments against *N*-acetylphenylalanine (**68**) were performed with valine (**25**) and leucine (**30**). The k_{rel} values obtained in this manner were consistently within 10% of the k_{rel} values determined against phenylalanine (**28**). To obtain estimates of reproducibility duplicate experiments were performed on *N*-acetylglycine (**61**), *N*-acetylalanine (**62**), *N*-acetylleucine (**65**), *N*-acetylnorleucine (**74**), and *N*-acetylisoleucine (**64**) and k_{rel} values were within 5% for each. Repeated determinations of product distributions for individual samples were consistently within 5%.

Chapter 4

Glycylalanylphenylalnine (**102**) and Cbz-phenylalanylleucylalanine were purchased from Bachem Ltd. Phenylalanylhomophenylalanylalanine (**104**) and *N*-(α-aminobutanoyl)-norvalylalanine (**105**) were produced to order by the Biomolecular Resource Facility, John Curtain School of Medical Research, The Australian National University. All amino acid residues in the above peptides had *S*-stereochemistry at the α-centre.

Cbz-Phenylalanylleucylalanine was deprotected by hydrogenation to give phenyl-alanylleucylalanine (**103**) using the following procedure: Cbz-phenylalanylleucylalanine (300 mg, 0.61 mmol) was dissolved in methanol (100 mL). To this palladium on carbon (10%) (~25 mg) was added. The solution was stirred under a hydrogen atmosphere overnight. The solution was filtered through celite, and the filtrate removed under reduced pressure to give a quantitative yield of phenylalanylleucylalanine (**103**) as a colourless powder (216 mg). ^{1}H NMR (MeOH-d_4, 500 MHz): δ 0.97 (d *J*=7Hz, 3H), 1.00 (d *J*=7Hz, 3H), 1.43 (d *J*=7Hz, 3H), 1.64 (m, 2H), 1.74 (m, 1H), 3.01 (dd *J*=9Hz *J*=14Hz, 1H), 3.30 (dd *J*=5Hz *J*=9Hz, 1H), 4.13 (dd *J*=5Hz *J*=9Hz, 1H), 4.38 (q *J*=7Hz, 1H), 4.50 (dd *J*=6Hz *J*=9Hz, 1H), 7.3 (m, 5H) ppm. ^{13}C NMR (MeOH-d_4, 125 MHz): δ δ 16.1, 20.7, 21.9, 24.3, 37.1, 40.7, 51.6, 54.0, 127.5, 128.7, 129.1, 157.9, 158.2, 158.6, 158.9 ppm. HRMS *m/z*: [M+H] (FTICR) calculated for $C_{18}H_{28}N_3O_4$, 350.2074; found 350.2080.

The period for which the peptides (**102-105**) were chlorinated was determined by the following procedure: the residue on which the majority of reaction was expected to occur was identified based on data in Figures 2.36 and 3.23. and an amount of the analogous *N*-acetylated amino acid (*N*-acetylphenylalanine (**68**), *N*-acetylhomophenylalanine (**76**), *N*-acetylleucine (**65**) or *N*-acetylnorvaline (**73**)) equivalent to 100 mg of the corresponding peptide was dissolved in 5 mL TFA in a quartz reaction vessel. The solution was then irradiated with a 300W broad spectrum sunlamp while it was saturated with molecular chlorine until approximately half of the *N*-acetylated amino acid was consumed, as determined by ^{1}H NMR spectroscopy.

The peptides were chlorinated under the following conditions: 100 mg of the peptide was dissolved in 5 mL TFA. The solution was then irradiated with a 300W broad spectrum sunlamp while it was saturated with molecular chlorine for the period determined as above. The solution was degassed with N_2, and then the solvent was removed under reduced pressure. The mixture of products was separated on a semi-preparative HPLC system. The isolated products were identified using ^1H and ^{13}C NMR spectroscopy and high resolution mass spectrometry.

Glycylalanylphenylalanine (**102**) (100 mg, 0.34 mmol) was chlorinated using the above procedure for 80 seconds. The product was purified by HPLC (80:20 H_2O+0.1% TFA/MeCN, 10 mL/min), and the required fractions were lyophilised. The peak at 8.38 min was identified as glycylalanyl-β-chlorophenylalanine (**106**), 58 mg of a colourless hygroscopic powder (52%, 73% based on recovered starting material). ^1H NMR (MeOH-d_4, 500 MHz): δ 1.36 (d *J*=7Hz, 3H), 3.70 (s, 2H), 4.47 (q *J*=7Hz, 1H), 4.92 (d *J*=5Hz, 1H), 5.60 (d *J*=5Hz, 1H), 7.31 (m, 5H) ppm. On standing at room temperature over several days (**106**) converts to the eneamide (**107**). δ ^1H NMR (MeOH-d_4, 500 MHz): 1.40 (d *J*=7Hz, 3H), 3.72 (s, 2H), 4.48 (q *J*=7Hz, 1H), 6.26 (d *J*=14Hz, 1H), 7.20 (m, *J*=5H), 7.39, (d *J*=14Hz, 1H) ppm. ^{13}C NMR (MeOH-d_4, 125 MHz): δ 17.2, 40.3, 49.5, 114.2, 122.3, 125.4, 126.6, 128.6, 136.5, 166.0, 171.2 ppm. HRMS *m/z*: $[M+H]^+$ (FTICR) calculated for $C_{13}H_{18}N_3O_2$, 248.1399; found, 248.1405

Phenylalanylhomophenylalanylalanine (**103**) (100 mg, 0.26 mmol) was chlorinated using the above procedure for 60 seconds. The product was purified by HPLC (95:5 H_2O+0.1% TFA/MeCN, 10 mL/min), and the required fractions were lyophilised. The peak at 13.86 min was identified as phenylalanyl-γ-chlorohomophenylalanylalanine (**108**), 59 mg of colourless a hygroscopic powder (54%, 69% based on recovered starting material). ^1H NMR (MeOH-d_4, 500 MHz): δ 1.43 (d *J*=7Hz, 3H), 2.20 (m, 2H). 3.01 (dd *J*=9Hz *J*=14Hz, 1H), 3.30 (dd *J*=5Hz *J*=9Hz, 1H), 4.38 (q *J*=7Hz, 1H), 4.50 (dd *J*=6Hz *J*=9Hz, 1H), 4.67 (dd *J*=5Hz *J*=10Hz, 1H), 5.00 (dd *J*=4Hz *J*=8Hz, 1H), 7.30 (m, 10H) ppm. ^{13}C NMR (MeOH-d_4,

125 MHz): δ 16.2, 37.5, 41.2, 49.5, 51.9, 55.1, 67.3, 127.7, 128.6, 129.5, 157.7, 157.8, 158.4, 158.5, 158.6, 158.7, 158.9 ppm. HRMS *m/z*: $[M+H]^+$ (FTICR) calculated for $C_{22}H_{27}ClN_3O_4$, 432.1685; found, 432.1689.

Phenylalanylleucylalanine (**104**) (100 mg, 0.29 mmol) was chlorinated using the above procedure for 60 seconds. The product was purified by HPLC (82:18 H_2O+0.1% TFA/MeCN, 10 mL/min), and the required fractions were lyophilised. The peak at 13.38 min was identified as phenylalanyl-γ-chloroleucylalanine (**109**), 16 mg of a colourless hygroscopic powder (15%, 47% based on recovered starting material). ^1H NMR (MeOH-d_4, 500 MHz): δ 1.36 (d *J*=7Hz, 3H), 1.59 (s, 3H), 1.61 (s, 3H), 2.10 (dd *J*=9Hz *J*=15Hz, 1H), 2.41 (dd *J*=6Hz *J*=15Hz, 1H), 3.19 (dd *J*=8Hz *J*=14Hz, 1H), 3.32 (dd *J*=8Hz *J*=14Hz, 1H), 4.47 (q *J*=7Hz, 1H), 4.52 (dd *J*=5Hz *J*=9Hz, 1H), 4.72 (dd *J*=6Hz *J*=9Hz, 1H), 7.31 (m, 5H) ppm. ^{13}C NMR (MeOH-d_4, 125 MHz): δ 16.5, 31.0, 32.5, 37.2, 46.5, 47.2, 54.8, 52.1, 66.7, 128.0, 127.7, 128.3, 157.7, 158.2, 158.8, 158.9 ppm. HRMS *m/z*: $[M+H]^+$ (FTICR) calculated for $C_{14}H_{19}ClN_3O_4$, 384.1690; found 384.1681.

N-(α-aminobutanoyl)-norvalylalanine (**105**) (100 mg, 0.36 mmol) was chlorinated using the above procedure for 80 seconds. The product was purified by HPLC (95:5 H_2O+0.1% TFA/MeCN, 10 mL/min), and the required fractions were lyophilised. The peak at 8.22 min was identified as *N*-(α-aminobutanoyl)-γ-chloronorvalylalanine (**111**), 10 mg of a colourless hygroscopic powder (9%, 30% based on recovered starting material). ^1H NMR (MeOH-d_4, 500 MHz): δ 1.02 (t *J*=8Hz, 3H), 1.04 (t *J*=8Hz, 3H), 1.42, (d *J*=7Hz, 3H), 1.43 (d *J*=7Hz, 3H), 1.56 (d *J*=6Hz, 3H), 1.58 (d *J*=6Hz, 3H), 1.89 (m, 2H), 2.09 (m, 1H), 2.24 (m, 1H), 3.81 (apparent t *J*=6Hz, 1H), 3.82 (apparent t *J*=6Hz, 1H), 4.17 (m, 1H), 4.22 (m, 1H), 4.37 (q *J*=7Hz, 1H), 4.43 (q *J*=7Hz, 1H), 4.63 (dd *J*=7Hz 6.5Hz, 1H), 4.71 (dd *J*=4Hz *J*=10Hz, 1H) ppm. ^{13}C NMR (MeOH-d_4, 125 MHz): δ 8.0, 16.1, 28.5, 29.4, 29.3, 43.8, 49.0, 51.5, 52.1, 52.6, 53.7, 127.4, 127.8, 129.0 pm. HRMS *m/z*: $[M+H]^+$ (FTICR) calculated for $C_{14}H_{19}ClN_3O_4$, 308.1372; found, 308.1387. The peak at 8.71 min was identified as *N*-(α-aminobutanoyl)-δ-chloronorvalylalanine (**112**), 9 mg of a colourless hygroscopic powder

(8%, 27% based on recovered starting material). ^{1}H NMR (MeOH-d_4, 500 MHz): δ 1.04 (t *J*=8Hz, 3H), 1.42, (d *J*=7Hz, 3H), 1.72 (m 2H), 1.83 (m, 2H), 1.89 (m, 2H), 3.60 (t *J*=6Hz, 3H), 3.82 (t *J*=6Hz, 1H), 4.38 (q *J*=7Hz, 1H), 4.45 (dd *J*=6Hz *J*=8Hz, 1H) ppm. ^{13}C NMR (MeOH-d_4, 125 MHz): δ 8.1, 16.2, 28.4, 29.5, 31.0, 45.3, 51.3, 51.6, 52.1, 127.7, 127.6, 128.7 ppm. HRMS *m/z*: $[M+H]^+$ (FTICR) calculated for $C_{14}H_{19}ClN_3O_4$, 308.1372; found, 308.1379.

Chapter 5

RSE and BDE values were calculated by Prof. L. Radom (*radom@chem.usyd.edu.au)* and Mr. G.P.F. Wood (*gwood@chem.usyd.edu.au*), University of Sydney, from whom the Gaussian archive entries for the optimised structures are available. The values were calculated at the RB3-LYP/6-311+G(3df,2p)//UB3-LYP/6-31G(d) level with scaled (0.9806) UB3-LYP/6-31G(d) zero-point vibrational energies.

Chapter 6

The amino acids (**12**), (**13**), (**15**), (**18**), (**21**), (**23**), (**25**), (**29-31**), (**37-40**), and (**113-115**) and *N*-acetylated amino acids (**61-67**), (**69-75**) and (**116-118**) were obtained from the same sources as for Chapters 2 and 3. Hydrogen peroxide was purchased from Merck. Deuterium peroxide was purchased from Icon Isotopes.

The rate of reaction of the amino acids (**12**), (**13**), (**15**), (**18**), (**21**), (**23**), (**25**), (**29-31**), (**37-40**), and (**113-115**) and acetamides (**61-67**), (**69-75**) and (**116-118**) were obtained using the following procedure: approximately 5 mg of each of two amino acids was dissolved in 0.5 mL D_2O in a quartz NMR tube. 1 drop of TFA was added to acidify the solution. To this, approximately 0.05 mL deuterium peroxide was added. The NMR tube was then fitted with a WILMAD® coaxial insert filled with a solution of benzoic acid in TFA. The ^1H NMR spectrum of the sample was obtained. The sample was irradiated in a photochemical reactor fitted with 16, 254 nm bulbs for between 20 and 60 minutes depending on the compounds. Afterwards a second ^1H NMR spectrum of the sample was obtained. The k_{rel} values were then determined using equation detailed in Chapter 2.

The k_{rel}^{H} values were identified by the following procedure. Using the data from the ^1H NMR spectra obtained during the determination of k_{rel}, the percentage of the starting amino acid reacted at the ω-methyl position was determined by comparison with authentic samples. The decimal percentage was then multiplied by the k_{rel} value of the appropriate amino acid then divided by three. This gives the k_{rel}^{H} for the ω-position of the amino acid side-chain

No detectable glycine (**12**) was obtained from reaction alanine (**13**).

The percentage of aspartic acid (**37**) obtained from reaction of α-aminobutyric acid (**15**) (36%) was determined by integration of the ^{1}H NMR signal (MeOH-d_4, 300 MHz) at 2.81 (d *J*=5Hz) ppm.

The percentage of glutamic acid (**18**) obtained from reaction of norvaline (**38**) (35%) was determined by integration of the ^{1}H NMR signals (MeOH-d_4, 300 MHz) at 3.03 (dd *J*=5Hz *J*=6Hz) and 3.02 (dd *J*=5Hz J=6Hz) ppm.

The percentage of α-aminoadipic acid (**122**) obtained from reaction of norleucine (**39**) (30%) was determined by integration of the ^{1}H NMR signals (MeOH-d_4, 300 MHz) at 3.00 (dd *J*=4Hz *J*=5Hz) and 3.06 (dd *J*=4Hz *J*=5Hz) ppm.

The percentage of β-methylaspartic acid (**123**) obtained from reaction of valine (**25**) (37%) was determined by integration of the ^{1}H NMR signal (MeOH-d_4, 300 MHz) at 3.00 (m) ppm.

The percentage of β,β-dimethylaspartic acid (**124**) obtained from reaction of *tert*-leucine (**40**) (100%) was determined by integration of the ^{1}H NMR signal (MeOH-d_4, 300 MHz) at 4.24 (s) ppm.

The percentage of *N*-acetylglycine (**61**) obtained from reaction of *N*-acetylalanine (**62**) (15%) was determined by integration of the ^{1}H NMR signal (MeOH-d_4, 300 MHz) at 3.50 (s) ppm.

The percentage of *N*-acetylaspartic acid (**70**) obtained from reaction of *N*-acetyl-α-aminobutyric acid (**72**) (26%) was determined by integration of the ^{1}H NMR signal (MeOH-d_4, 300 MHz) at 2.61(ABX *J*=6Hz *J*=8Hz *J*=16Hz) ppm.

The percentage of *N*-acetylglutamic acid (**69**) obtained from reaction of *N*-acetylnorvaline (**73**) (15%) was determined by integration of the ^{1}H NMR signals (MeOH-d_4, 300 MHz) at 2.97 (dd *J*=5Hz *J*=7.5Hz) and 3.01 (dd *J*=5Hz *J*=7.5Hz) ppm.

The percentage of *N*-acetyl-α-aminoadipic acid obtained from reaction of *N*-acetylnorvaline (**73**) (10%) was determined by integration of the ^{1}H NMR signals (MeOH-d_4, 300 MHz) at 3.01 (dd *J*=4Hz *J*=5Hz) and 3.05 (dd *J*=4Hz *J*=5Hz) ppm.

The percentage of *N*-acetyl-β-methylaspartic acid obtained from reaction of *N*-acetylvaline (**63**) (100%) was determined by integration of the ^{1}H NMR signal (MeOH-d_4, 300 MHz) at 2.80 (m) ppm.

The percentage of *N*-acetyl-β,β-dimethylaspartic acid obtained from reaction of *N*-acetyl-*tert*-leucine (**75**) (100%) was determined by integration of the ^{1}H NMR signal (MeOH-d_4, 300 MHz) at 4.56 (s) ppm.

References

[1] Wieland, T.; Bodanszky, M., *The World of Protiens*. Heidelberg, 1991.

[2] Prigge, S. T.; Mains, R. E.; Eipper, B. A.; Amzel, L. M., *Cellular and Molecular Life Sciences* **200,** *57*, 1236.

[3] Dustin, P., *Microtubules*. New York, 1984.

[4] Hunt, S., In *Chemistry and Biochemsitry of the Amino Acids*, ed. Barrett, G. C. New York, 1985; p 55.

[5] Hardy, P. M., In *Chemistry and Biochemistry of the Amino Acids*, ed. Barrett, G. C. New York, 1985; p 6.

[6] Lubec, G.; Rosenthal, G. A., *Amino Acids. Chemistry, Biology and Medicine*. ESCOM Science Publishers B.V.: 1990.

[7] Greenstien, J. P.; Winitz, M., *Chemistry of the Amino Acids*. John Wikey & Sons: 1961.

[8] Wolff, S. P.; Dean, R. T., *Biochemical Journal* **1986,** *234*, 399.

[9] Wolff, S. P.; Garner, A.; Dean, R. T., *Trend in Biochemical Sciences* **1986,** *11*, 27.

[10] Davies, K. J. A., *Journal of Biological Chemistry* **1987,** *262*, 9895.

[11] Stadtman, E. R., *Science* **1992,** *257*, 1220.

[12] Davies, M. J.; Dean, R. T.; Geisig, S., *Trends in Biochemical Sciences* **1993,** *18*, 437.

[13] Brattin, W. J.; Glende, E. A.; Recknagel, R. O., *Free Radicals in Biology and Medicine* **1985,** *1*, 27.

[14] Ames, B. N.; Kohen, R.; Yamamoto, Y.; Cundy, K. C., *Proceedings of the National Acadamy of Sciences (USA)* **1988,** *85*, 3175.

[15] Henriksen, T.; Melo, T. B.; Saxebol, G., In *Free Radicals in Biology*, ed. Pryor, W. A. New York.

[16] Markesbury, W. R., *Free Radicals in Biology and Medicine* **1997,** *23*, 134.

[17] Yang, C. Y.; Gu, Z. W.; Yang, H. X.; Yang, M.; Gotto, A. M.; Smith, C. V., *Free Radicals in Biology and Medicine* **1997,** 2, 161.

[18] Pryor, W. A.; Dooley, M. M.; Church, D. F., *Advances in Free Radical Biology and Medicine* **1986,** 2, 161.

[19] Dean, R. T.; Fu, S.; Stocker, R.; Davies, M. J., *Biochemical Journal* **1997,** *324*, 1.

[20] Berlett, B. S.; Stadtman, E. R., *The Journal of Biological Chemistry* **1997,** *272*, (33), 20313.

[21] Davies, M. J.; Dean, R. T., *Radical-Mediated Protien Oxidation*. New York, 1997.

[22] Stubbe, J.; Donk, W. A. v. d., *Chemical Reviews* **1998,** *98*, 705.

[23] Stadtman, E. R.; Berlett, B. S., *Journal of Biological Chemistry* **1991,** *266*, 17201.

[24] Dooley, D. M.; Ruggiero, C. E.; Smith, J. A.; Tanizawa, K., *Biochemistry* **1997,** *36*, 1953.

[25] Eriksson, L. A.; Himo, F., *Journal of the Chemical Society, Perkin Transactions 2* **1998,** 305.

[26] Frey, P. A., *Chemical Reviews* **1990,** *90*, 1343.

[27] Jones, J. P.; Manchester, J. I.; Dinnocenzo, J. P.; Higgins, L., *Journal of the American Chemical Society* **1997,** *119*, 5069.

[28] Klinman, J. P.; Miller, S. M., *Biochemistry* **1985,** *24*, 2114.

[29] Mansuy, D.; Battioni, P., In *Activation and Functionalisation of Alkanes*, ed. Hill, C. L. 1989; p 195.

[30] Easton, C. J.; Eichiger, S. K.; Pitt, M. J., *Tetrahedron* **1997,** *53*, 5609.

[31] Spiro, T. G., *Metal Ion Activation of Dioxygen*. New York, 1980.

[32] Danen, W. C.; Warner, R. J.; Arudi, R. L., Nucleophillic Reactions of Superoxide Anion Radical. In *Organic Free Radicals*, ed. Pryor, W. A. 1978.

[33] Fossey, J.; Lefort, D.; Sorba, J., *Free Radicals in Organic Chemistry*. 1995.

[34] Brockmann, H.; Pampus, G.; Manegold, J. H., *Chemische Berichte* **1959,** *92*, 1294.

[35] Dettwiler, J. E.; Belec, L.; Lubell, W. D., *Canadian Journal of Chemistry* **2005,** *83*, (6-7), 793.

[36] Saito, H.; Yamada, T.; Okumura, K.; Yonezawa, Y.; Shin, C.-G., *Chemistry Letters* **2002,** *11*, 1098.

[37] Sugiyama, M.; Kumagai, T., *Journal of Bioscience and Bioengineering* **2002,** *93*, (2), 105.

[38] Boger, D. L.; Patane, M. A.; Zhou, J., *Journal of the American Chemical Society* **1994,** *116*, (19), 8544.

[39] Ueda, K.; Xiao, J. Z.; Doke, N.; Nakatsuka, S., *Tetrahedron Letters* **1992,** *33*, (37), 5377.

[40] Hojati, Z.; Milne, C.; Harvey, B.; Gordon, L.; Borg, M.; Flett, F.; Wilkinson, B.; Sidebottom, P. J.; Rudd, B. A. M.; Hayes, M. A.; Smith, C. P.; Micklefield, J., *Chemistry & Biology* **2002,** *9*, (11), 1175.

[41] Liu, H.-W.; Sherman, D. H.; Zhao, L., WO 2002029035, 2002.

[42] Bryskier, A.; Klich, M., *Antimicrobial Agents* **2005**, 816.

[43] Bonnington, L. S.; Tanaka, J.; Higa, T.; Kimura, J.; Yoshimura, Y.; Nakao, Y.; Yoshida, W. Y.; Scheuer, P. J., *Journal of Organic Chemistry* **1997,** *66*, (22), 7765.

[44] Traber, R.; Keller-Juslen, C.; Rudolf, L. H.; Kuhn, M.; Von Wartburg, A., *Helvetica Chimica Acta* **1979,** *62*, (4), 1252.

[45] Miyata, T.; Iwanaga, S., *Domyaku Koka* **1996,** *23*, (9), 499.

[46] Raffauf, R. F.; Zennie, T. M.; Onan, K. D.; Le Quesne, P. W., *Journal of Organic Chemistry* **1984,** *49*, (15), 2714.

[47] Oka, M.; Yaginuma, K.; Numata, K.; Konishi, M.; Oki, T.; Kawaguchi, H., *Journal of Antibiotics* **1988,** *41*, (10), 1338.

[48] Randazzo, A.; Bifulco, G.; Giannini, C.; Bucci, M.; Debitus, C.; Cirino, G.; Gomez-Paloma, L., *Journal of the American Chemical Society* **2001,** *123*, (44), 10870.

[49] Pisarewicz, K.; Mora, D.; Pflueger, F. C.; Fields, G. B.; Mari, F., *Journal of the American Chemical Society* **2005,** *127*, (17), 6207.

[50] Blunden, G.; Patel, A. V.; Adrian-Romero, M.; Melendez, P., *Biochemical Systematics and Ecology* **2004,** *32*, (12), 1153.

[51] Narayanan, S.; Iyengar, M. R. S.; Ganju, P. L.; Rengaraju, S.; Shomura, T.; Tsuruoka, T.; Inouye, S.; Niida, T., *Journal of Antibiotics* **1980,** 33, (11), 1249.

[52] Johnson, J. H.; Tymiak, A. A.; Bolgar, M. S., *Journal of Antibiotics* **1990,** *43*, (8), 920.

[53] Kato, T.; Hinoo, H.; Terui, Y.; Kikuchi, J.; Shoji, J., *Journal of Antibiotics* **1988,** *41*, (6), 719.

[54] O'Sullivan, J.; McCullough, J. E.; Tymiak, A. A.; Kirsch, D. R.; Trejo, W. H.; Principie, P. A., *The Journal of Antibiotics* **1988,** *41*, 1740.

[55] Koehn, F. E.; Longley, R. E.; Reed, J. K., *Journal of Natural Products* **1992,** *55*, (5), 613.

[56] Hagenmaier, H.; Keckeisen, A.; Zaehner, H.; Koenig, W. A., *Liebigs Annalen der Chemie* **1979**, (10), 1494.

[57] Sun, Q.; Ishida, K.; Matsuda, H.; Murakami, M., *Tennen Yuki Kagobutsu Toronkai Koen Yoshishu* **1998**, 499.

[58] Isogai, A.; Suzuki, A.; Higashikawa, S.; Kuyama, S.; Tamura, S., *Peptide Chemistry* **1980**, 125.

[59] Wieland, T., *Apotheker Zeitung* **1976,** *116*, (23), 805.

[60] Chandrasekhar, S.; Chandrashekar, G., *Tetrahedron: Asymmetry* **2005,** *16*, (13), 2209.

[61] Shoji, J.; Hinoo, H.; Katayama, T.; Nakagawa, Y.; Ikenishi, Y.; Iwatani, K.; Yoshida, T., *Journal of Antibiotics* **1992,** *45*, (6), 824.

[62] Chen, Z.; Ye, T., *Syntheic Letters* **2005**, (18), 2781.

[63] Farver, D. K.; Hedge, D. D.; Lee, S. C., *Annals of Pharmacotherapy* **2005,** *39*, (5), 863.

[64] Khokhlov, A. S.; Shutova, K. I., *Journal of Antibiotics* **1972,** *25*, (9), 501.

[65] Harris, C. M.; Harris, T. M., *Journal of the American Chemical Society* **1982,** *104*, (15), 4293.

[66] H, F.; A, B.; H, B.; T, W., *Biochemistry* **1980,** *19*, (14), 334.

[67] Morita, H.; Kayashita, T.; Shimomura, M.; Takeya, K.; Itokawa, H., *Heterocycles* **1996,** *43*, (6), 1279.

[68] Zerbe, K.; Pylypenko, O.; Vitali, F.; Zhang, W.; Rouset, S.; Heck, M.; Vrijbloed, J. W.; Bischoff, D.; Bister, B.; Süssmuth, R. D.; Pelzer, S.; Wohlleben, W.; Robinson, J. A.; Schlichting, I., *The Journal of Biological Chemistry* **2002,** *277*, (49), 47476.

[69] Baldwin, J. E.; Adlington, R. M.; Domayne-Hayman, B. P.; Knight, G.; Ting, H.-H., *Journal of the Chemical Society, Chemical Communications* **1987,** *21*, 1661.

[70] Baldwin, J. E.; Abraham, E. P.; Adlington, R. M.; Chakravarti, B.; Derome, A. E.; Murphy, J. A.; Field, L. D.; Green, N. B.; Tong, H.-H.; Usher, J. J., *Journal of the Chemical Society, Chemical Communications* **1983,** *22*, 1317.

[71] Baldwin, J. E.; Adlington, R. M.; Turner, N. J.; Domayne-Hayman, B. P.; Ting, H.-H.; Derome, A. E.; Murphy, J. A., *Journal of the Chemical Society, Chemical Communications* **1984,** *17*, 1167.

[72] Baldwin, J. E.; Wan, T. S., *Journal of the Chemical Society, Chemical Communications* **1979**, 249.

[73] Baldwin, J. E.; Adlington, R. M.; Bohlmann, R., *Journal of the Chemical Society, Chemical Communications* **1985**, 357.

[74] Elson, S. W.; Baggaley, K. H.; Gillett, J.; Holland, S.; Nicholson, N. H.; Sime, J. T.; Woroniecki, S. R., *Journal of the Chemical Society, Chemical Communications* **1987**, 1736.

[75] Ingold, K. U., Rate Constants for Free Radical Reactions. In *Free Radicals*, ed. Kochi, J. K. 1973; 'Vol.' I, p 37.

[76] Poutsma, m. L., Halogenation. In *Free Radicals*, ed. Kochi, J. K. 1973; 'Vol.' 2, p 159.

[77] Russel, G. A., Reactivity, Selctivity, and Polar Effects in Hydrogen Atom Transfer Reaction. In *Free Radicals*, ed. Kochi, J. K.; Wiley: 1973; 'Vol.' 1.

[78] Traynham, J. G., Alphatic and Aromatic Free-Radical Reactions. In *Frontiers of Free Radical Chemistry*, ed. Pryor, W. A. 1980; p 283.

[79] Pryor, W. A.; Church, D. F.; F.Y., T.; R.H, T., The Role of Polar Effects and Bond Dissociation Energies (BDE) in Radical Reactivities: The Iodination of Toluene. In *Frontiers of Free Radical Chemistry*, ed. Pryor, W. A. 1980; p 355.

[80] Rüchardt, C., *Angewandte Chemie, International Edition in English* **1970,** *9*, 830.

[81] Rüchardt, C.; Beckhaus, H. D., *Angewandte Chemie, International Edition in English* **1980,** *19*, 429.

[82] Balaban, A. T., *Revue Roumaine de Chimie* **1971,** *16*, 725.

[83] Balaban, A. T.; Caproiu, M. T.; Negoita, N.; Baican, R., *Tetrahedron* **1977,** *33*, 2249.

[84] Balaban, A. T.; Istratoiu, R., *Tetrahedron Letters* **1973,** *21*, 1879.

[85] Balaban, A. T.; Negoita, N.; Baican, R., *Tetrahedron Letters* **1973,** *21*, 1877.

[86] Katritzky, A. R.; Soti, F.; Baldcock, R. W.; Hudson, P., *Journal of the Chemical Society, Perkin Transactions I* **1974**, 1422.

[87] Katritzky, A. R.; Soti, F., *Journal of the Chemical Society, Perkin Transactions I* **1974**, 1427.

[88] Katritzky, A. R.; Baldcock, R. W.; Hudson, P.; Soti, F., *Heterocycles* **1973,** *1*, 67.

[89] Viehe, H. G.; Merényi, R.; Stella, L.; Janousek, Z., *Angewandte Chemie International Edition in English* **1979,** *18*, 979.

[90] Korth, H. G.; Sicking, W., *Journal of the Chemical Society, Perkin Transactions* 2 **1997**, 715.

[91] Pasto, D. J.; Kranasnsky, R.; Zercher, C., *Journal of Organic Chemistry* **1987,** *52*, 3062.

[92] Pasto, D. J., *Journal of the American Chemical Society* **1988,** *110*, 8164.

[93] Rüchardt, C.; Beckhaus, H. D.; Birkhofer, H.; Hadrich, J., *Angewandte Chemie, International Edition in English* **1987,** *26*, 573.

[94] Rüchardt, C.; Brocks, J. J.; Welle, F. W.; Beckhaus, H. D., *Tetrahedron Letters* **1997,** *38*, 7721.

[95] Easton, C. J.; Hay, M. P., *Journal of the Chemical Society, Chemical Communications* **1985**, 425.

[96] Easton, C. J.; Hay, M. P.; Love, S. G., *Journal of the Chemical Society, Perkin Transactions I* **1988**, 265.

[97] Easton, C. J.; Hay, M. P., *Journal of the Chemical Society, Chemical Communications* **1986**, 55.

[98] Easton, C. J.; Burgess, V. A.; Hay, M. P., *Journal of the American Chemical Society* **1989,** *111*, 1047.

[99] Rüchardt, C.; Brocks, J. J.; Beckhaus, H. D.; Beckwith, A. L. J., *Journal of Organic Chemistry* **1998,** *63*, 1935.

[100] Rauk, A.; Yu, D.; Taylor, J.; Shustov, G. V.; Block, D. A.; Armstrong, D. A., *Biochemistry* **1999,** *38*, (28), 9089.

[101] Wong, M. W.; Pross, A.; Radom, L., *Journal of the American Chemical Society* **1994,** *116*, (26), 11938.

[102] Henry, D. J.; Parkin, C. J.; Mayer, P. M.; Radom, L., *Journal of Physcial Chemistry A* **2001,** *105*, 6750.

[103] Galano, A.; Alvarez-Idaboy, J. R.; Agacino-Valdés, E.; Ruiz-Santoyo, M. E., *Journal of Molecular Structure (Theochem)* **2004,** *676*, 97.

[104] Galano, A.; Alvarez-Idaboy, J. R.; Bravo-Pérez, G.; Ruiz-Santoyo, M. E., *Journal of Molecular Structure (Theochem)* **2002,** *617*, 77.

[105] Galano, A.; Alvarez-Idaboy, J. R.; Cruz-Torres, A.; Ruiz-Santoyo, M. E., *International Journal of Chemical Kinetics* **2003,** *35*, 212.

[106] Galano, A.; Alvarez-Idaboy, J. R.; Cruz-Torres, A.; Ruiz-Santoyo, M. E., *Journal of Molecular Structure (Theochem)* **2003,** *629*, 165.

[107] Galano, A.; Alvarez-Idaboy, J. R.; Montero, L. A.; Vivier-Bunge, A., *Journal of Computational Chemistry* **2001,** *22*, (11), 1138.

[108] Kollonitsch, J.; Rosegay, A.; Doldouras, G., *Journal of the American Chemical Society* **1964,** 86, 1857.

[109] Kollonitsch, J.; Scott, A. N.; Doldouras, G. A., *Journal of the American Chemical Society* **1966,** *88*, (15), 3624.

[110] Kollonitsch, J.; Doldouras, G. A.; Verdi, V. F., *Journal of the Chemical Society (B)* **1967,** 1093.

[111] Dixon, H. B. F.; Karpeiskii, M. Y.; Shlyapnikov, S. V.; Oseledchik, V. S.; Turchin, K. F., *Zhurnal Obshchei Khimii* **1967,** *37*, (6), 1237.

[112] Armstrong, W. A.; Humphreys, W. G., *Canadian Journal of Chemistry* **1967,** *45*, 2589.

[113] Taniguchi, H.; Fukui, K.; Ohnishi, S.; Hatano, H.; Hasegawa, H.; Maruyama, T., *The Journal of Physical Chemistry* **1968,** *72*, (6), 1926.

[114] Paul, V. H.; Fischer, H., *Berichte der Bunsengesellschaft für Physikalische Chemie* **1969,** *73*, (10), 972.

[115] Neta, P.; Simic, M.; Hayon, E., *The Journal of Physical Chemistry* **1970,** *74*, (6), 1214.

[116] Smith, P.; Fox, W. M.; McGinty, D. J.; Stevens, R. D., *Canadian Journal of Chemistry* **1970,** *48*, 480.

[117] Taniguchi, H.; Hatano, H.; Hasegawa, H.; Maruyama, T., *The Journal of Physical Chemistry* **1970,** *74*, (16), 3063.

[118] Neta, P.; Fessenden, R. W., *The Journal of Physical Chemistry* **1971,** *75*, (6), 738.

[119] Paul, v. H.; Fischer, H., *Helvetica Chimica Acta* **1971,** *54*, 485.

[120] Taniguchi, H.; Hasumi, H.; Hatano, H., *Bulletin of the Chemical Society of Japan* **1972,** *45*, 3380.

[121] Faulstich, H.; Dölling, J.; Michl, K.; Wieland, T., *Liebigs Annelen der Chemie* **1973**, 560.

[122] Livingston, R.; Doherty, D. G.; Zeldes, H., *Journal of the American Chemical Society* **1975,** *97*, (11), 3198.

[123] Rao, P. S.; Hayon, E., *The Journal of Physical Chemistry* **1975,** *79*, (2), 109.

[124] Joshi, A.; Rustgi, S.; Moss, H.; Riesz, P., *International Journal of Radiation Biology* **1978,** *33*, (3), 205.

[125] Burgess, V. A.; Easton, C. J., *Spectroscopy Letters* **1991,** *24*, (9), 1059.

[126] Hawkins, C. L.; Davies, M. J., *Biochimica et Biophysica Acta* **2001,** *1504*, 196.

[127] Hawkins, C. L.; Davies, M. J., *Journal of the Chemical Society, Perkin Transactions 2* **1998**, 2617.

[128] Nukuna, B. N.; Goshe, M. B.; Anderson, V. E., *Journal of the American Chemical Society* **2001,** *123*, 1208.

[129] Goshe, M. B.; Chen, Y. H.; Anderson, V. E., *Biochemistry* **2000,** *39*, 1761.

[130] Mita, H.; Shirakura, N.; Yokoyama, H.; Nomoto, S.; Shimoyama, A., *Advances in Space Research* **2004**, *33*, (8), 1282.

[131] Nord, L. I.; Vaag, P.; Duus, J.. *Analytical Chemistry* **2004**, *76*, (16), 4790.

[132] Walling, C.; Gibion, M. J. Journal of the American Chemical Society **1965**, *87*, 3361

[133] Laver, W. G.; Neuberger, A.; Scott, J. J., *Journal of the Chemical Society, Abstracts* **1959**, 483

[134] Miller S. L.; Urey, H. C., *Science* **1959,** *130,* 245.

[135] Kvenvolden K, Lawless J, Pering K, Peterson E, Flores J, Ponnamperuma C, Kaplan IR, Moore C., *Nature* **1970**, *923* 228